

UNCLASSIFIED

AD 269 846

*Reproduced
by the*

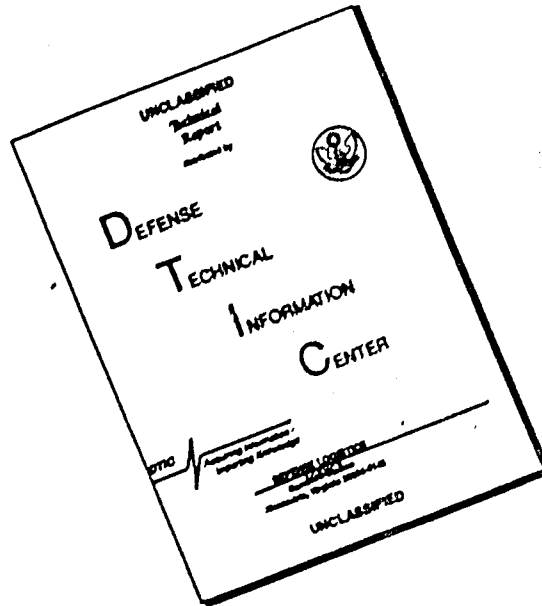
**ARMED SERVICES TECHNICAL INFORMATION AGENCY
ARLINGTON HALL STATION
ARLINGTON 12, VIRGINIA**



UNCLASSIFIED

NOTICE: When government or other drawings, specifications or other data are used for any purpose other than in connection with a definitely related government procurement operation, the U. S. Government thereby incurs no responsibility, nor any obligation whatsoever; and the fact that the Government may have formulated, furnished, or in any way supplied the said drawings, specifications, or other data is not to be regarded by implication or otherwise as in any manner licensing the holder or any other person or corporation, or conveying any rights or permission to manufacture, use or sell any patented invention that may in any way be related thereto.

DISCLAIMER NOTICE



THIS DOCUMENT IS BEST QUALITY AVAILABLE. THE COPY FURNISHED TO DTIC CONTAINED A SIGNIFICANT NUMBER OF PAGES WHICH DO NOT REPRODUCE LEGIBLY.

CATALOGED BY ASTIA
AS AD NO. _____

2698

269 846

Tunnel Diode Circuits at Microwave Frequencies

JOHN REINDEL

62-1-6
XEROX

ASTIA
RECEIVED
JAN 20 1962
TIPDB

SYLVANIA ELECTRONIC SYSTEMS
 Government Systems Management
 for **GENERAL TELEPHONE & ELECTRONICS**



**ELECTRONIC
 DEFENSE
 LABORATORIES**
 MOUNTAIN VIEW, CALIFORNIA



PREPARED FOR THE U.S. ARMY SIGNAL CORPS



ELECTRONIC DEFENSE LABORATORIES

P. O. Box 205

Mountain View, California

TECHNICAL MEMORANDUM

No. EDL-M397

15 August 1961

TUNNEL DIODE CIRCUITS AT MICROWAVE FREQUENCIES

John Reindel

Approved for publication F. E. Butterfield
Manager
Equipment Engineering Laboratory

R. E. Booth
Head
Tubes and Components Section

Prepared for the U.S. Army Signal Research and Development
Laboratory under Signal Corps Contract DA 36-039 SC-87475.

SYLVANIA ELECTRIC PRODUCTS INC.

ASTIA AVAILABILITY NOTICE

QUALIFIED REQUESTORS MAY OBTAIN COPIES OF
THIS REPORT FROM ASTIA.

ELECTRONIC DEFENSE LABORATORIES

P. O. Box 205

Mountain View, California

Addendum No. 1 to Technical Memorandum EDL-M397

ERRATA

The following changes should be made in the original publication. Each corrected page should be marked "Revised 19 December 1961" in the upper right-hand corner under "EDL-M397."

Page 8. Change Equation (4) to read:

$$f_0 = \frac{1}{2\pi} \sqrt{\frac{1}{L_s C_D} - \left(\frac{1}{R_D C_D}\right)^2} \quad (4)$$

Page 8. In the sixth line of the first paragraph of Section 3.3, change "germanimum" to "germanium".

Page 23. In the last line on the page, change " P_{ow} " to " P_{av} ".

Page 33. In the lower part of Figure 26, the words "BYPASS CAPACITOR" should be shown to refer to the 1/16- by 7/16-inch rectangular block just to the right of the shaded area.

Page 59. In Figure 46, change "(FIG 34)" to "(FIG 37)"; change "(FIG 35)" to "(FIG 38)"; change "(FIG 37 AND 40)" to "(FIG 40 AND 43)"; and change "2N2939" to "1N2939".

Page 66. In the upper left-hand part of Figure 50, change "IF INPUT" to "IF OUTPUT".

Page 67. In the first line of Section 4.4, change "in the instant report" to "in this report".

Page 5. In equations (1) and (2), change "C" to " C_D " (three places); and change "L" to " L_g " (four places).

Page 29. In the second line of the last paragraph on the page, change "2N2939" to "1N2939".

Page 30. In the upper left-hand corner of Figure 24, change "2N2939 DIODE" to "1N2939 DIODE".

Page 31. In the upper part of Figure 25, change "2N2939" to "1N2939".

Page 32. In the ninth line from the top of the page, change "2N2939" to "1N2939".

Page 35. In the upper part of Figure 28, change "2N2939" to "1N2939".

Page 46. In the upper part of Figure 37, change "2N2939" to "1N2939".

CONTENTS

Section	Title	Page
1.	ABSTRACT	1
2.	INTRODUCTION	1
3.	TUNNEL DIODE CHARACTERISTICS	1
3.1	Mechanism of Tunneling	1
3.2	Diode Circuit Parameters	2
3.3	Diode Construction	8
3.4	Measurement of Diode Parameters	9
3.5	Stability Criteria	13
3.6	Biasing Technique	14
4.	APPLICATIONS FOR THE TUNNEL DIODE	15
4.1	Oscillators	15
4.2	Amplifiers	23
4.2.1	Hybrid Technique	40
4.2.2	Circulator Technique	48
4.2.3	Broad-banding Techniques	48
4.2.4	Broad-band Stabilizing Network	52
4.2.5	Amplifier Noise Figure	55
4.3	Frequency Converters	60
4.4	Superregenerative Amplifier	67
5.	TEMPERATURE CHARACTERISTICS	71
6.	SUMMARY	71
7.	REFERENCES	73

ILLUSTRATIONS

Figure	Title	Page
1	Static Characteristic Curve of Sylvania D4115A Tunnel Diode	3
2	Small-Signal Equivalent Circuit	3
3	Junction Conductance	4
4	Modified Diode Equivalent Circuit	6
5	Equivalent Shunt Circuit	6
6	Variation of Junction Conductance with Bias at Various Frequencies	6
7	Terminal Negative Conductance	7
8	Terminal Capacitance	7
9	Sylvania D4115 Microwave Tunnel Diode Cartridge	10
10	Distributed Diode Configurations	10
11	Cylindrical Cavity for Measurement of Frequency of Oscillation	12
12	Graphic Illustration of Biasing Requirement	12
13	Bias Circuit for Stable DC Operation	16
14	Coaxial Bypass Capacitor with Low Series Inductance	17
15	Tracing Circuit	17
16	Tunnel Diode Test Mount	18
17	Tracing Circuit and Diode Test Mount	19

ILLUSTRATIONS -- Continued

Figure	Title	Page
18	Typical Characteristics of Some Commercially Available Microwave Tunnel Diodes	20
19	Single-Tuned Circuits	21
20	Experimental C-band Oscillator	24
21	Tunable Cavity in Waveguide	25
22	Single-Tuned Amplifier Circuits	26
23	Transducer Gain	28
24	Single-Tuned UHF Amplifier	30
25	Single-Tuned Stripline One-port Amplifier	31
26	Gain Measurement Technique for One-port Amplifier	33
27	One-port VHF Amplifier	34
28	Single-Tuned Stripline Two-port Amplifier	35
29	Amplifier Circuit and Cross-Sectional View	36
30	S-band Amplifier Gain	37
31	S-band One-port Amplifier.	38
32	Capacitive-Tuned Circuit	39
33	Schematic of Capacitive-Tuned S-band Amplifier	41
34	Capacitive-Tuned S-band Amplifier	42
35	Dynamic Range of Amplifier	43
36	Hybrid-Coupled Amplifier	44

ILLUSTRATIONS -- Continued

Figure	Title	Page
37	Hybrid-Coupled Amplifier Employing an Electromagnetic Quarter-Wave Coupler	46
38	Hybrid-Coupled Amplifier Using a 3-branch Coupler	47
39	Wye Circulator	49
40	Amplifier with Circulator	50
41	Wide-banding Filter Networks	51
42	Impedance of Wye Ferrite Circulator	53
43	Wide-banded S-band Amplifier	54
44	Block Diagram of Stabilizing Network	56
45	Stripline Configuration of Stabilizing Network	57
46	Measured Noise Figures	59
47	Conversion Conductance and Average Conductance at Three Bias Points	61
48	L-band Mixer Circuit Schematic and Component Layout	64
49	Stripline L-band Mixer	65
50	Miniature Tunnel Diode Down Converter	66
51	Miniature Solid-State Receiver	68
52	Capacitive-Tuned Down Converter	69
53	Superregenerative Amplifier	70
54	Temperature Characteristics of Sylvania D4115A Tunnel Diode	72

DEFINITION OF SYMBOLS

A_R	reflected gain (Equation 24).
A_T	transducer gain.
c	velocity of light.
C_b	barrier capacitance.
C_d	diffusion capacitance.
C_s	capsule capacitance.
C_D	shunt diode capacitance.
C_E	terminal capacitance.
e	electron charge.
f_q	quench frequency.
f_r	resistive cut-off frequency.
f_0	self-resonant frequency.
F	noise figure.
$F(\theta)$	stability parameter (Equation 12).
g_d	diffusion conductance.
g_t	tunnel conductance.
$g(t)$	time-varying conductance.
$-g_D$	shunt tunneling conductance.
g_0	average tunneling conductance.
g_1	conversion conductance.
GaAs	gallium arsenide .

DEFINITION OF SYMBOLS -- Continued

GaSb	gallium antimonide.
Ge	germanium.
G_E	negative terminal conductance.
G_{11}	transducer gain of 2-port amplifier at input port.
G_{41}	transducer gain of 2-port amplifier at output port.
I_p	peak tunneling current.
I_0	net dc diode current.
I_1	fundamental ac diode current.
k	Boltzmann's constant.
l	length of transmission line.
L_s	capsule inductance.
n	number of side-band frequencies.
P_o	output power.
r_{eff}	effective diode radius.
r_{in}	mixer input resistance.
r_{out}	mixer output resistance.
r_2	cavity outer radius.
R_s	bulk resistance.
R_1, R_0	bias resistors.
T	absolute temperature ($^{\circ}$ Kelvin).
Z_0	characteristic impedance of transmission line.

DEFINITION OF SYMBOLS -- Continued

α, β, γ	gain parameters (Equation 37).
ϵ_r	relative dielectric constant.
θ	diode constant (Equation 11).
ρ	reflection coefficient.

TUNNEL DIODE CIRCUITS AT MICROWAVE FREQUENCIES

John Reindel

1. ABSTRACT.

This report presents results of recent studies in tunnel diode microwave circuits at the Electronic Defense Laboratories. Descriptions are also offered of an S-band low-noise amplifier with a voltage gain bandwidth product of 6000 megacycles and of designs of mechanically tunable down-converters. The prime features of the tunnel diode, its small size and low dc power requirements, are taken advantage of in the circuit designs.

2. INTRODUCTION.

The tunnel diode is one of the newest semiconductor devices; it consists of a single abrupt p-n junction between two heavily doped regions. Its principal characteristic is a negative differential resistance over a small range of applied bias. The device, also known as the Esaki diode, has created widespread interest due to its potential use in microwave circuits, and its relatively small size and low dc power requirements. The frequency range of the device extends from dc into the gigacycle region. Numerous applications have been reported, the most promising of which are as oscillators, amplifiers, and converters. The object of this study is to

- (a) summarize and evaluate recent investigations of tunnel diodes and their circuits and
- (b) discuss experimental tunnel diode circuits recently fabricated at EDL.

3. TUNNEL DIODE CHARACTERISTICS.

3.1 Mechanism of Tunneling.

The diode is named for its principle of operation, called tunneling. The tunneling process is a quantum mechanical penetration of electrons of the p-n junction potential barrier.¹ Several papers describe the

3.1 -- Continued.

effect and formulate the characteristics of the junction from purely theoretical considerations;² although, for a number of reasons,³ these do not provide a quantitative description of the observed phenomenon. However, a qualitative description of the tunneling process is useful even to the casual reader and is contained in other papers written on this subject:^{4, 5, 6}

3.2 Diode Circuit Parameters.

A typical current-voltage curve of a tunnel diode is shown in Figure 1. A negative conductance region exists where the current falls from a high value at low forward voltage to a value somewhat above what would be representative of a normal p-n junction characteristic at a higher forward voltage. Figure 2 shows a small-signal equivalent circuit that describes the diode behavior from low frequencies up to and including microwave frequencies.⁷ The symbols represent the following semiconductor characteristics: Tunnel conductance, g_t ; diffusion conductance, g_d ; barrier capacitance, C_b ; diffusion capacitance, C_d ; capsule capacitance, C_s ; bulk resistance, R_s ; and capsule inductance, L_s .

The effect of the diffusion conductance and capacitance is masked by the much larger tunnel conductance and barrier capacitance. The tunnel conductance varies with bias; this is best shown (Figure 3) by plotting the differential of the curve in Figure 1. The diode is normally biased at the point of maximum negative conductance (or conversely the point of minimum negative resistance). The barrier capacitance increases with bias voltage however this increase is relatively small in the region of negative conductance.

In relatively large p-n junctions (junction diameter of several mils), the capacitance is large (10 picofarads and up), and the bulk resistance is small (5 ohms or less). As the junction diameter is reduced to 1 mil or less, the capacitance decreases to 1 or 2 picofarads or less and the bulk resistance increases to about 10 ohms or more. A figure of merit for the tunnel diode at microwave frequencies is the time constant C_b/g_t . Presently, it is less than $2 \cdot 10^{-11}$ second for the best germanium diodes. The time constant of the diode at the input terminals is modified by the other diode circuit parameters and is, therefore, frequency dependent and greater than C_b/g_t .

It is common practice to exclude the capsule capacitance, since it is negligible, and to include the diffusion parameters with the barrier

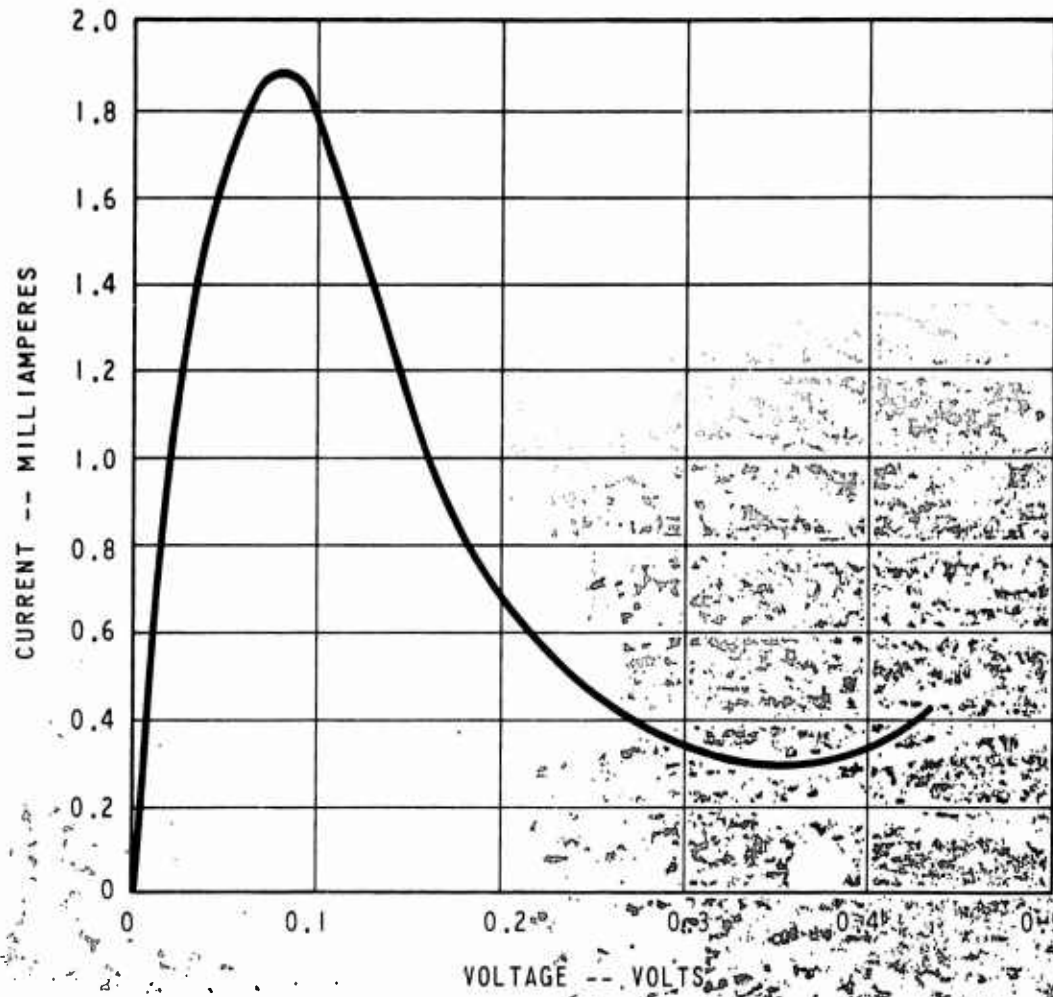


Figure 1
 Static Characteristic Curve of Sylvania
 D4115A Tunnel Diode

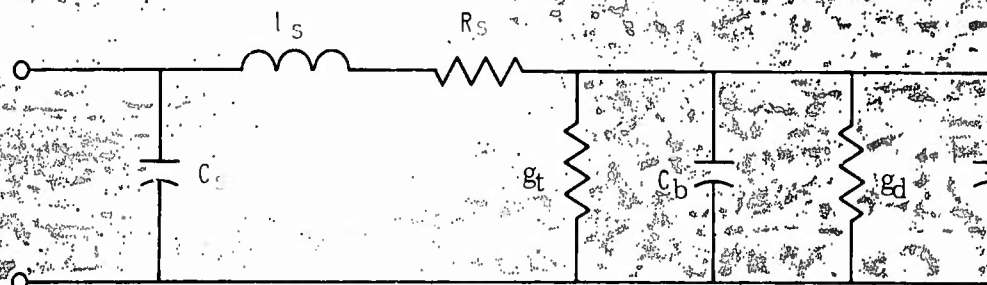


Figure 2
 Small-Signal Equivalent Circuit

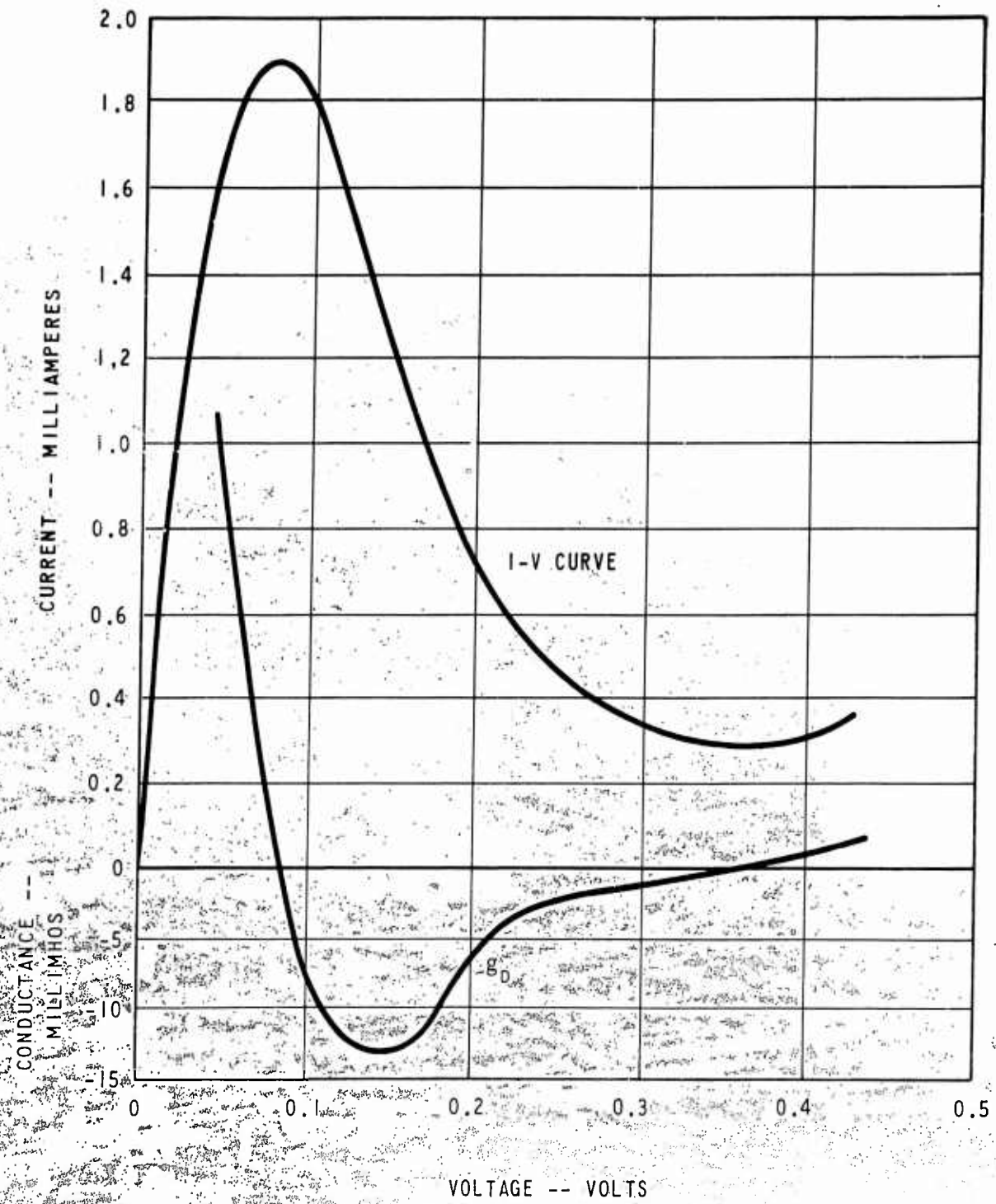


Figure 3
Junction Conductance

3.2 -- Continued.

capacitance and tunnel conductance. The diode equivalent circuit then takes the form shown in Figure 4,^{8,9} and consists of only the following four elements:

- L_s = series (lead inductance),
- R_s = series (bulk) resistance,
- C_D = shunt (barrier) capacitance,
- $-g_D$ = shunt (tunneling) conductance.

These elements are essentially frequency independent. An equivalent shunt circuit is found by circuit analysis, as shown in Figure 5. The negative terminal conductance, G_E , and the terminal capacitance, C_E , are frequency dependent.

$$G_E = g_D \frac{\left(1 + R_s g_D \left[1 + \left(\frac{\omega C}{g_D} \right)^2 \right] \right)}{\left(1 - \omega^2 LC + R_s g_D \right)^2 + (\omega g_D)^2 \left(1 + \frac{R_s C_D}{g_D} \right)^2} \quad (1)$$

$$C_E = C \frac{\left[1 - \frac{Lg_D}{C_D} - \omega^2 LC_D \right]}{\left(1 - \omega^2 LC_D + R_s g_D \right)^2 + (\omega g_D)^2 \left(1 + \frac{R_s C_D}{g_D} \right)^2} \quad (2)$$

Representative plots⁷ of G_E as a function of frequency are shown in Figure 6. The conductance can be plotted directly as a function of frequency^{10, 11} if the diode is assumed biased at the point of maximum negative conductance. The negative conductance of a typical tunnel diode (Figure 7) shows increasing values of series inductance. The terminal conductance is zero at the resistive cutoff frequency, f_r . From Equation 1, f_r can be shown to be:

$$f_r = \frac{1}{2\pi R_D C_D} \sqrt{\frac{R_D}{R_s} - 1} \quad (3)$$

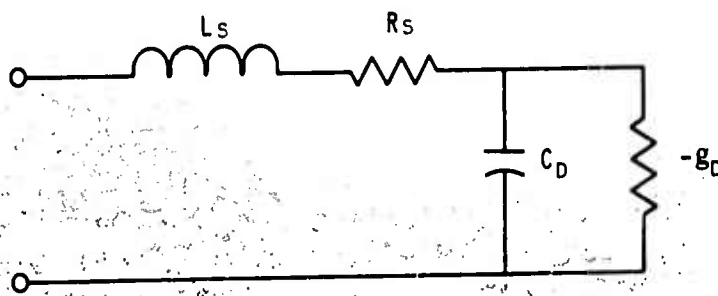


Figure 4
Modified Diode Equivalent Circuit

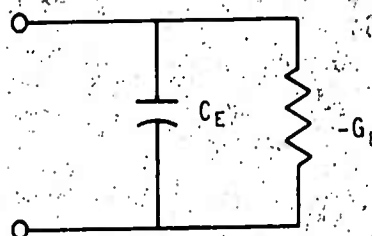


Figure 5
Equivalent Shunt Circuit

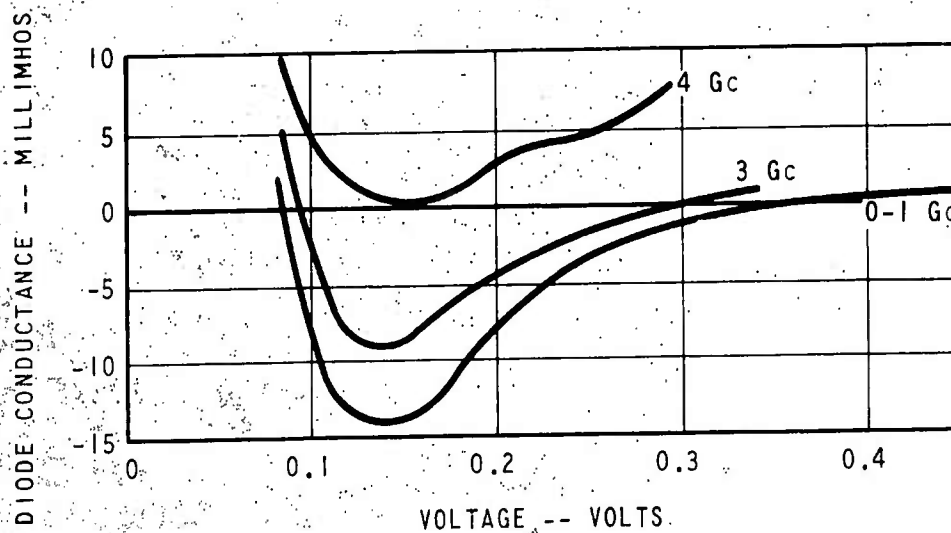


Figure 6
Variation of Junction Conductance with
Bias at Various Frequencies

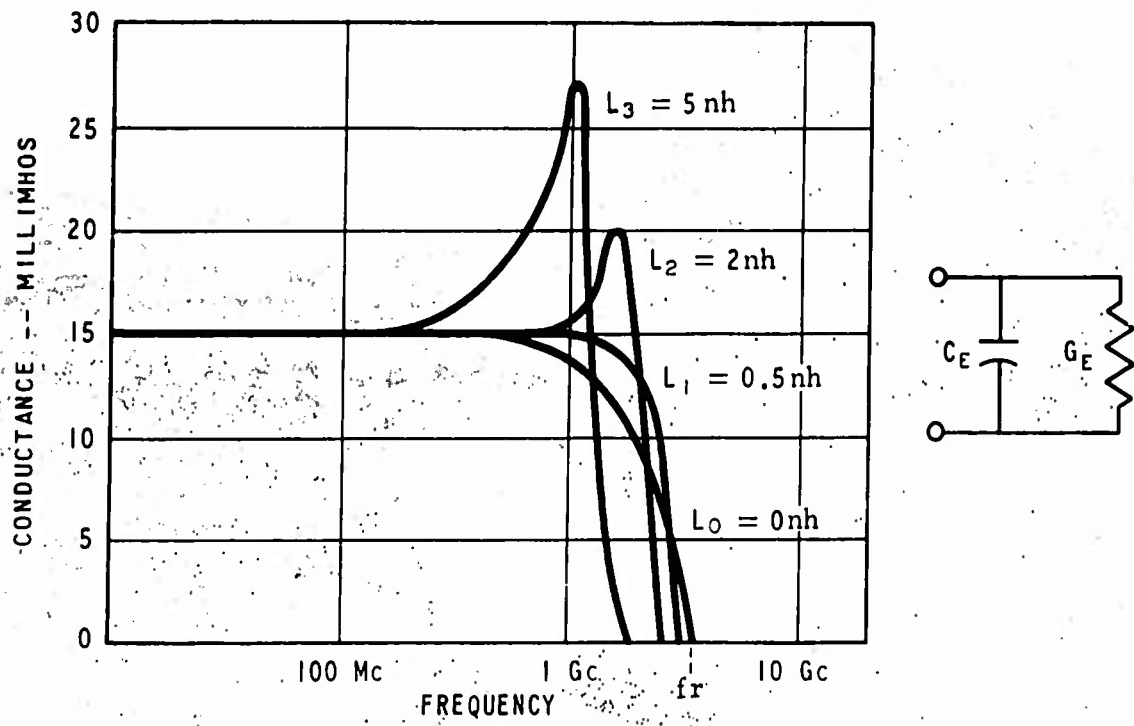


Figure 7
Terminal Negative Conductance

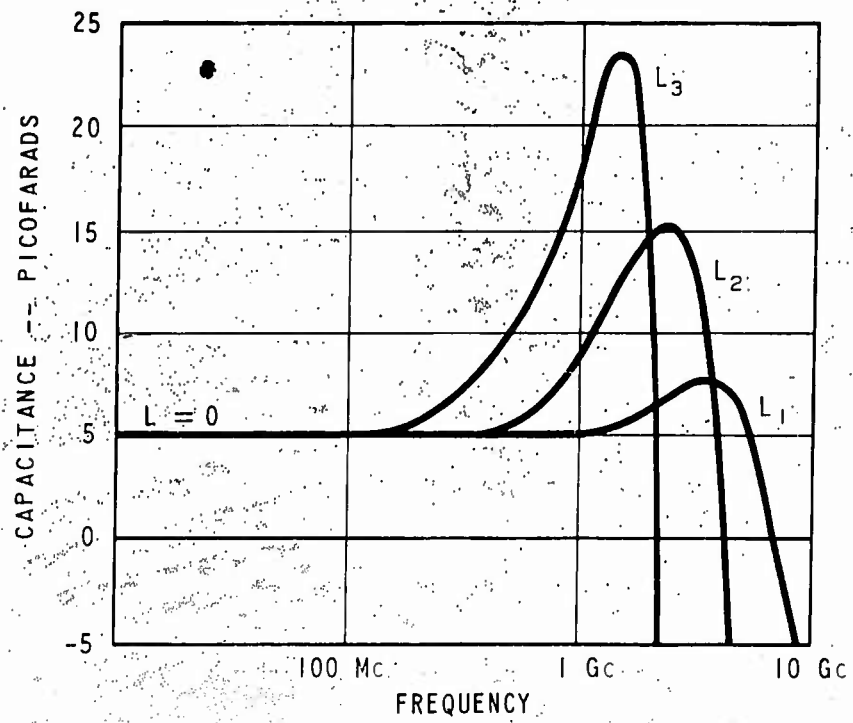


Figure 8
Terminal Capacitance

3.2 -- Continued.

where

$$R_D = 1/g_D.$$

It can be seen from Equation 3 that f_r is not a function of capsule inductance L_s . Figure 7 shows the intercept of the conductance curve (for $L = 0$) with the frequency axis as f_r . The curves also indicate that the conductance is nearly constant from dc to about 1/3 of f_r when the inductance is low (less than 0.5 nanohenry). If the diode capsule inductance or external lead inductance is increased (to 2 and 5 nanohenries), the conductance changes radically at a much lower frequency. At the inductive (or self) resonant frequency, f_0 , the inductance and capacitance will resonate if the device terminals were ac short circuited:

$$f_0 = \frac{1}{2\pi L_s C_D} \sqrt{1 - \frac{L_s}{R_D^2 C_D}} \quad (4)$$

The terminal capacitance varies with frequency^{10, 11} as shown in Figure 8; this variation is negligible at low frequencies, but is large near the cutoff frequencies. C_E is negative above f_0 , i. e., the terminal susceptance is inductive.

3.3 Diode Construction.

In contrast to many other semiconductor devices, the tunnel diode is made of very heavily doped materials. The space-charge layer separating the two semiconductor materials is extremely thin (less than 100 Å). Since propagation of waves through the layer takes place with the velocity of light, the high-frequency response is limited only by the junction capacitance. The capacitance of germanium (Ge) diodes is given approximately as 8 picofarads per square mil of junction diameter. A typical high-frequency Ge diode may have a junction diameter of 0.0005 inch and a capacitance of 2 picofarads.

The most commonly used semiconductor materials are Ge, gallium arsenide (GaAs) and gallium antimonide (GaSb). Other useful materials have been reported but are not presently used in commercially available tunnel diodes. GaAs diodes have a higher voltage and current swing in the negative conductance region and therefore a higher power capability. GaAs junctions also offer lower capacitance per unit area and can be used at higher frequencies; however, GaAs diodes have not been as dependable as the Ge and GaSb diodes. The GaAs diodes have

3.3 -- Continued.

a peak current degradation phenomenon that so far has not been completely solved. In addition, the GaAs diodes inherently have a higher noise figure than either the Ge or GaSb diodes. GaSb diodes with an especially low noise figure have been introduced.

Tunnel-diode circuit devices can be operated over an appreciable frequency range only if the negative terminal conductance is nearly constant. The curves in Figure 7 indicate that the diode series inductance must be made as small as possible. Wire stems about 1/8-inch long connecting to a semiconductor junction have an inductance of roughly 5 nanohenries and are therefore useless for applications at frequencies above 500 megacycles. Even the standard microwave crystal cartridge has higher inductance than can be tolerated at frequencies in the L-band and higher. Figure 9 shows a diode cartridge with an estimated inductance of 0.25 nanohenry; this cartridge has been used for diodes having capacitance as low as 0.7 picofarad and an f_0 greater than 12 gigacycles.

Since the junction area determines the diode current (as well as the capacitance), and therefore the available power output, the high-frequency diodes have very low power capability (estimated power at 10.8 gigacycles for a diode having a capacitance of 0.8 picofarad is 2 microwatts¹²). In addition to the single-spot diode, other geometries have been suggested¹³ as a means to obtain greater power capacity at high frequencies. Of the suggested geometries, the most likely to be used is the narrow-line distributed diode either in straight or in circular form (Figure 10). In addition to the problems of forming such a junction, there will be moding problems, i. e., the problem of suppressing unwanted spurious oscillations. Although a solution of these problems has been suggested,¹³ no distributed diode circuit has yet been built and tested.

3.4 Measurement of Diode Parameters.

Measurement of equivalent circuit parameters is of importance for control of diode fabrication as well as for application in practical circuits, as commercially available diodes often have wide limits of parameter specifications. For example, the G. E. tunnel diode Type 1N3219 reportedly has a median capacitance of 7 picofarads, and limits of 1.5 picofarads minimum and 10 picofarads maximum. The negative conductance reportedly is between 10 and 25 millimhos.

The series elements are readily determined for the four parameters

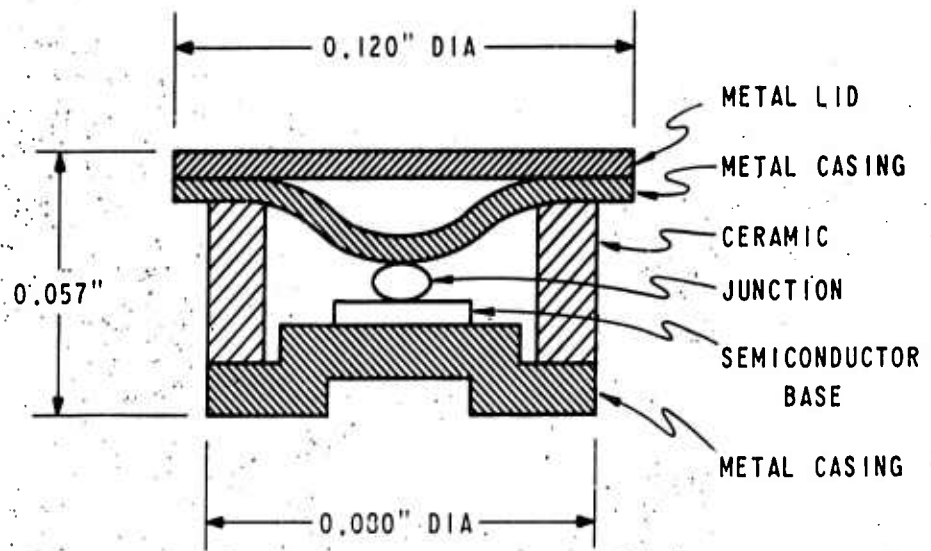


Figure 9

Sylvania D4115 Microwave Tunnel Diode Cartridge

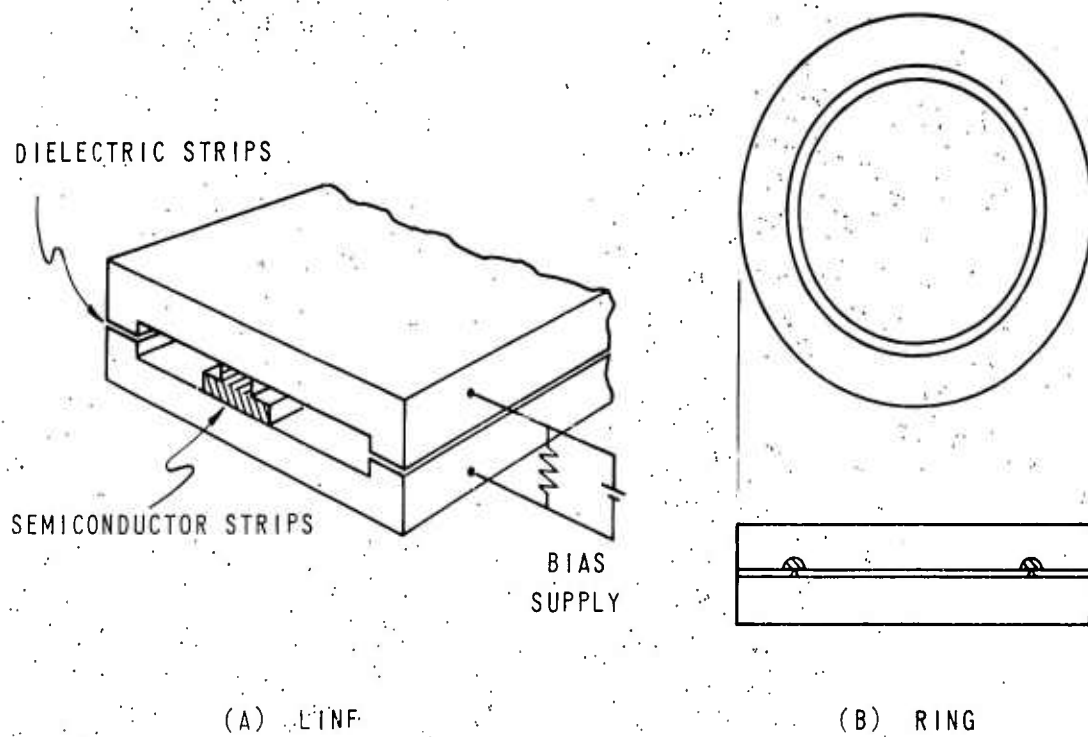


Figure 10

Distributed Diode Configurations

3.4 -- Continued.

shown in Figure 4. The series inductance of microwave capsulated diodes (similar to the diode shown in Figure 9) is determined almost entirely by the physical size of the capsule. A rough estimate of the inductance may be made by bridge measurements of a short-circuited capsule. Studies have shown that the series inductance can be found by measurements of frequencies of oscillation when the diode is placed in several different circular cylindrical cavities having various outer radii.¹⁴ The inductance of a cavity, as shown in Figure 11, is given by:

$$L = 4.60 h \mu_r \log \frac{r_2}{r_{\text{eff}}} \text{ nanohenries} \quad (5)$$

where

h is cavity height (cm)

r_2 is outer radius of cavity

μ_r is permittivity of cavity

r_{eff} is effective diode radius as defined by the equation

$$\frac{1}{f^2} = K \log \frac{r_2}{r_{\text{eff}}} \quad (6)$$

where

K is a constant.

When $\frac{1}{Kf^2}$ is plotted versus r_2 on a semilogarithmic scale, the curve (a straight line) intersects the abscissa at a value given by $r_{\text{eff}} = r_2$, since

$$\frac{1}{f^2} = K \log \frac{r_2}{r_{\text{eff}}} = 0 \quad \text{for } r_2 = r_{\text{eff}} \quad (7)$$

The experimental data¹⁴ indicate that r_{eff} equals 0.015 inch for the diode shown in Figure 10 and that the minimum inductance of the diode is approximately 0.24 nanohenry. The diode inductance varies little among diodes.

The series resistance, R_s , is most easily measured by the back-bias

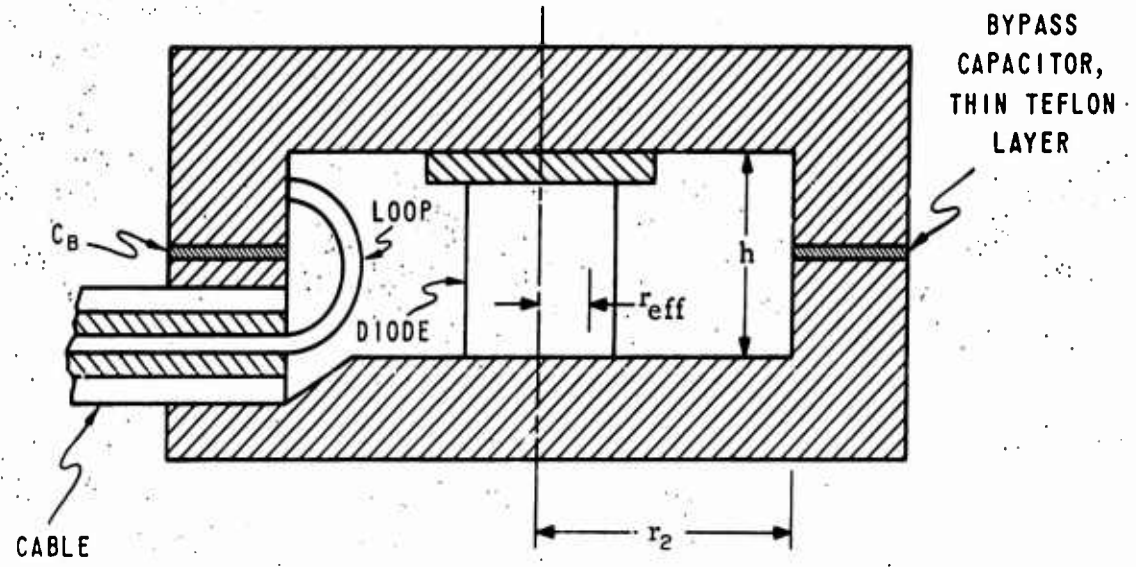
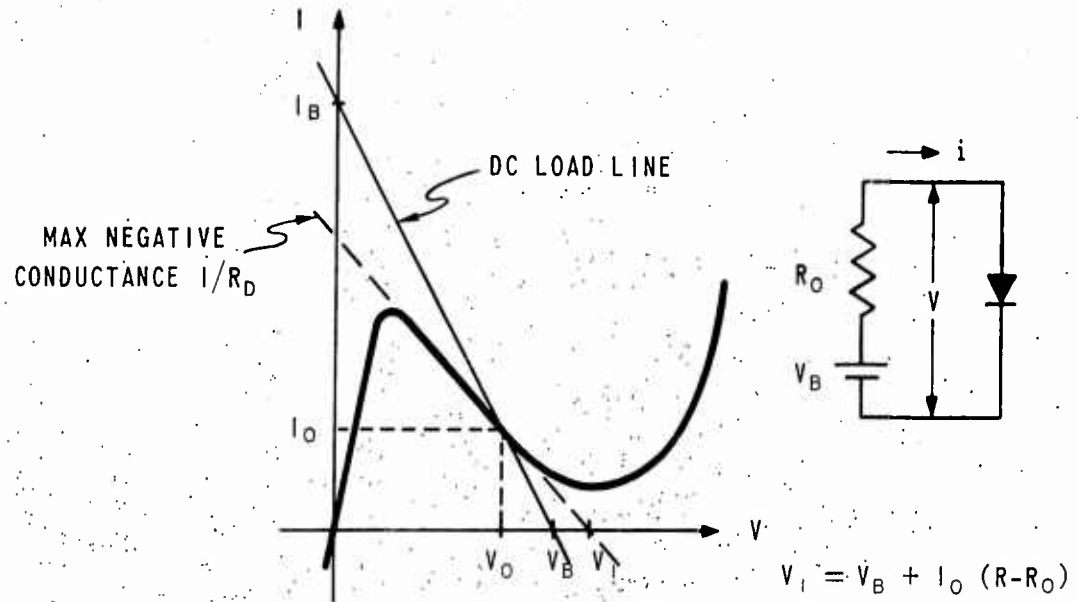


Figure 11

Cylindrical Cavity for Measurement of Frequency of Oscillation



$$R_0 = \frac{V_B}{I_B} < R_D + R_S$$

Figure 12

Graphic Illustration of Biasing Requirement

3.4 -- Continued.

measurement technique. The actual resistance measured with the diode back-biased is the series combination of the back resistance and R_s . However, the back resistance for large bias is very small and can be neglected.

The negative conductance g_D is theoretically frequency-independent. At dc and low frequencies, Equation 1 reduces to

$$G_E = \frac{g_D}{1 + R_s g_D} \quad (8)$$

and

$$R_E = R_s + R_D \quad (9)$$

R_E can therefore be measured graphically from a static current-voltage (I-V) characteristic curve^{2, 3, 15, 16} or with a bridge circuit operated at frequencies well below the cut-off frequencies.^{17, 18}

The diode capacitance, C_D , can similarly be found by bridge measurements of the terminal capacitance, C_E . At low frequencies,

$$C_E = C_D \left(1 - \frac{L}{C_D R^2} \right), \quad \text{when } R_D \gg R_s \quad (10)$$

C_E can also be calculated by measurements of the frequency of oscillation when the cavity inductance is known with sufficient accuracy.

3.5 Stability Criteria.

Certain stability criteria must be met in measurements of the I-V curve, in bridge measurements as well as in practical applications of a diode. If a diode is terminated in a load resistance, R_L , then conditions sufficient for stability^{8, 13} are as follows:

$$\frac{L_s g_D}{C} < R_T < \frac{1}{g_D}, \quad \text{Condition A}$$

where R_T is the sum of R_s and R_L . If a diode is short circuited

3.5 -- Continued.

($R_L = 0$), we have for requirements:

$$\frac{R_s}{R_D} < 1 \quad \text{Condition B}$$

and

$$\sqrt{\frac{L_s}{C}} < R_D \quad \text{Condition C}$$

A new theorem on the stability of tunnel diodes¹⁹ states that Conditions B and C are sufficient but not necessary, because C can be replaced by the somewhat milder requirement

$$\frac{L}{R_D^2 C} < F(\theta) \quad \text{Condition D}$$

where

$$\theta = \frac{1}{2\pi f_r RC} \quad (11)$$

and

$$F(\theta) = \frac{\theta^3}{(1 + \theta^2)(\theta - \arctan \theta)} \quad (12)$$

where f_r is defined by Equation 3. $F(\theta)$ varies in value from 3 to 1 as R_s/R_D takes on values from zero to 1. A rigorous proof²⁰ exists for the case of $R_s/R_D = 0$.

Condition B is satisfied by all commercially available diodes, but Condition D is not always satisfied, although stability can always be obtained by adding a small positive (loading) resistance in series with the diode.

3.6 Biasing Techniques.

A stable dc operating point in the negative-resistance region³ requires that the source resistance be less than the magnitude of the minimum negative resistance. The dc load line then intersects the I-V curve in only one place, as shown in Figure 12. The bias voltage usually is of the order of a few tenths of a volt which can conveniently be obtained

3.6 -- Continued.

with a circuit where $R_0 < R_D + R_S$ (Figure 13). This circuit also reduces the external inductance of the voltage supply, V_B , by a factor of approximately $(R_1/R_0)^2$.

The high-frequency stability may easily be adversely affected by the parasitic elements of the biasing circuit. An external series inductance will, as shown by Condition A, seriously affect the stability criteria, if the size of the inductance is comparable to the inductance of the diode cartridge. Figure 13 shows how the ac path is completely separated from the biasing circuit by the large bypass capacitor, C_B .

The bypass capacitor must be specially designed for use at ultrahigh frequencies. Figures 11 and 14 show the construction of some useful bypass capacitors in which the series inductance of the capacitors is much smaller than the diode inductance. Figure 15 depicts a widely-used curve-tracing circuit; Figure 16 illustrates a low-inductance diode mount used for a tracing circuit; and Figure 17 is a photo of the mount and curve tracer.

Figure 18 presents data characteristics of some available microwave tunnel diodes.

4. APPLICATIONS FOR THE TUNNEL DIODE.

The negative resistance of the tunnel diode can be put to use in a variety of circuits with many useful properties. Two major types of operation are possible: (a) small-signal operation around a bias point in the negative-resistance region, and (b) large-signal switching. Only the small-signal operation at microwave frequencies will be considered here. Three types of circuits will be analyzed and described in detail; in these, the negative resistance provides oscillation, amplification, and conversion. Other circuits will be mentioned briefly.

4.1 Oscillators.

The terminal reactance can be resonated either in series or in shunt with the load,³ (Figure 19, A and B). The maximum frequency of oscillation for both circuits is the resistive cut-off frequency, f_r , as given by Equation 3; however, this can only be reached when the load resistance, R_L , equals zero.

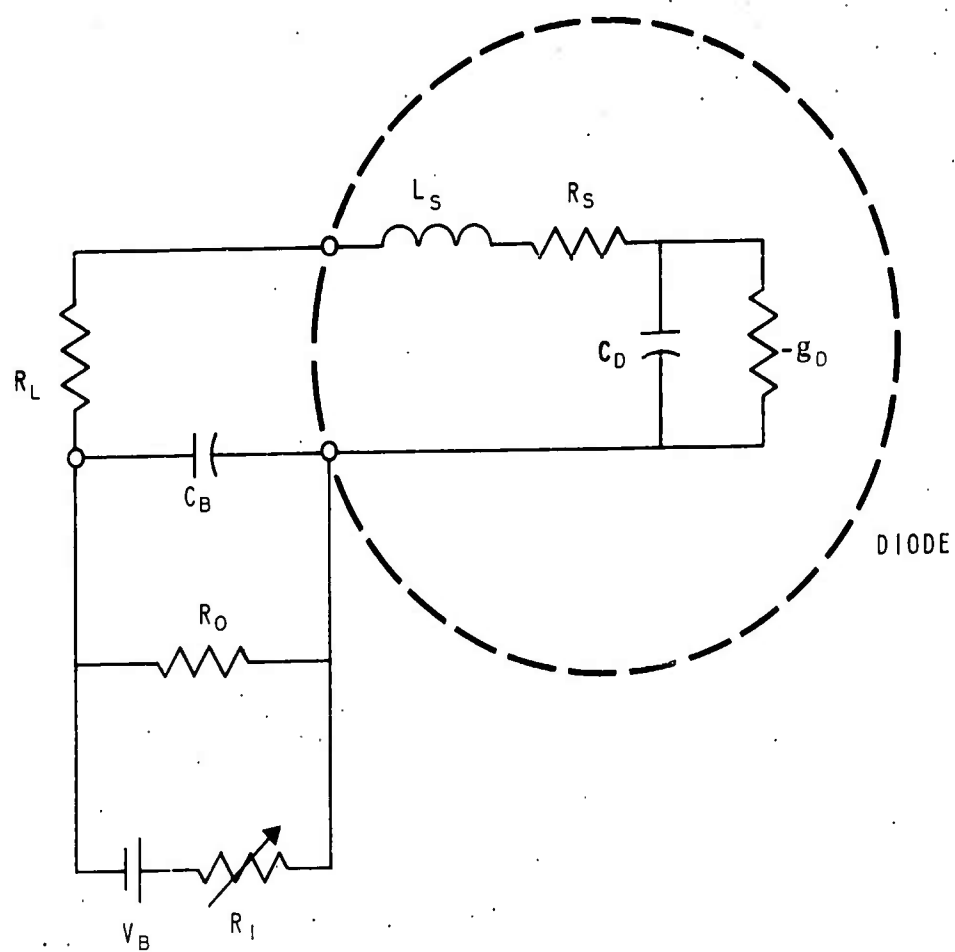


Figure 13
Bias Circuit for Stable DC Operation

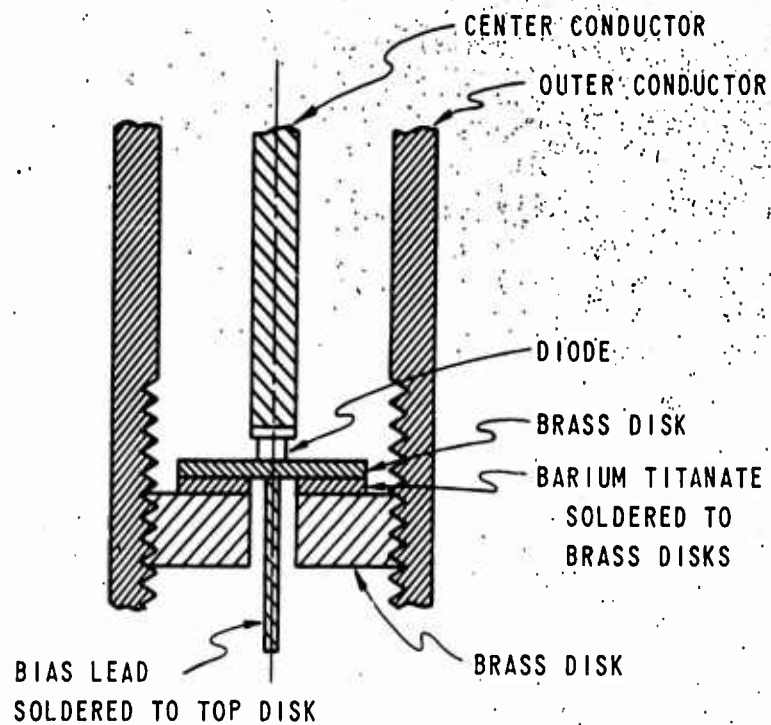


Figure 14
 Coaxial Bypass Capacitor with
 Low Series Inductance

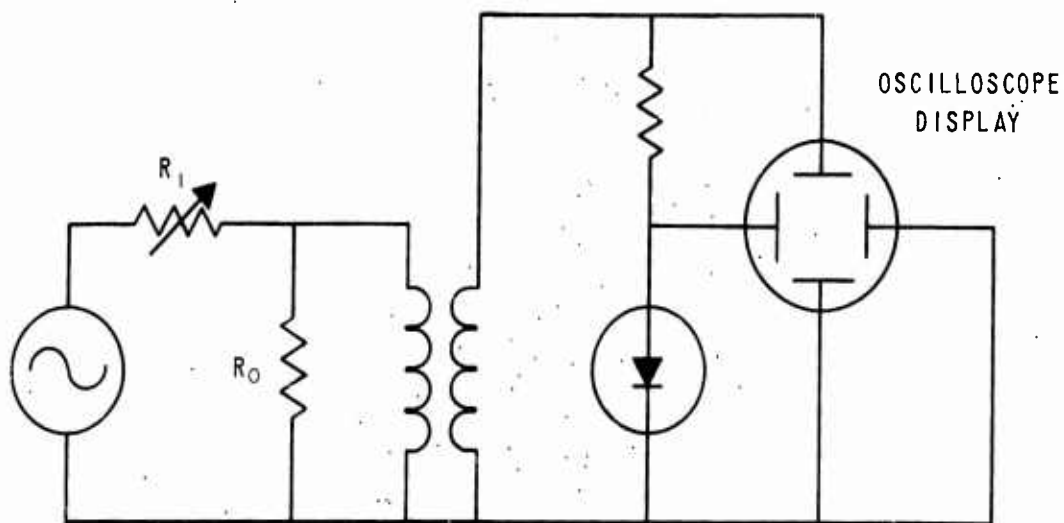


Figure 15
 Tracing Circuit

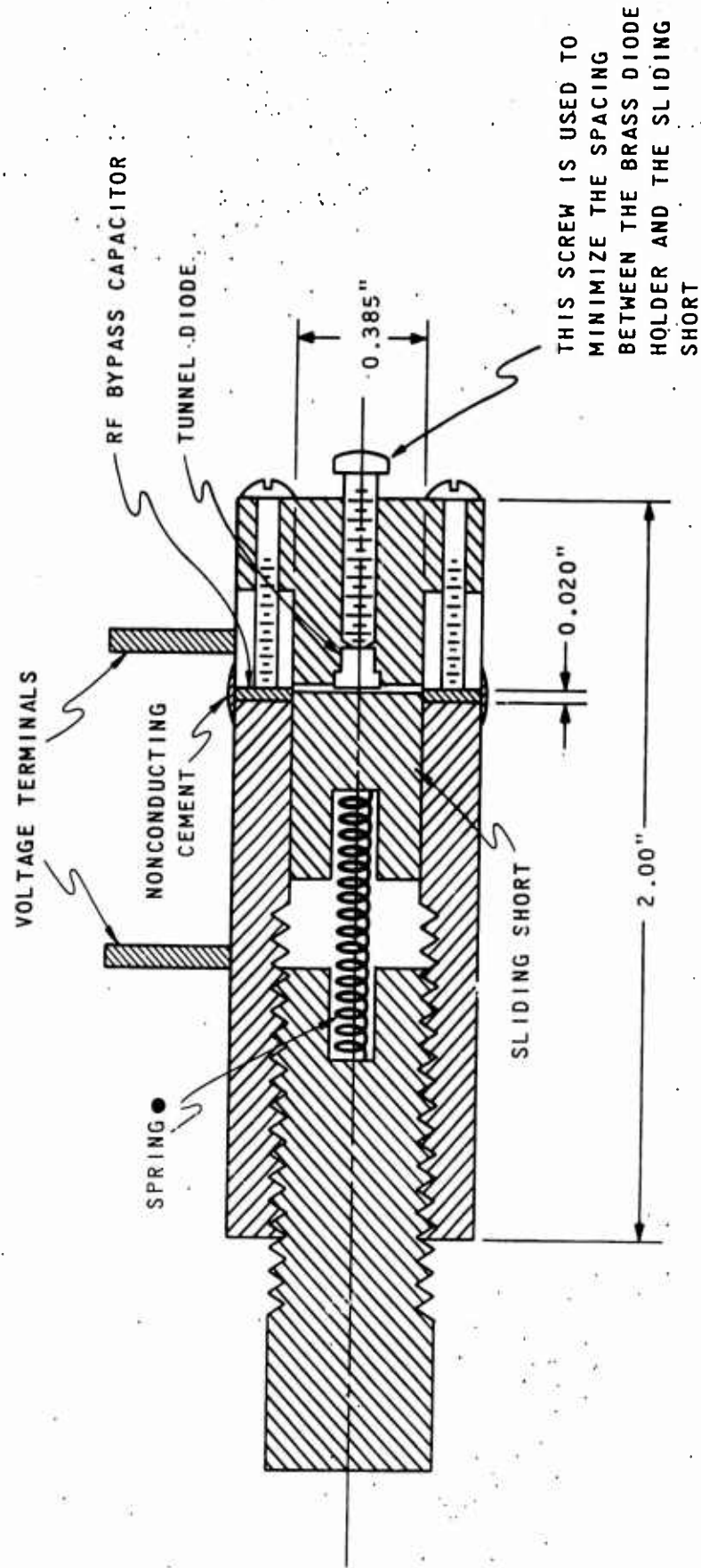


Figure 16
Tunnel Diode Test Mount

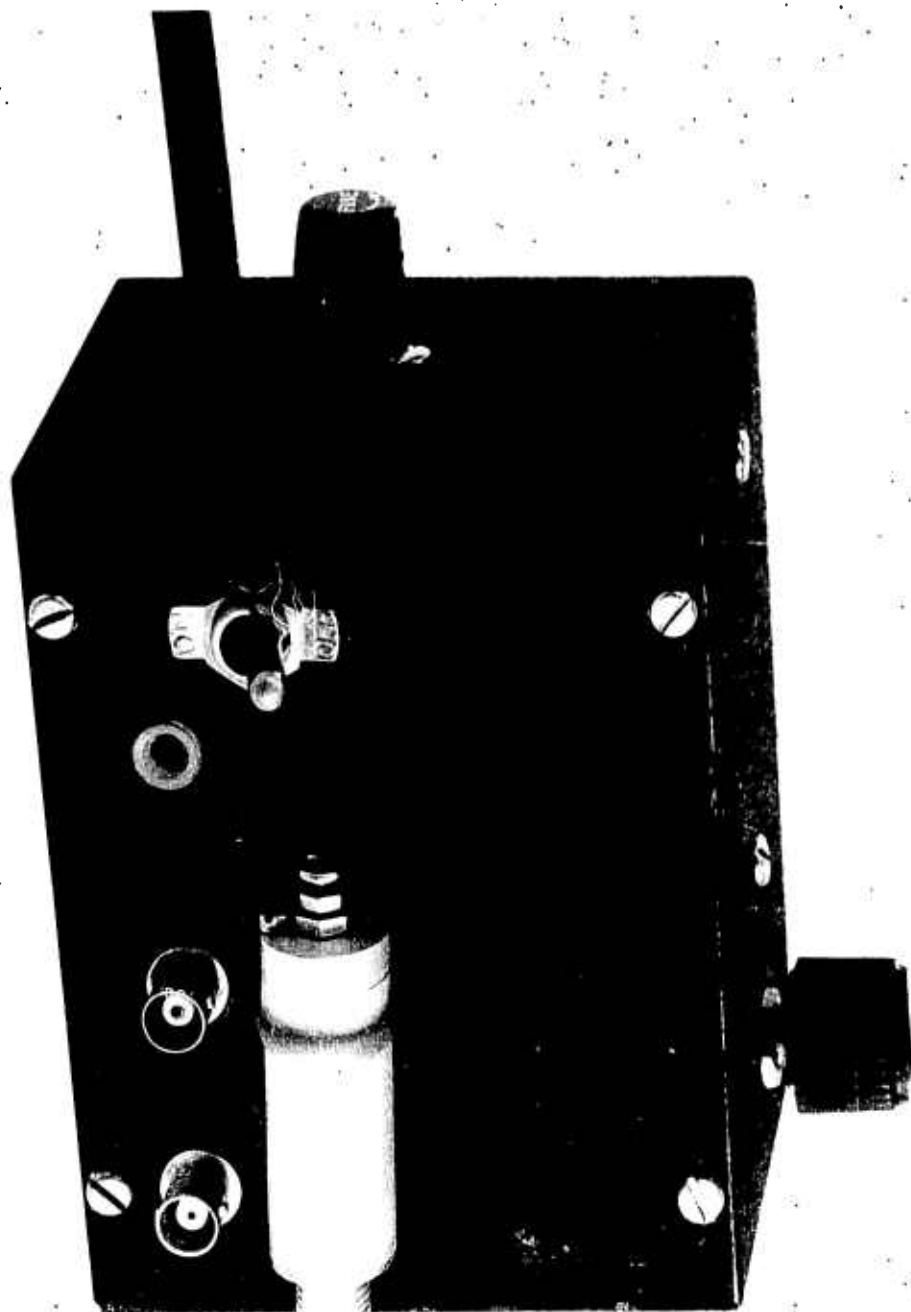
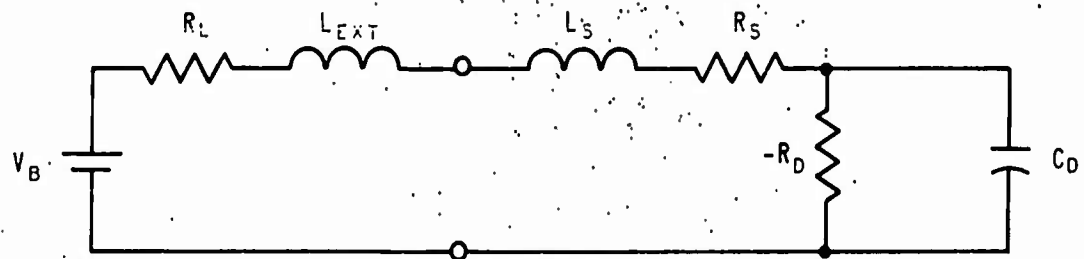


Figure 17
Tracing Circuit and Diode Test Mount

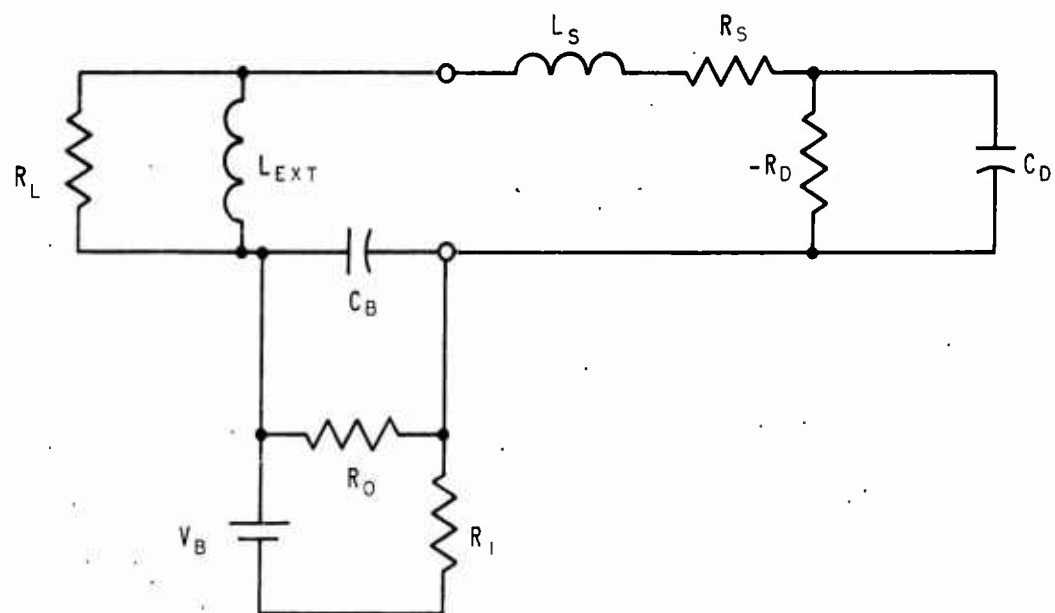
TYPE	L_s nh	R_s ohms	C_D pf	g_D mmho	f_R Gc	I_p
G. E. 1N2939	6	1.5	5	6.6	2.2	1.0
1N2941	6	0.5	25	30	1.6	4.7
1N2969	6	1.0	8	16	2.5	2.2
Sony 1T 1103	0.3	2.0	5	20		1.8
RCA TD 104	0.4	0.4	60	30		50
Sylvania D4115	0.4	1.0	8	18	>2	1.8
D4115A	0.4	2	6	20	>3	1.7
D4115B	0.4	3	4	20	>4	1.6
D4168D	0.3	5	2	25	>10	2.0
Microstate M 5225	0.3	2	2.5	25	>5.5	3.5
M 233	0.3	3	4	18	>3	1.0
M 234	0.3	3	5	50	>4	3.0

Figure 18

Typical Characteristics of Some Commercially Available Microwave Tunnel Diodes



(A) SERIES RESONANT CIRCUIT



(B) SHUNT RESONANT CIRCUIT

Figure 19
Single-Tuned Circuits

4.1 -- Continued.

The series circuit in Figure 19 A shows the diode resonated with an external inductor. The steady-state frequency of oscillation of the series circuit is given by

$$\omega = \left[\frac{1}{LC_D} - \frac{1}{(R_D C_D)^2} \right]^{\frac{1}{2}} \quad (13)$$

where L is the sum of the internal and external series inductance ($L = L_s + L_{ext}$). The requirements for steady-state oscillation³ are

$$R_D > R_s + R_L \quad \text{Condition E}$$

and

$$L/C_D = (R_s + R_L) R_D \quad \text{Condition F}$$

R_D and C_D in Equation 13 and Conditions E and F are effective steady-state values that may differ from the small-signal values because the diode characteristics are nonlinear. At frequencies from dc to f_0 , the terminal susceptance is capacitive (C_E is positive) and the diode is resonated with an external inductor, as shown in Figure 19. Oscillation above the self-resonant frequency is theoretically possible if the external circuit presents a capacitive reactance and if the resistive cut-off frequency is higher than the self-resonant frequency.

Assuming $L_{ext} \gg L_s$, the frequency of oscillation of the shunt circuit of Figure 19 B is given by

$$\omega = \left[\left(\frac{1}{L_{ext} C_D} \right) \left(\frac{1 - R_s/R_D}{1 + R_s/R_L} \right) \right]^{\frac{1}{2}} \quad (14)$$

The requirement for stable oscillation is that $R_L > R_D$. Assuming that $R_s \ll R_D$, the available power output is given by

$$P = \frac{V^2}{8R_D} \left(1 - \frac{f^2}{f_R^2} \right) \quad (15)$$

where V is the linear rms voltage swing.²¹ Equation 15 shows how the

4.1 -- Continued.

power output drops to zero at the resistive cut-off frequency f_r ; the power is down 3 db at $1/\sqrt{2}$ times the cut-off frequency. The voltage swing, V , depends mainly on the semiconductor material. Experimental data²² gives $V = 0.1$ volt for Ge, and $V = 0.15$ volt for GaAs. R_D is related to the current swing, I , and the junction capacitance, C_D . The negative resistance is typically from 30 to 60 ohms, but may be as high as 150 ohms or as low as a few ohms. Power output at a given frequency is maximized with a given ratio I/C ; however, this ratio may vary from about 0.6 to 6 for Ge diodes^P for frequencies ranging from 1 to 10 gigacycles.

A schematic of an experimental C-band oscillator built at EDL is shown in Figure 20. The shunt (cavity) inductance is continuously variable from 0.3 to 1.2 nanohenries. When using a diode with a capacity of 2 picofarads, the oscillator was tunable from 3.5 to 6.1 gigacycles. Available power was measured as -25 dbm at 6 gigacycles. Power was coupled out by a loop into a coaxial cable. The cavity could also be built into a waveguide as illustrated in Figure 21. The standard waveguide height is stepped down to present the proper load at the diode cavity. Bias is provided through the piston. The thin epoxy film on the piston prevents dc currents through the moving parts and it provides a good RF bypass capacitance.

Calculations have indicated that the optimum available power of Ge and GaAs diodes varies from 3.7 milliwatts at 1 gigacycle to 0.1 milliwatt at 10 gigacycles.²³ Other measurements taken by Burrus gave the output power of GaAs diodes as 50 microwatts at 17 gigacycles, 25 microwatts at 40 gigacycles, and 2 microwatts at 90 gigacycles.²⁴ These figures reveal that the tunnel diode oscillator is a very-low-power generator at microwave frequencies. The tunnel diode can therefore be expected to be of better use in such devices as preamplifiers and down-converters, where the signal power need not exceed a few microwatts.

4.2 Amplifiers.

The single series- and shunt-tuned circuits in Figure 19, A and B, can also be used for amplification, provided the stability requirements of Condition A are met. The generator and load resistance may be separated as shown in Figure 22, A and B. The transducer gain, A_T , is defined as the ratio of power from the amplifier delivered into the load, P_o , and the available power from the generator, P_{ow} . Assuming

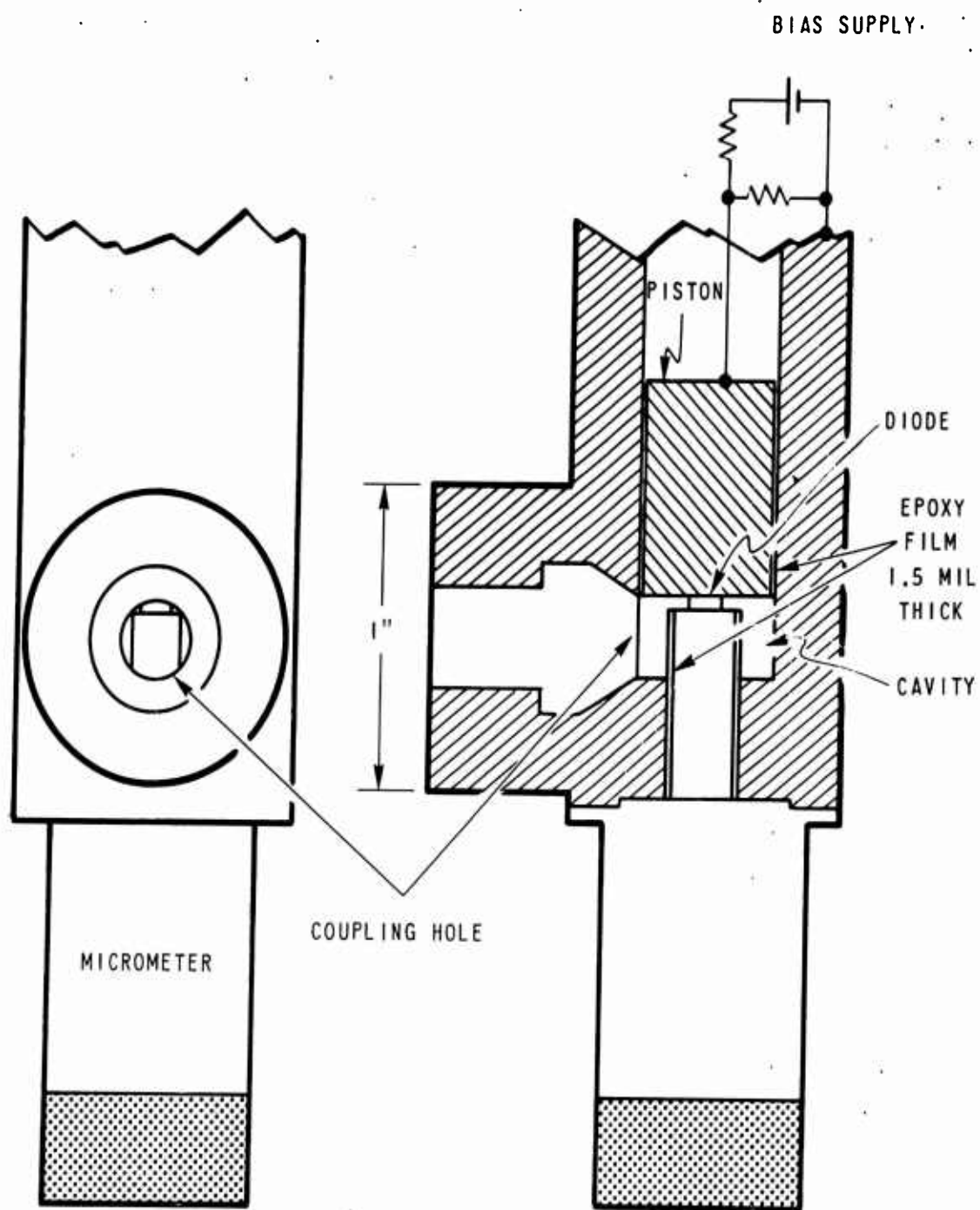


Figure 20
Experimental C-band Oscillator

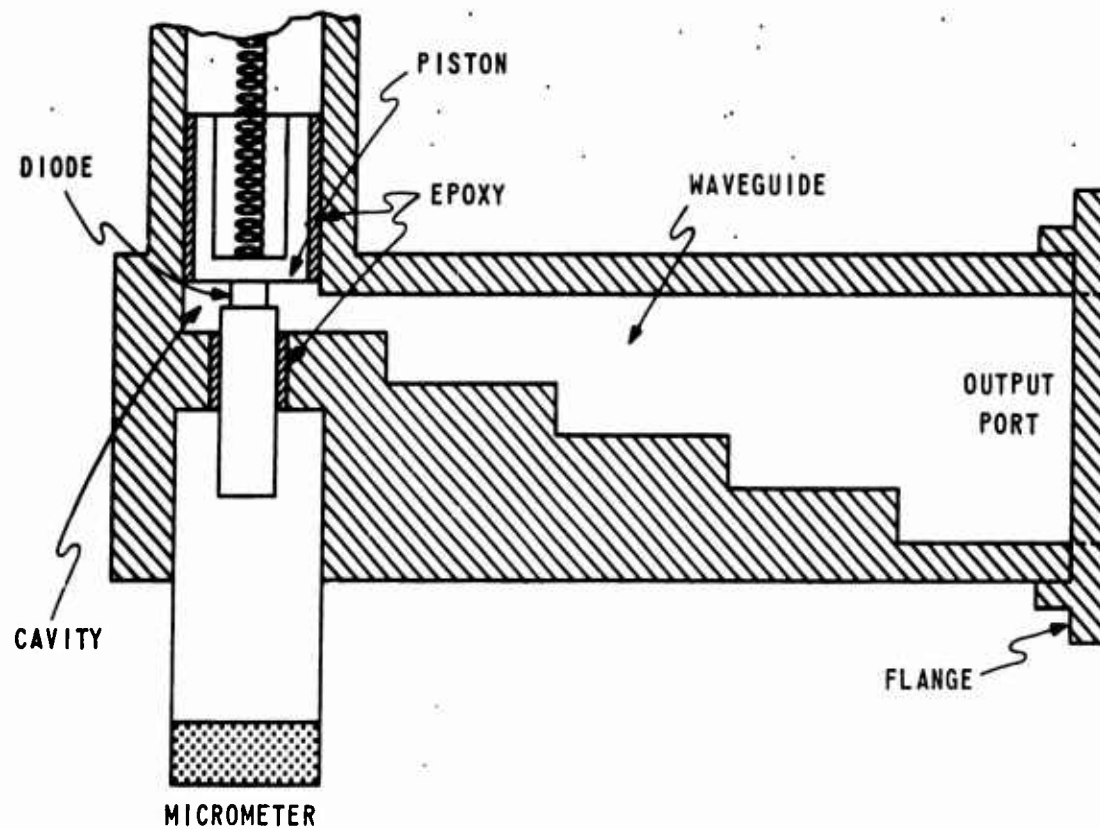
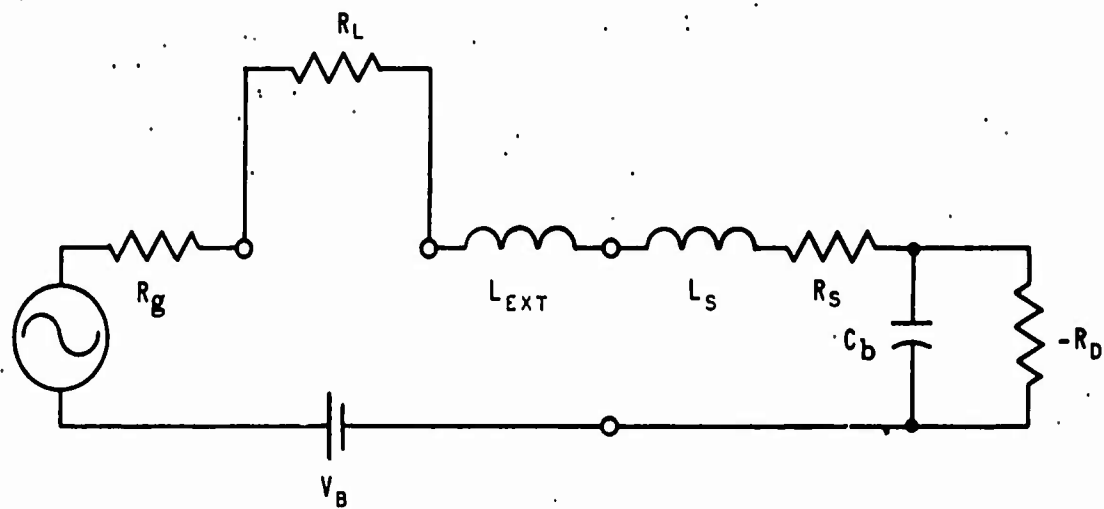
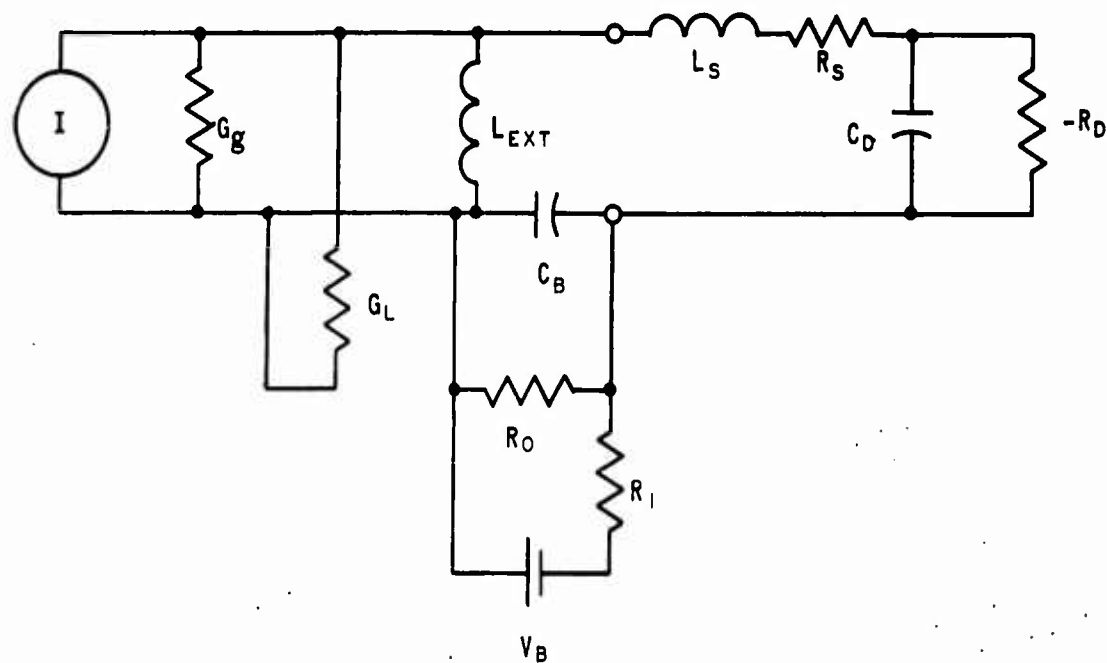


Figure 21
Tunable Cavity in Waveguide



(A) SERIES RESONATED AMPLIFIER



(B) PARALLEL RESONATED AMPLIFIER

Figure 22
Single-Tuned Amplifier Circuits

4.2 -- Continued.

$R_s \ll R_D$, the transducer gain, A_{Ts} , at circuit resonance is given by

$$A_{Ts} = \frac{P_o}{P_{av}} = \frac{4 R_g R_L}{(R_g + R_L - R_D)^2} \quad (16)$$

and

$$A_{Tp} = \frac{P_o}{P_{av}} = \frac{4 G_g G_L}{(G_g + G_L - G_D)^2} \quad (17)$$

where the second subscripts s and p refer to the circuit configuration, s for series and p for parallel.⁸ The reflected gain, A_R , is defined as the ratio of power from the amplifier delivered back into the generator resistance, P_g , and the available power from the generator, P_{av} . At resonance, A_R is given by:

$$A_{Rs} = \frac{P_g}{P_{av}} = \frac{4 (R_L - R_D)^2}{(R_g + R_L - R_D)^2} \quad (18)$$

and

$$A_{Rp} = \frac{P_g}{P_{av}} = \frac{4 (G_L - G_D)^2}{(G_g + G_L - G_D)^2} \quad (19)$$

The transducer gain can be made much larger than the reflected gain by making $(R_L - R_D)$ or $(G_L - G_D)$ small.

If $R_L = R_G = R/2$ and $G_L = G_G = G/2$, Equations 16 and 17 reduce to

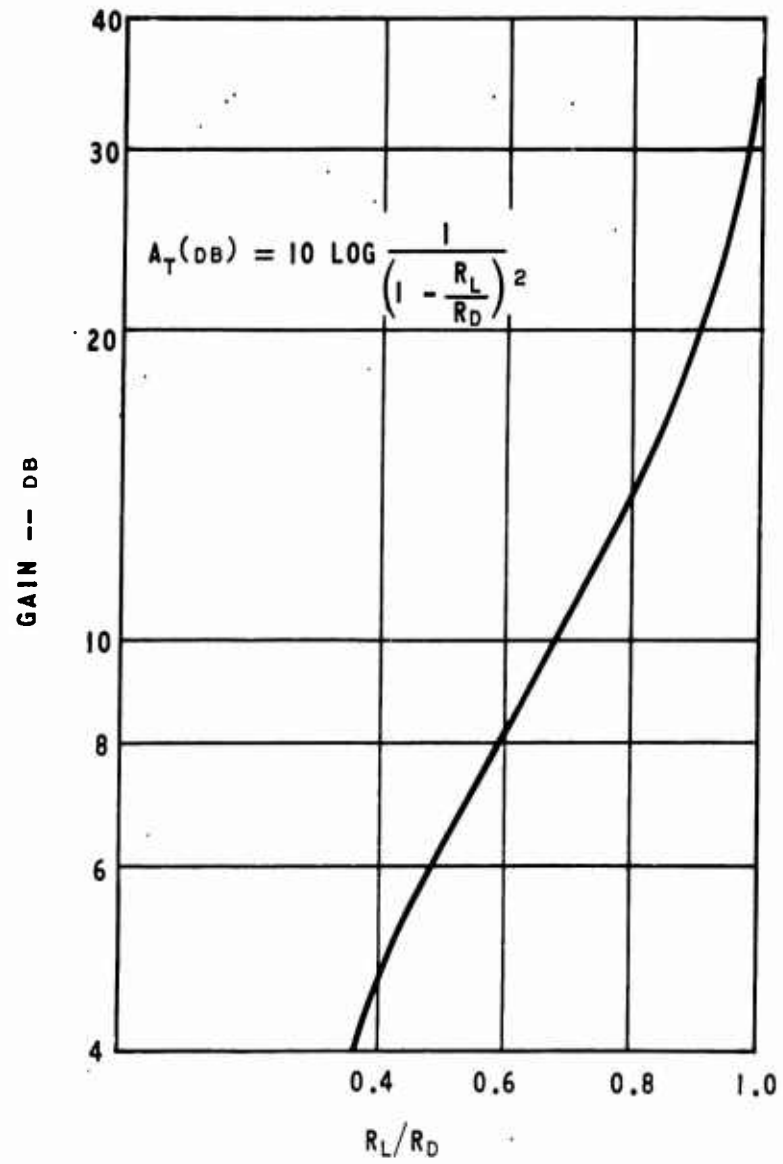
$$A_{Ts} = \frac{1}{\left(1 - \frac{R_D}{R}\right)^2} \quad (20)$$

and

$$A_{Tp} = \frac{1}{\left(1 - \frac{G_D}{G}\right)^2} \quad (21)$$

Equation 21 is plotted in Figure 23. Transducer gain of the single-tuned amplifier varies with frequency by

TRANSDUCER GAIN



EDL-U77

Figure 23
Transducer Gain

4.2. -- Continued:

$$A_{Tp} = \frac{1}{\left(1 - \frac{G_D}{G}\right)^2 + \left(\frac{C_D}{G}\right)^2 \cdot (4\pi f')^2} \quad (22)$$

where f' is the frequency deviation.

Single-tuned amplifiers have an optimum voltage gain-bandwidth product, $\sqrt{A_T} \cdot B$, given by:

$$\sqrt{A_T} \cdot B = \frac{1}{2\pi R_D C_D} \quad (23)$$

where B is the bandwidth in cycles per second.³

NOTE: When reference is made to a gain-bandwidth product, it is always to the voltage gain-bandwidth product and when reference is made to gain it is always to power gain.

A typical diode (Sylvania D4168) with a capacitance of 2 picofarads and a negative resistance of 56 ohms will give an optimum gain-bandwidth product of about 2 gigacycles, i. e., if the load resistance is 50 ohms the mid-band gain (by Equation 21) is 20 db and the optimum bandwidth is 200 megacycles. The bandwidth can be decreased by using a non-inductive capacitor in parallel with the diode, which can conveniently be used for tuning of the circuit. Figure 24 shows a practical circuit that may be used for amplification at frequencies up to 100 megacycles. The tuned circuit consists of the diode capacitance in parallel with the short-circuited coaxial transmission line. The capacitance of the micrometer adds to that of the diode and allows tuning over a limited range.

A stripline cavity version of the circuit shown in Figure 24 was reported by Schaffner. This amplifier, using a 2N2939 diode, was tunable from 405 to 460 megacycles and the gain-bandwidth product approached 100 megacycles. A stripline one-port version of the same circuit was built by EDL (Figure 25). The length of the shorted stripline is determined by

$$l = \frac{\lambda}{2\pi} \arccot(2\pi f_0 Z_0 C_D), \quad (24)$$

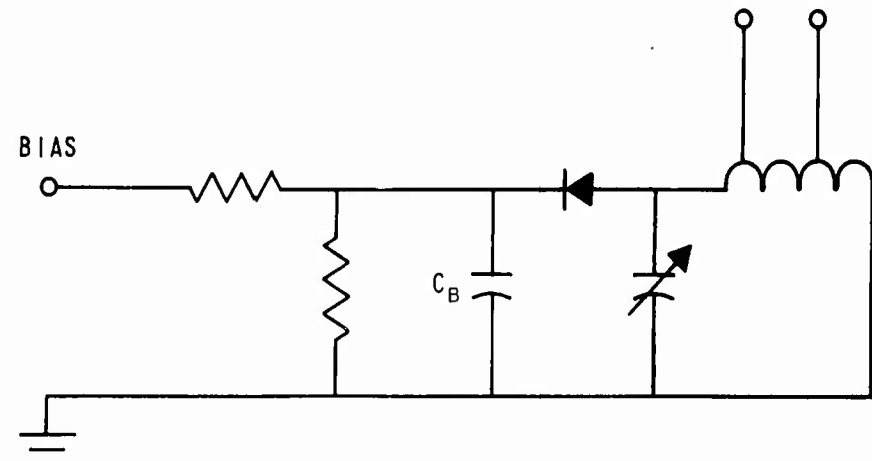
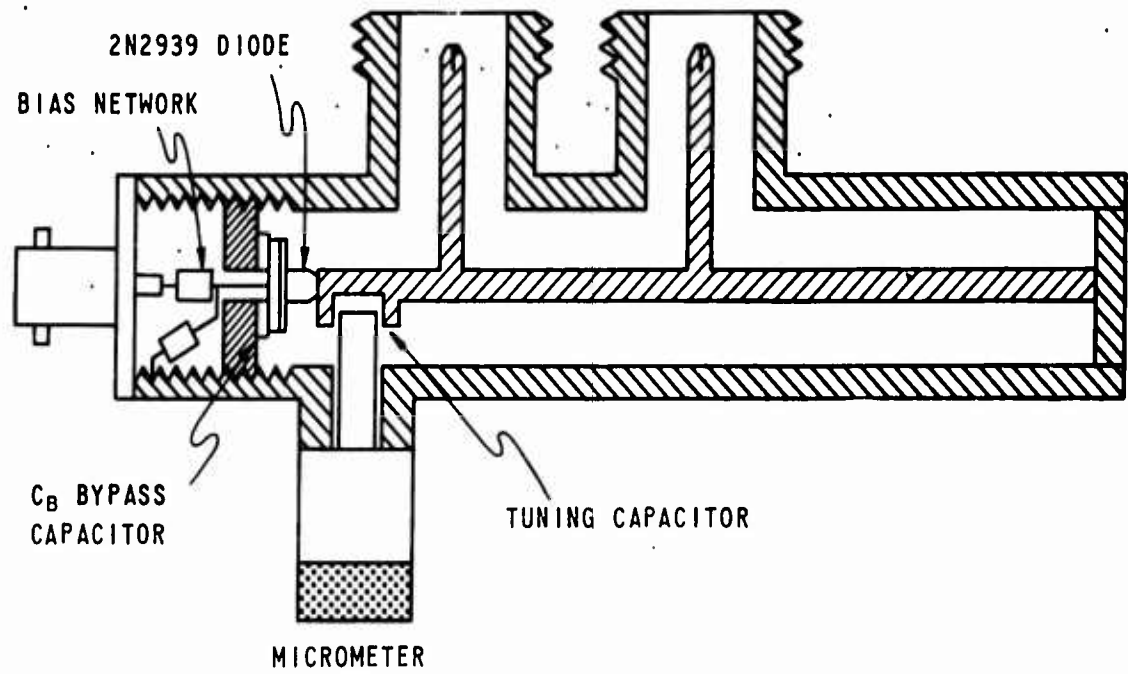
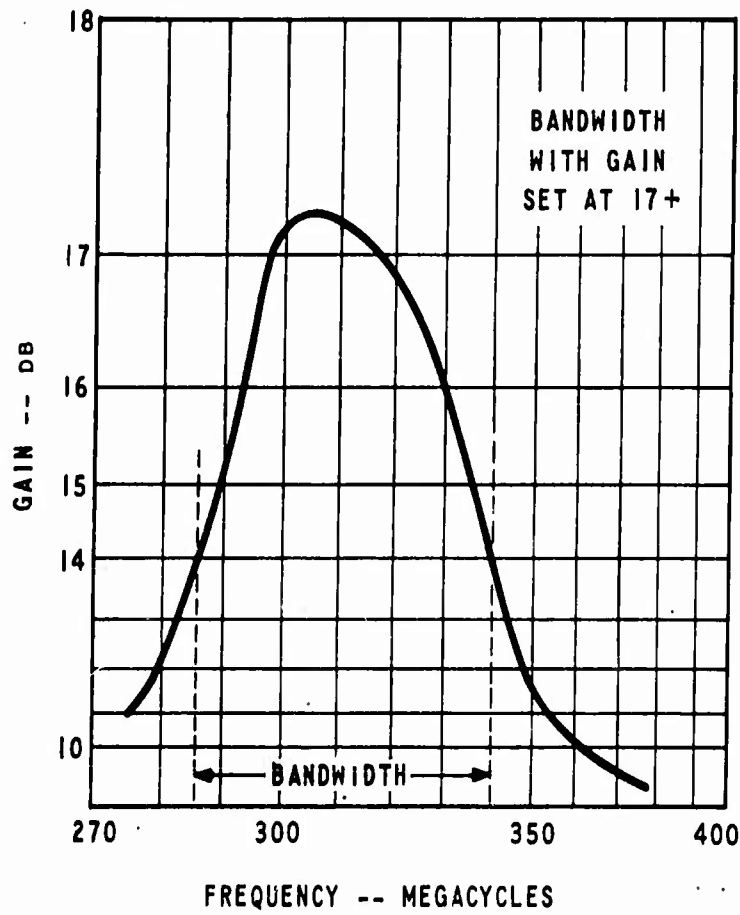
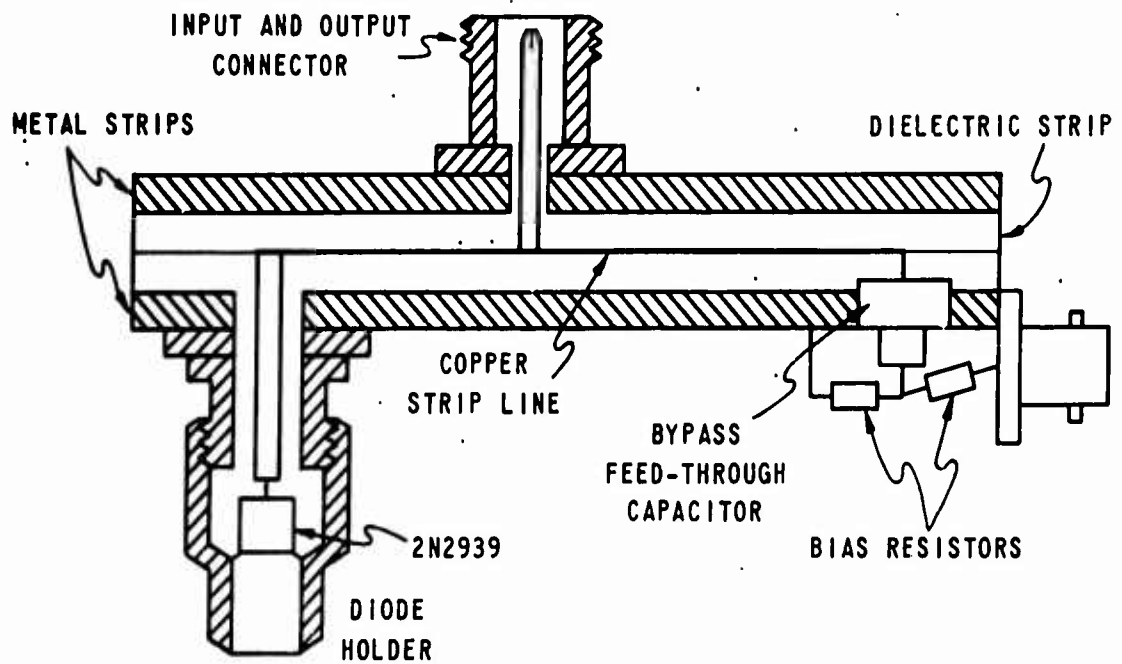


Figure 24
Single-Tuned UHF Amplifier



MEASURED PERFORMANCE		
AT(DB)	B(Mc)	$B \sqrt{AT}$ Mc
17	52	370
19	46	410
22	27	340
24	21	330

GAIN AND BANDWIDTH OBTAINED BY VARYING TAP POINTS

Figure 25
Single-Tuned Stripline One-port Amplifier

4.2 -- Continued.

where

λ is the transmission line wavelength at the desired frequency, f_0 , and Z_0 is the characteristic impedance of the line.

For short lengths ($l < \lambda/6$), Equation 24 can be approximated by

$$l = \frac{c}{(2\pi f)^2 Z_0 C_D \sqrt{\epsilon_r}} \quad (25)$$

where

c is the velocity of light, and

ϵ_r is the relative dielectric constant.

The amplifier used a 2N2939 diode fitted into a BNC connector. Amplifier gain was measured using reflectometer techniques as shown in Figure 26. Gain could be varied from 10 to 30 db by adjusting the tap point on the transformer. The $B\sqrt{A_T}$ was greater than 300 megacycles. A photo of the amplifier is shown in Figure 27; a similar model with separate input and output connectors is shown in Figure 28. The transducer gain and the reflected gain can be adjusted by moving the transformer tap points. Figure 28 shows a measured difference of A_T and A_R of greater than 10 db. This is achieved when $G_L \approx G_D$ and $G_g \ll G_L$, as indicated by Equations 15 and 17.

A tunable S-band amplifier using a Sylvania D4168 diode is shown in Figure 29. The resonant frequency is varied by adjusting the length of the shorted coaxial line. To maintain stability and high gain over a large frequency range, the ratio of R_L/R_D must be kept constant and near unity. The input transmission line is therefore coupled directly to the diode circuit (rather than by a loop) and impedance-transforming line sections are eliminated by using a selected diode with a negative resistance value of about 60 ohms. Figure 30 shows the amplifier gain measured with the reflectometer technique shown in Figure 26. Gain-bandwidth product is about 1200 megacycles. A photo of the amplifier with a mercury-cell power supply is shown in Figure 31.

An amplifier circuit with capacitive tuning was suggested by Sommers;⁶ this circuit is illustrated in Figure 32. Length of line, l_1 , is given by Equation 24. The desired mode has a null at the point where the

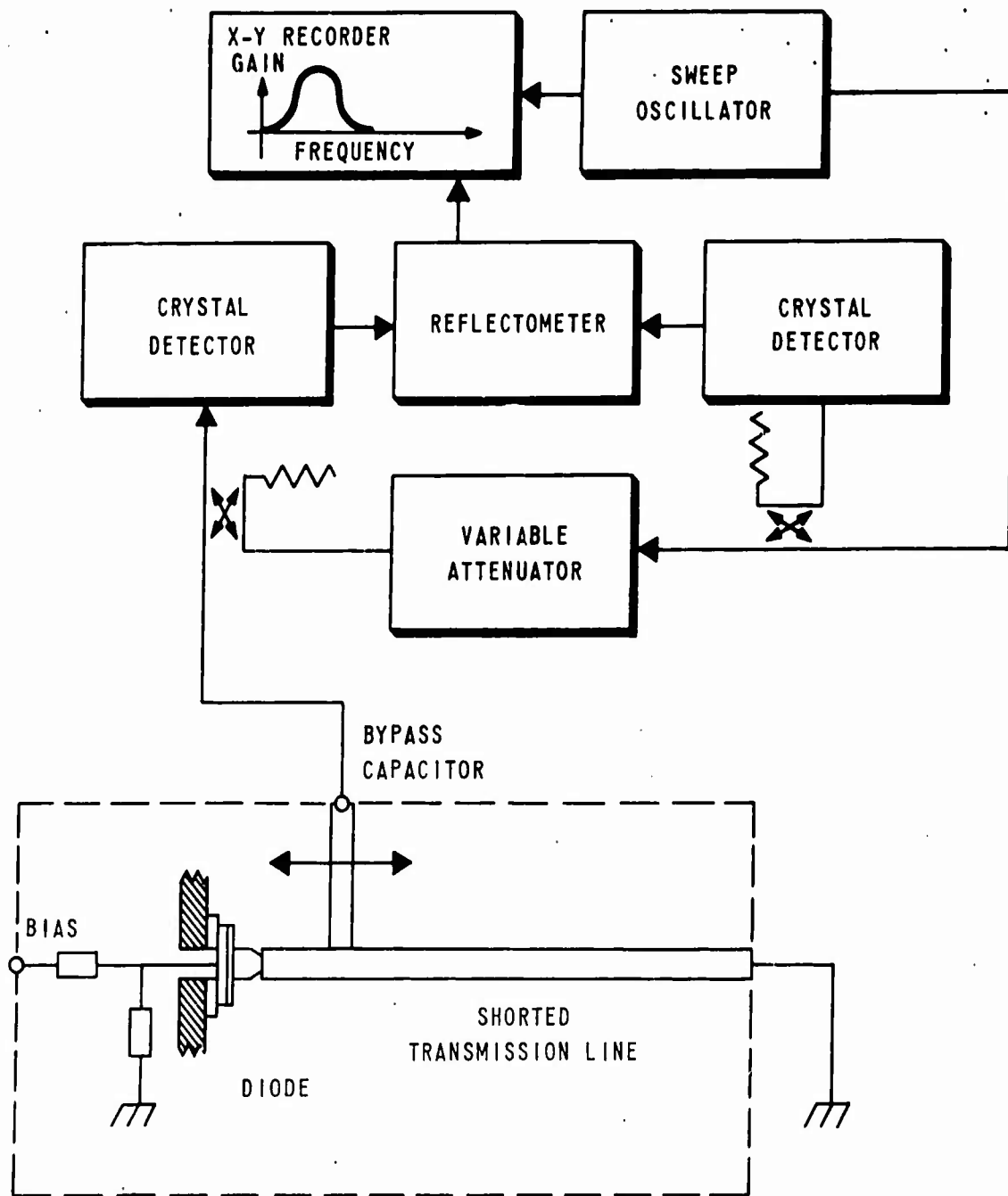


Figure 26

Gain Measurement Technique for One-port Amplifier

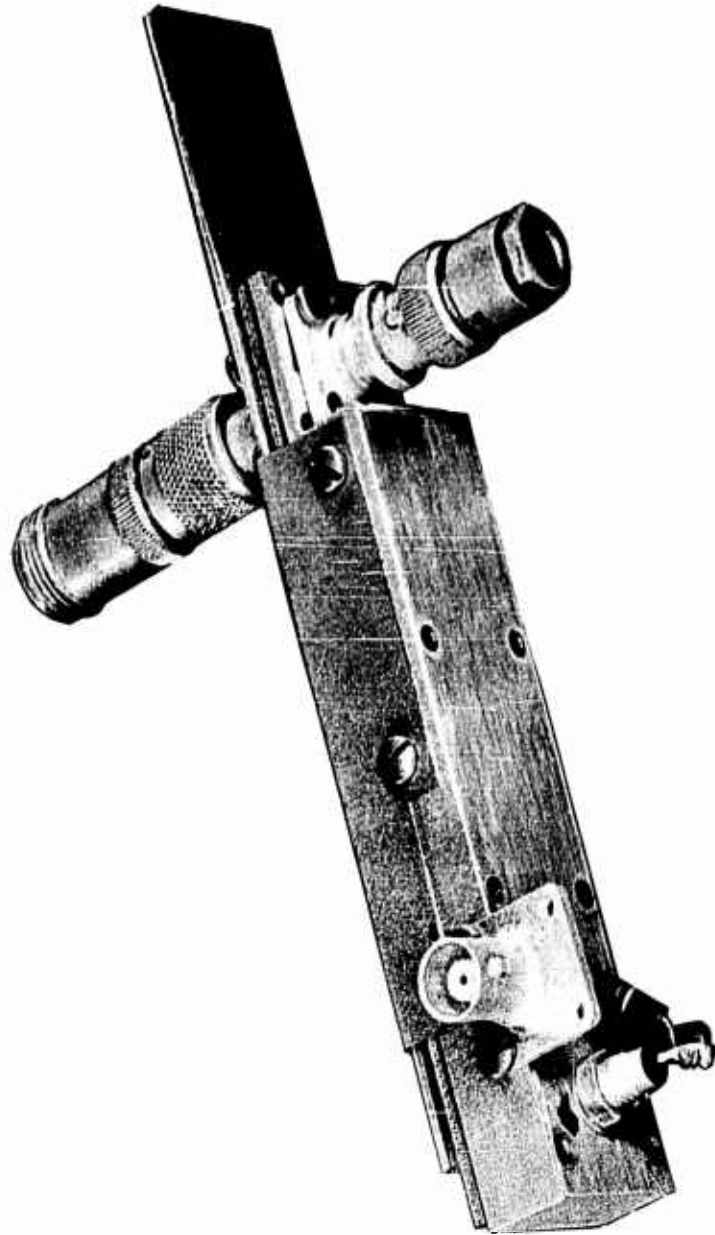


Figure 27
One-port VHF Amplifier

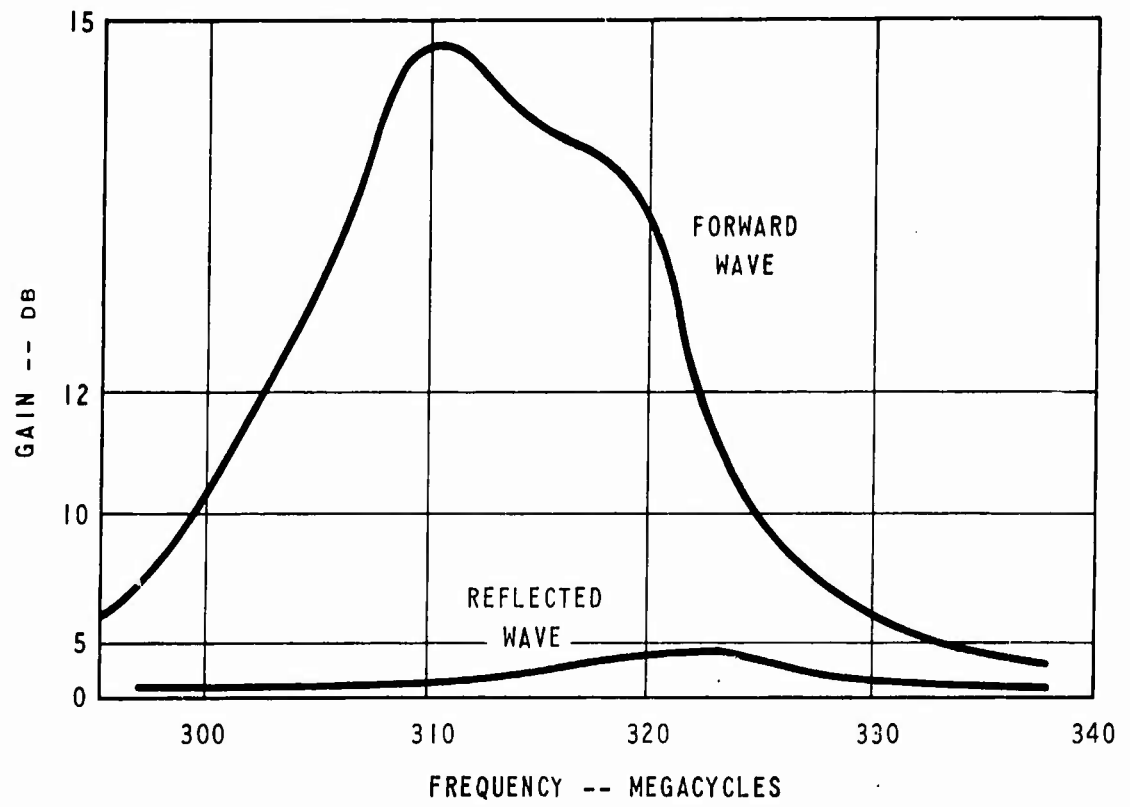
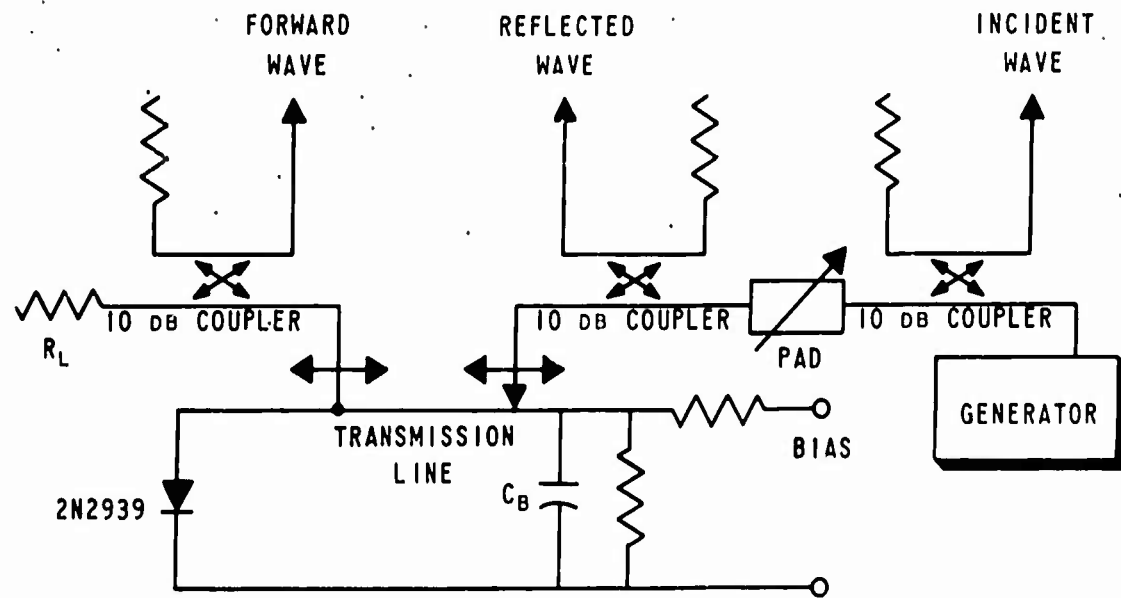


Figure 28

Single-Tuned Stripline Two-port Amplifier

AMPLIFIER CIRCUIT AND CROSS SECTIONAL VIEW

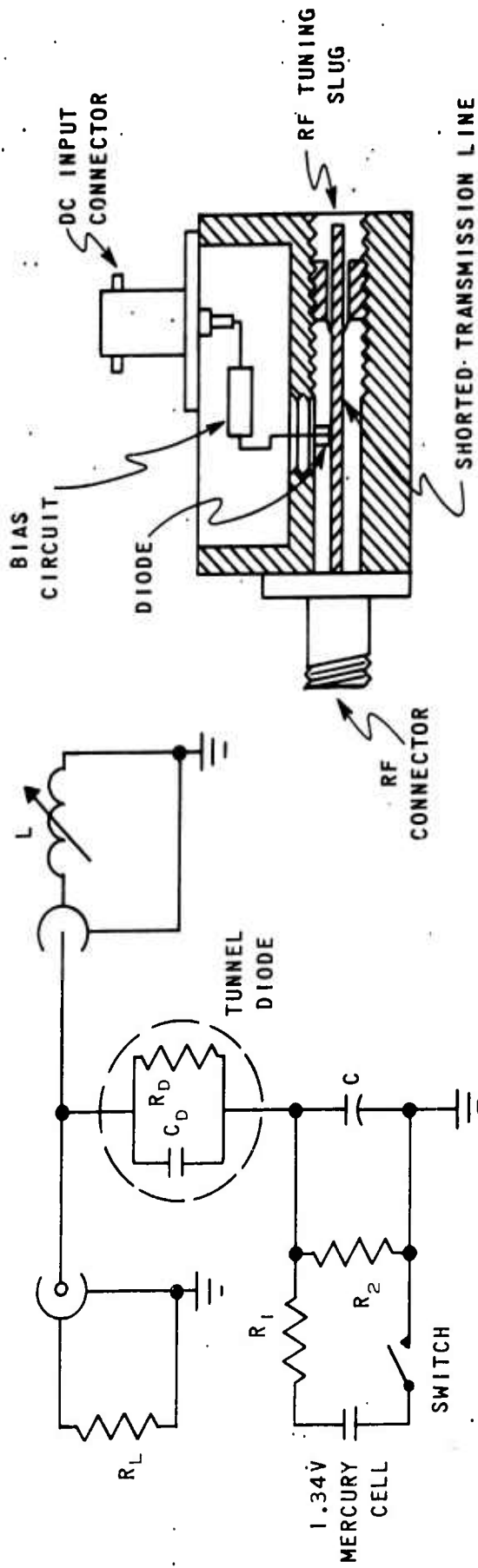


Figure 29

Amplifier Circuit and Cross-Sectional View

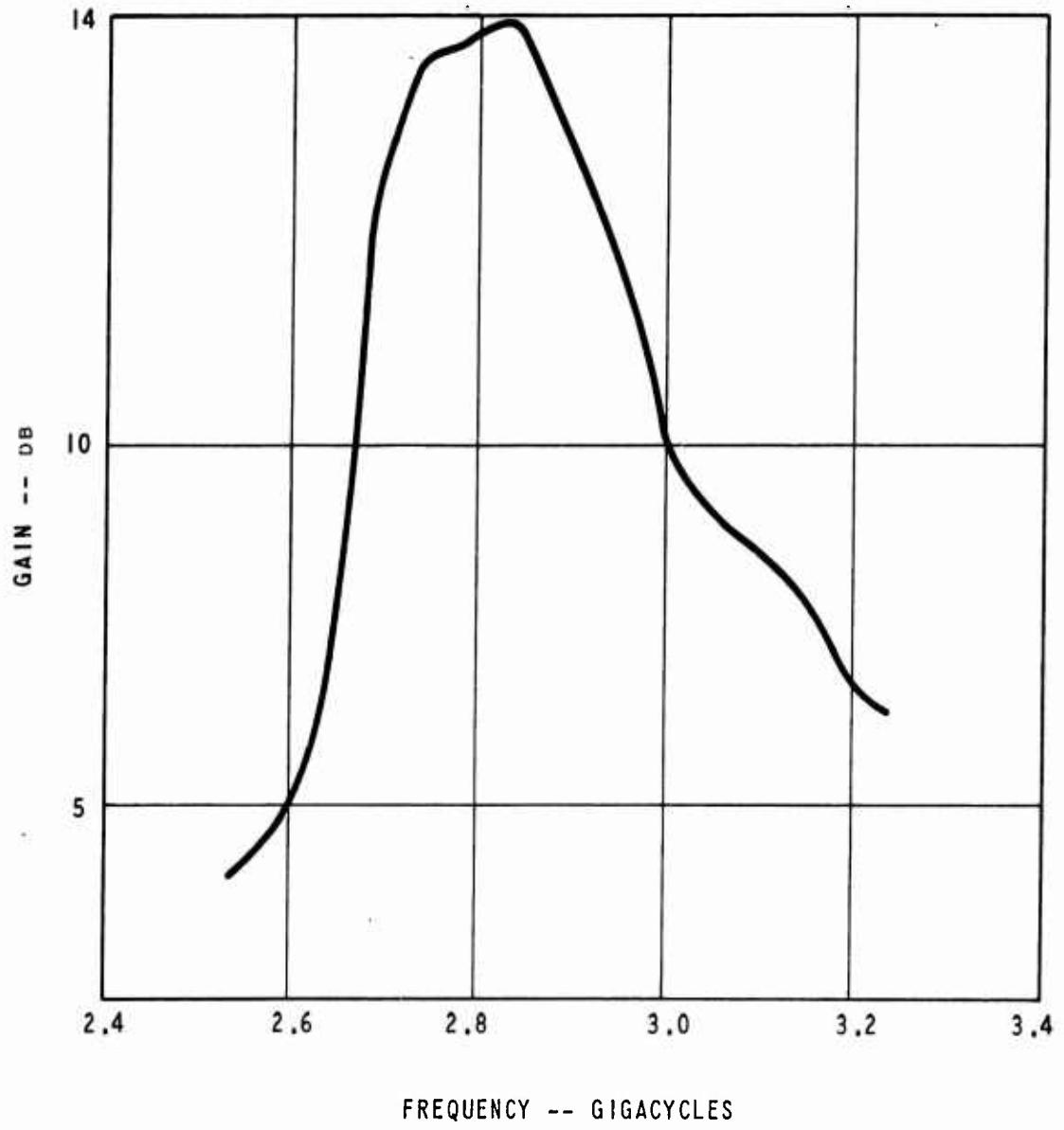


Figure 30
S-band Amplifier Gain



Figure 31
S-band One-port Amplifier

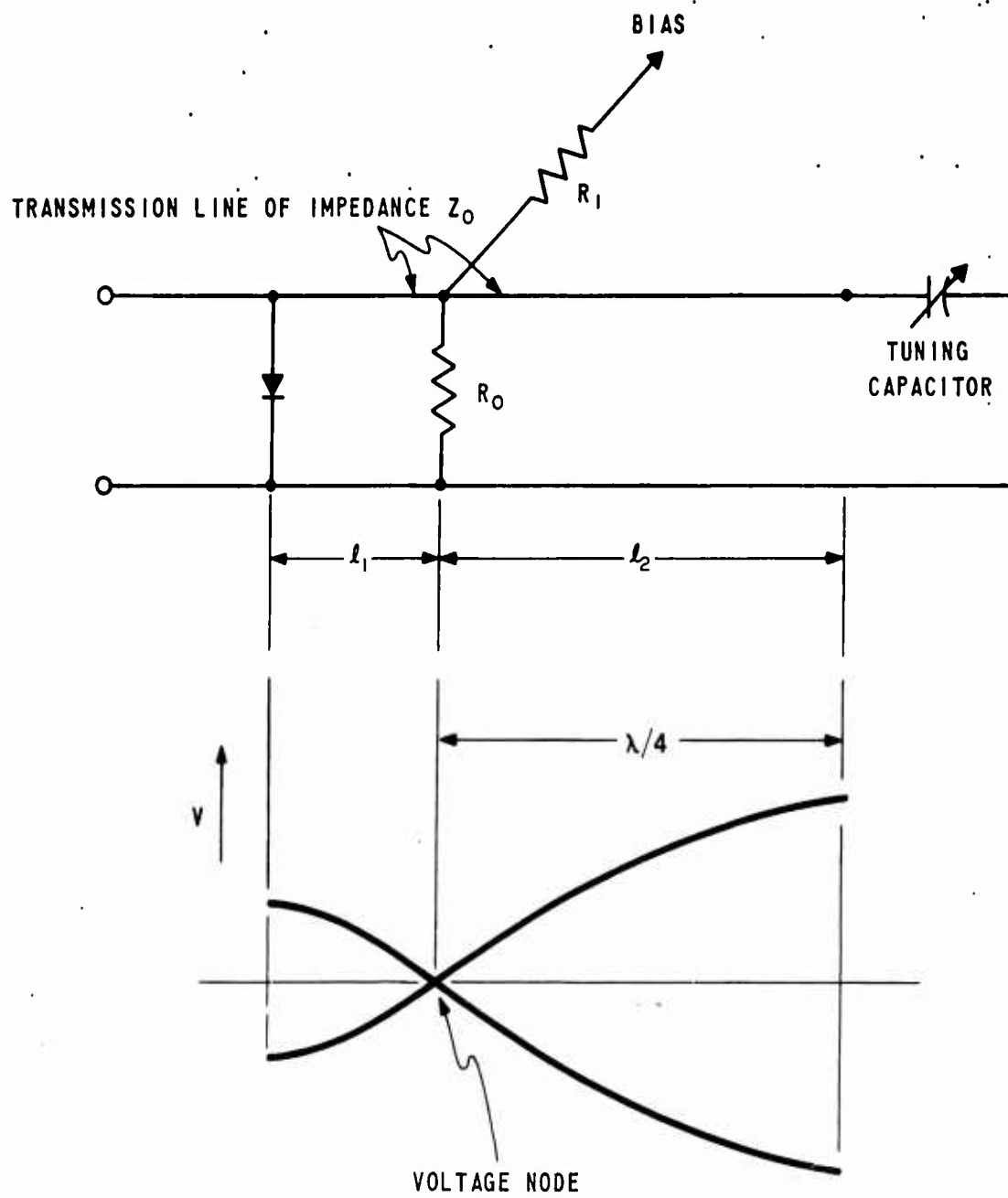


Figure 32
Capacitive-Tuned Circuit

4.2 -- Continued.

(noninductive) bias resistor, R_0 , is located. The total electrical length of the line l_2 and the capacitor is a quarter wavelength. (The length of l_2 is therefore somewhat smaller.) As the effective null point is changed when the capacitor is tuned, the bias resistor will load the RF circuit and reduce gain of the amplifier. A direct-coupled capacitive-tuned S-band amplifier is shown in Figure 33 and a photo of the amplifier follows in Figure 34. This amplifier is tunable from 2.5 to 2.9 gigacycles, the bandwidth is nearly constant at 65 megacycles and the gain varies from 15 to 20 db.

Dynamic range of a tunnel-diode amplifier is limited by noise at the low power level and by saturation at the high power level; gain is flat from the low power level to about -40 dbm, while the total range is greater than 50 db. Gain of an amplifier as a function of signal power is shown in Figure 35.

Separation of input and amplified wave may be accomplished in various ways. Figure 28 shows a two-port amplifier in which part of the amplified wave is returned to the generator and part goes to the load resistor, R_L . In this case, the separation is not complete. Descriptions are available of other two-port amplifier circuits using filter circuits.^{20,24}

4.2.1 Hybrid Technique. The hybrid-coupled amplifier is a two-port bidirectional device; either port can be used as input or output. It consists of two matched one-port amplifiers and a hybrid junction (3-db coupler) with a phase difference of 90 degrees between output arms. Two commonly used transmission-line hybrids have the required phase characteristics, the quarter-wave electromagnetic coupler and the branch coupler. These are illustrated in Figure 36, A and B.

In operation under ideal conditions, the input signal power splits evenly and is amplified by the matched one-port amplifiers at ports 2 and 3. The amplified waves cancel at port 1 and add in-phase at port 4. Ideally, the gain of the hybrid amplifier equals the gain of a single reflective one-port amplifier.

The conditions for ideal operation are that (a) the one-port amplifiers are exactly alike, (b) the hybrid is perfect (i. e., has no loss, equal power split and infinite directivity), and (c) perfect input and output match, i. e., reflection coefficients at ports 1 and 4 (ρ_1 and ρ_4) equal zero. If condition C is not met, the gain at port 4 for the hybrids shown in Figure 36 is

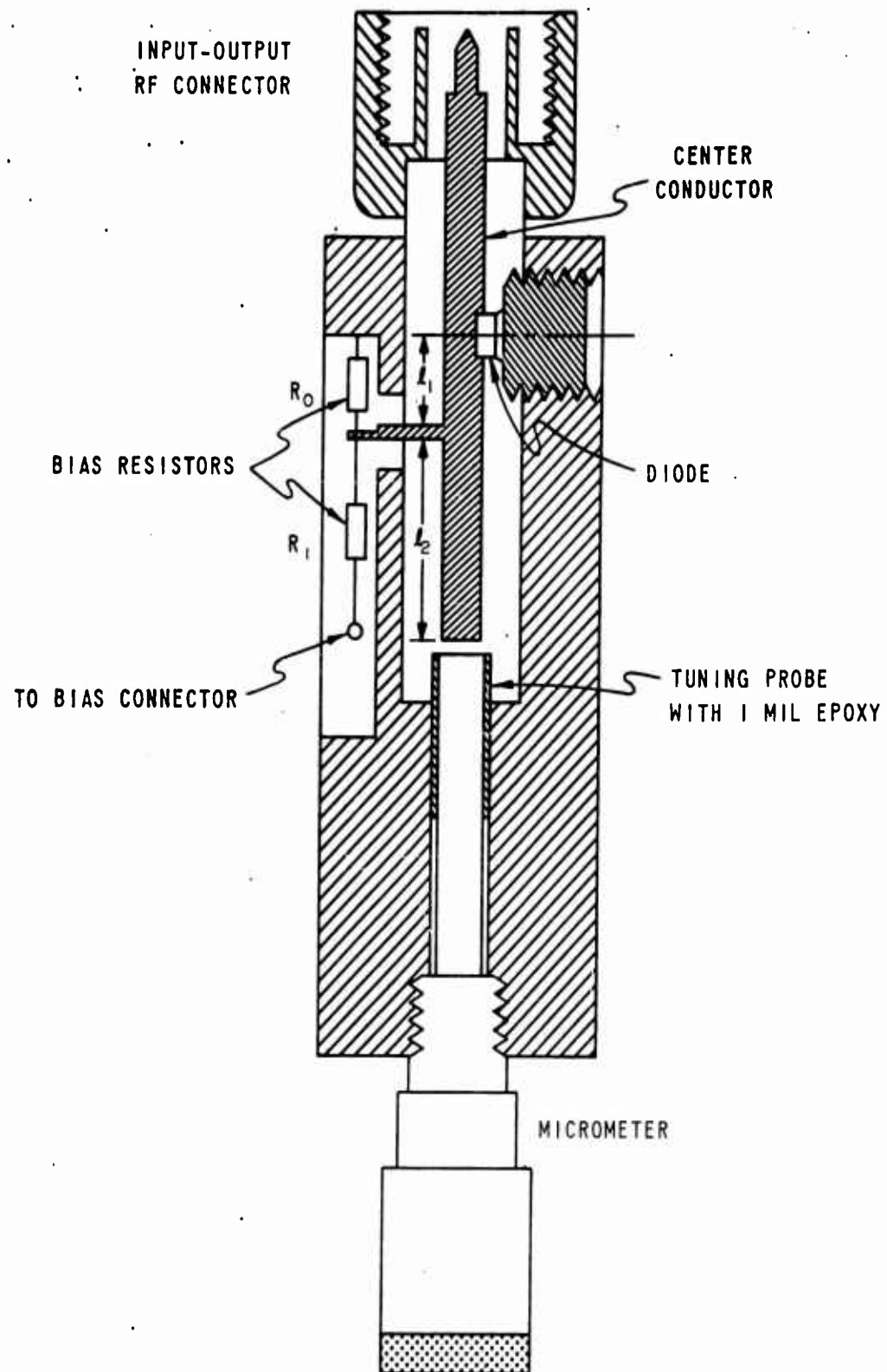


Figure 33

Schematic of Capacitive-Tuned S-band Amplifier

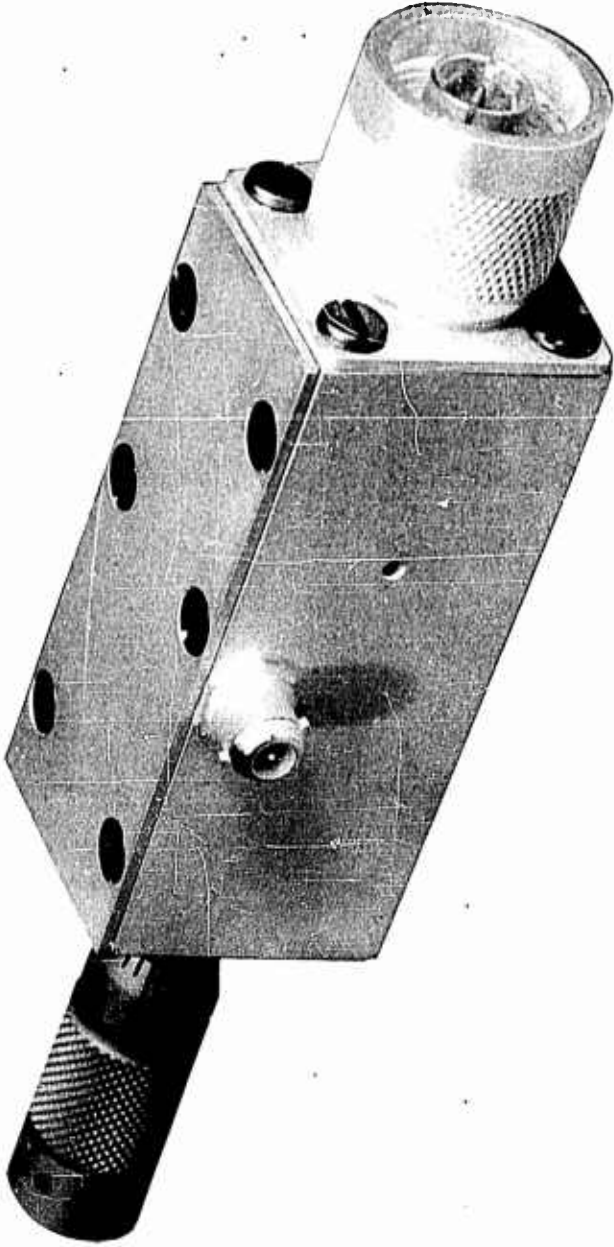
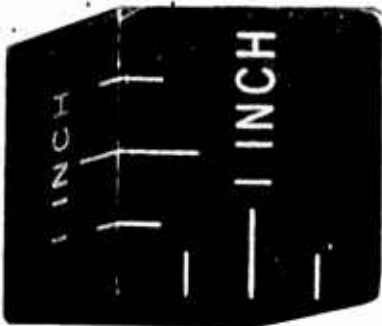


Figure 34
Capacitive-Tuned S-band Amplifier

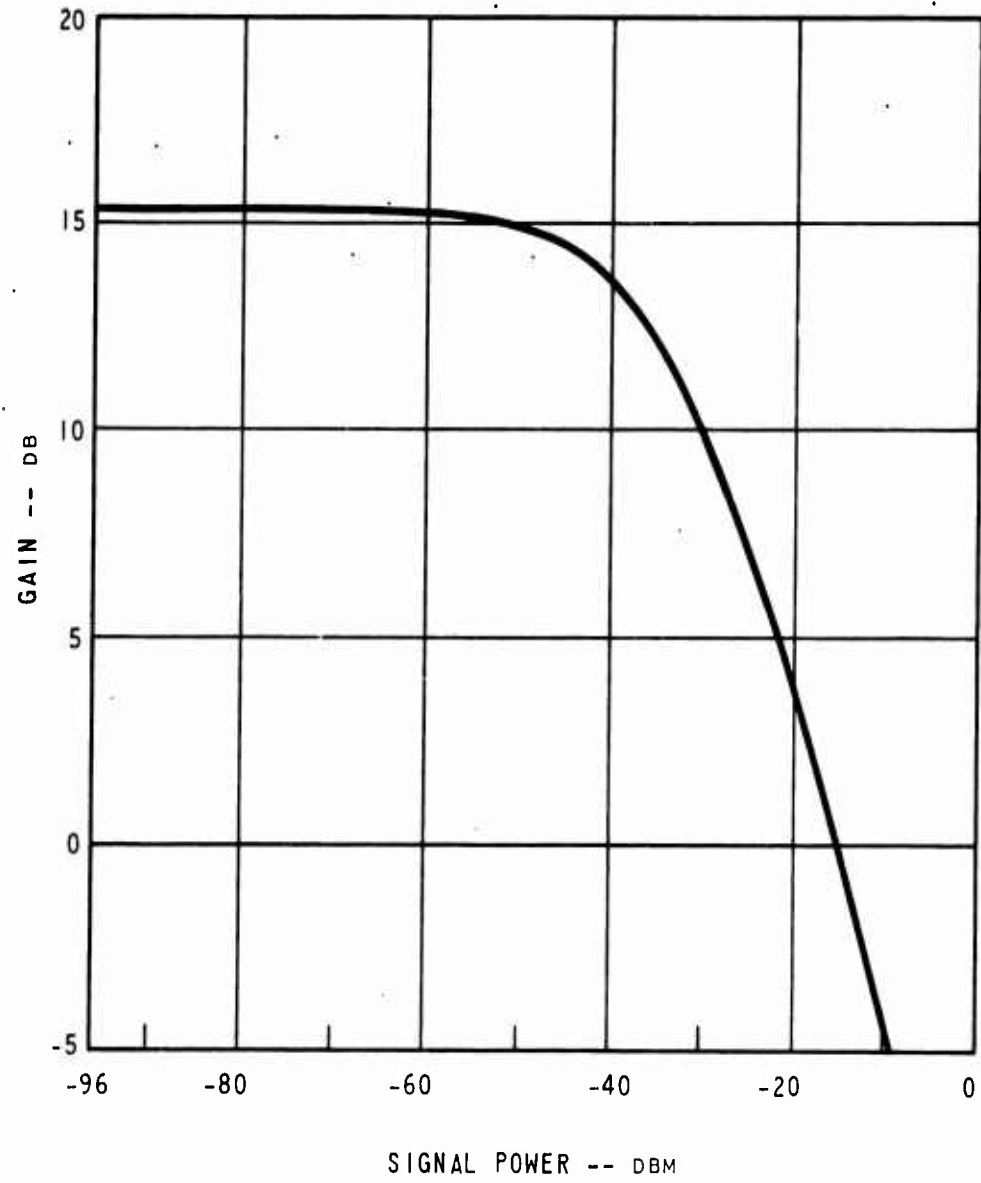
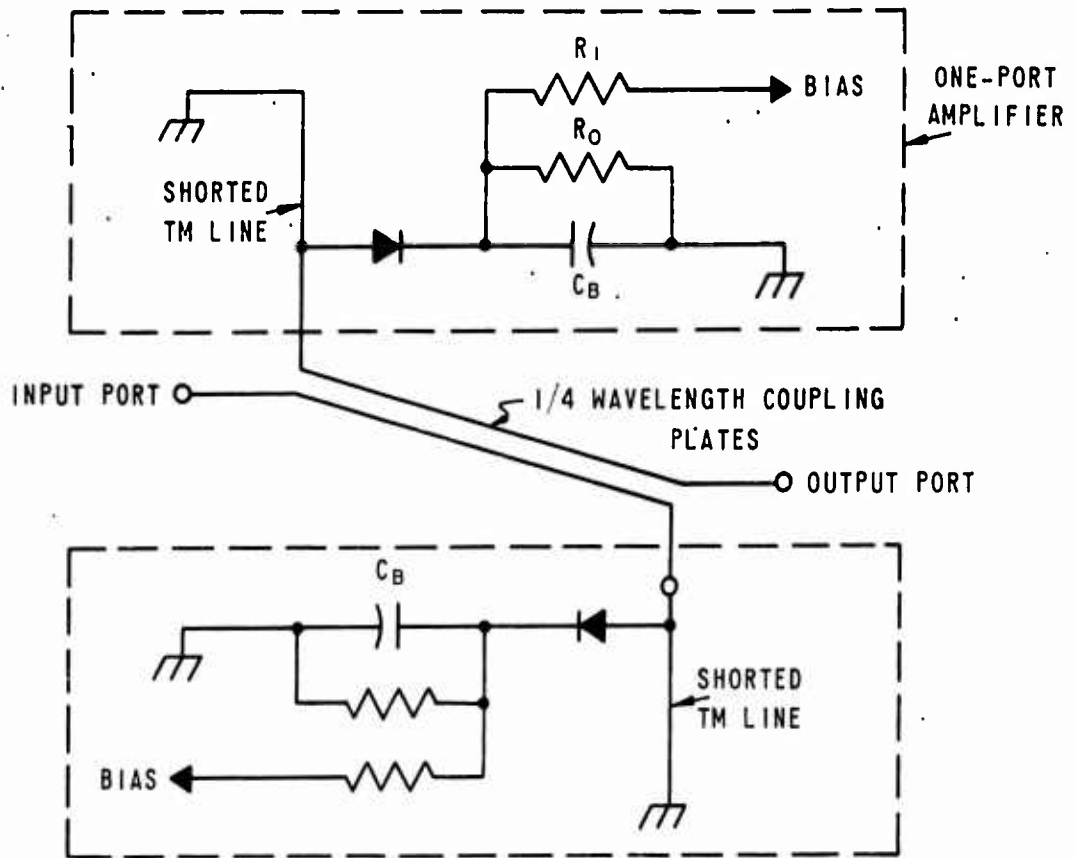
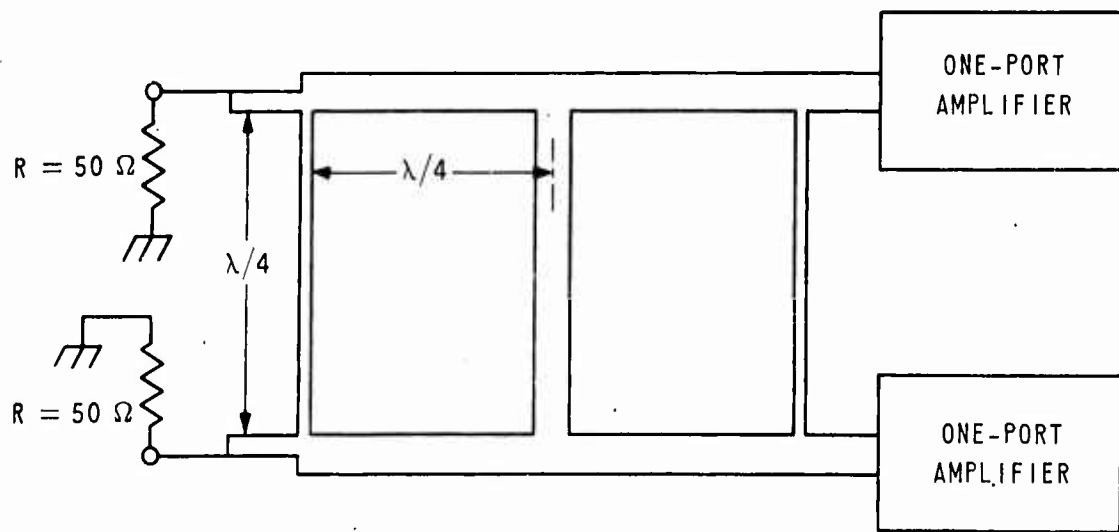


Figure 35
Dynamic Range of Amplifier



(A) $\lambda/4$ ELECTROMAGNETIC COUPLER



(B) 3-BRANCH COUPLER

Figure 36
Hybrid-Coupled Amplifier

4. 2. 1 -- Continued.

$$G_{41} = \frac{A_T}{(1 + \rho_1 \rho_4 A_T)^2} \quad (26)$$

The requirement for stability is:

$$\rho_1 \rho_4 < \left(1 - \frac{G_D}{G}\right)^2 = 1/A_T \quad (27)$$

If, for example, the one-port amplifier has a gain of 20 db ($A_T = 100$), the hybrid amplifier can, at most, tolerate an input and output VSWR of 1.2. However, this stability requirement, Equation 27, only ensures that the device will not oscillate. A large margin of stability is further required to obtain the desired 20-db gain of the hybrid amplifier. If condition C is not met, the hybrid amplifier will also have a reflected gain, G_{11} , as defined by Equation 19. Assuming Equation 27 is adequately met, the reflected gain is given approximately by

$$G_{11} = (\rho_4 \cdot A_T)^2 \quad (28)$$

Since G_{11} should be much smaller than unity to achieve a good input match, the output reflection coefficient must be exceptionally good ($\rho_4 < 1/A_T$). Assuming $A_T = 100$, as in the example above, ρ_4 can be no larger than 0.01. This means that the output termination must have a VSWR < 1.02 .

Conditions A and B, the stability requirement, Equation 27, and the requirement that $G_{11} < 1$ usually restricts use of the hybrid amplifier to a maximum gain of 10 to 12 db. The electromagnetic coupler of Figure 36 A is best suited for wide-band amplifiers. An ultra-high-frequency hybrid amplifier using a stripline coupler is shown in Figure 37. The amplifier has a gain of 8 db from 280 to over 480 megacycles. The amplifier remained stable with an input VSWR of up to 10 if the VSWR of the output termination was less than 1.06.

The branch coupler provides a well-matched coupling over a 20 per cent band and a very good isolation in the same band. A hybrid-coupled amplifier using a 3-branch coupler is shown in Figure 38. The 3-db bandwidth is about 160 megacycles and midband gain is 11 db.

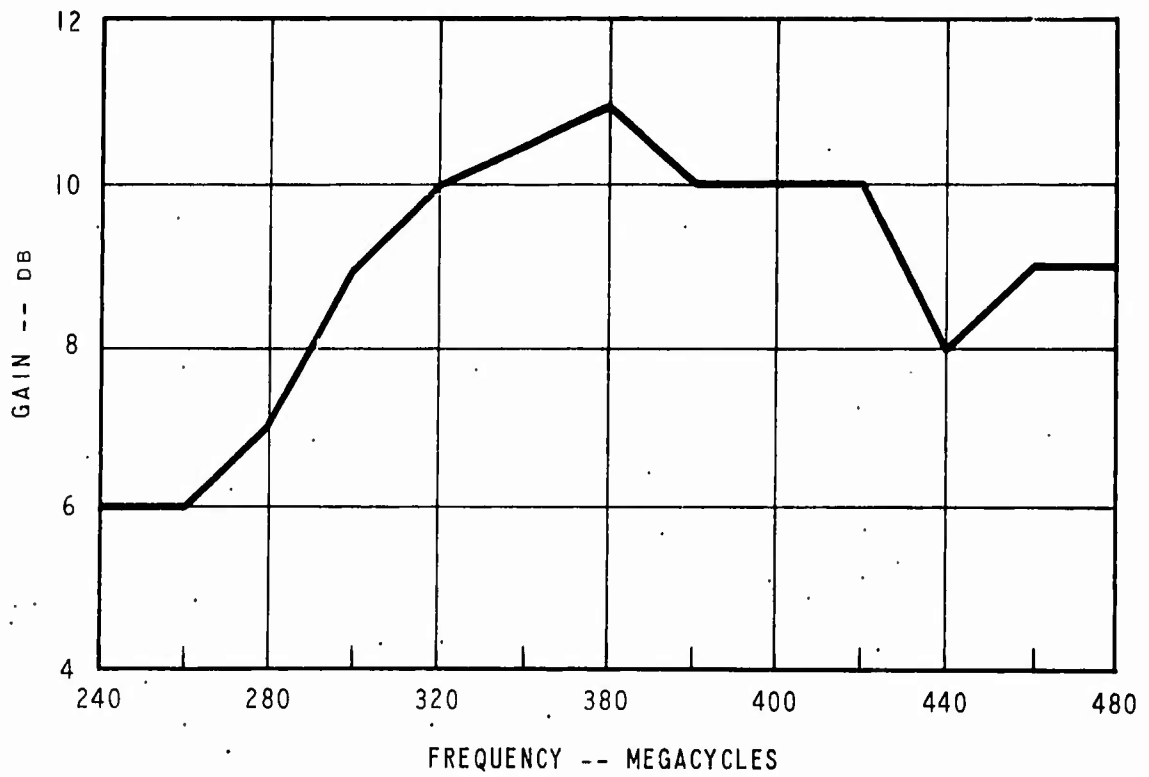
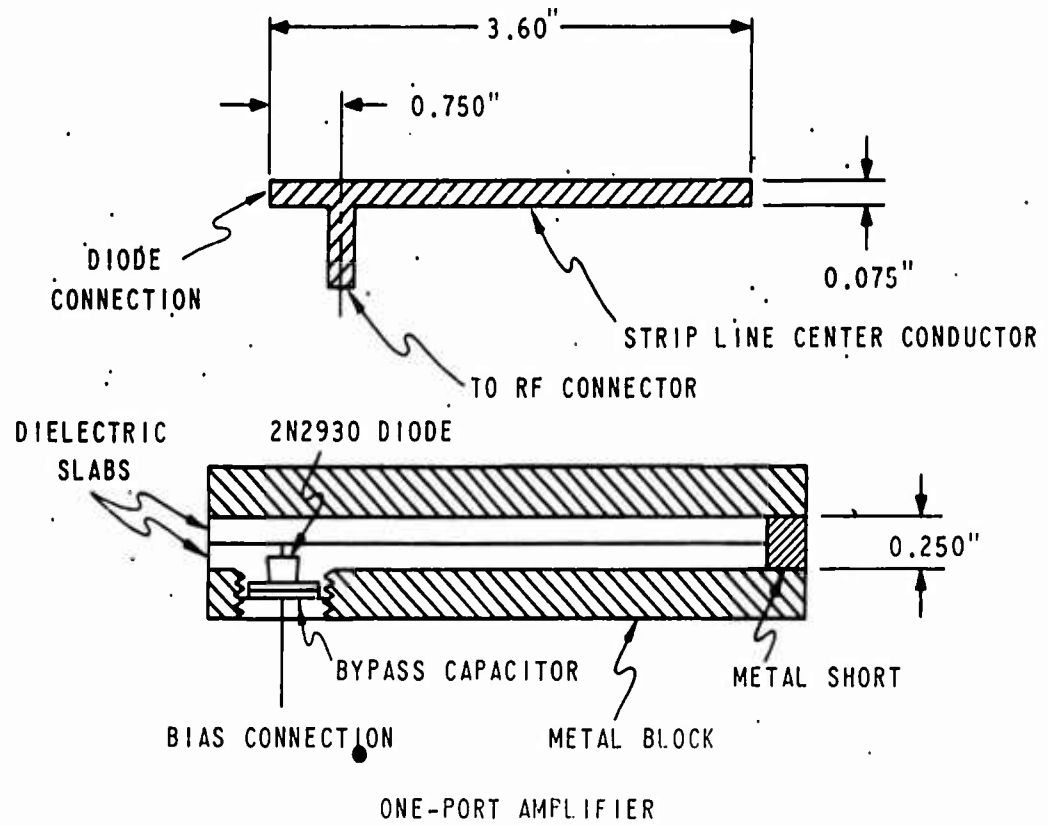


Figure 37
 Hybrid-Coupled Amplifier Employing an
 Electromagnetic Quarter-Wave Coupler

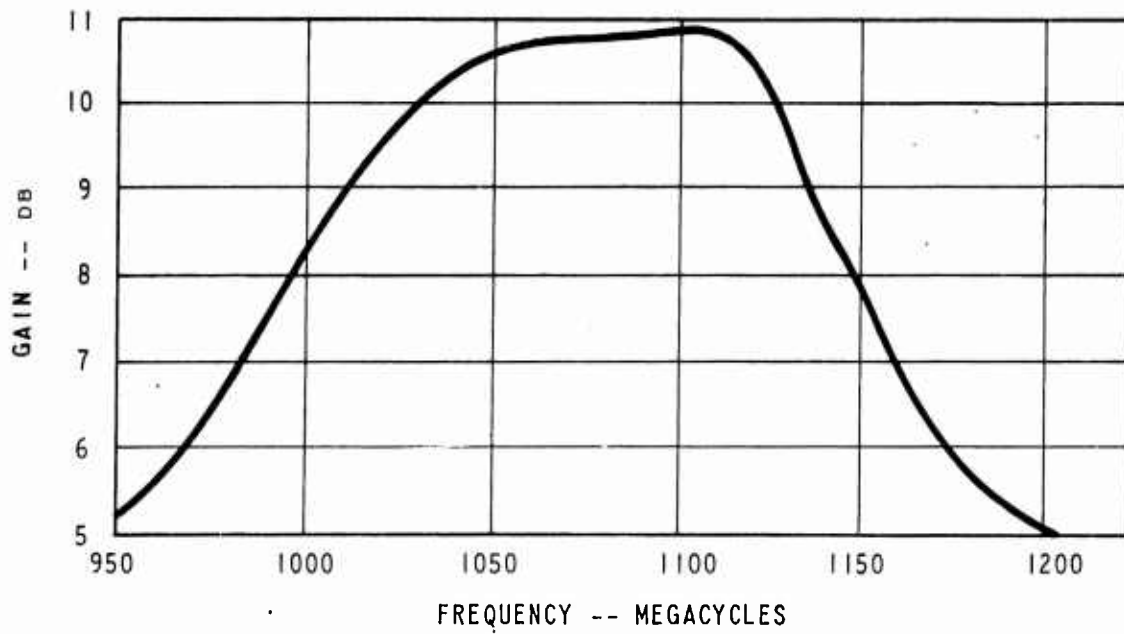
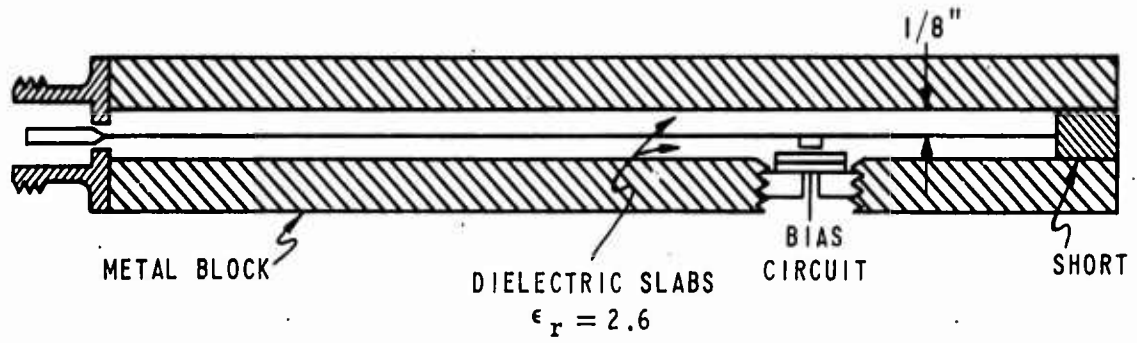
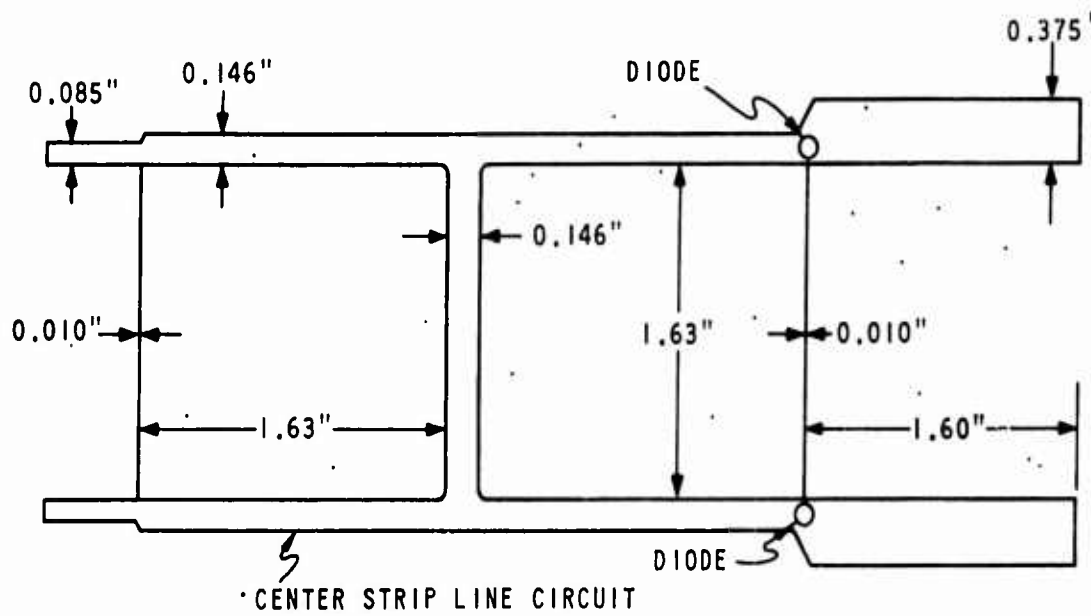


Figure 38
 Hybrid-Coupled Amplifier
 Using a 3-branch Coupler

4. 2. 2 Circulator Technique. The circulator method of separating the input and reflected waves of a one-port amplifier is illustrated in Figure 39. The circulator has a preferred direction of propagation, as indicated by the arrows. The amplified wave is diverted out port 3. A typical S-band 3-port circulator has a loss from port 1 to port 2 of a few tenths of a db over a bandwidth of 300 to 400 megacycles and an isolation from port 1 to port 3 greater than 20 db over 200 megacycles. Circulators are presently available commercially at frequencies higher than 500 megacycles.

A circulator in the S-band measures about 1.5 inches in diameter and 1 inch thick. Figure 40 is a photo of an S-band amplifier with a circulator. The amplifier has an attached mercury-cell power supply.

4. 2. 3 Broad-banding Techniques. The maximum gain-bandwidth product of a single-tuned amplifier is set by Equation 23. It can only be obtained at high gain and provided the diode is not shunted by any external capacitance. It has been shown, however, that the bandwidth can be improved greatly by using a filter circuit (also called an equalizer) instead of the single-tuned circuit.^{20, 26, 27} Two broad-banding filter circuits are shown in Figure 41. If the filter circuit is of the maximally flat type, the invariant gain-bandwidth product becomes $B \cdot (A_T)^{\frac{1}{n}}$, where n is the number of poles in the filter.²⁶ The product reduces to $B \sqrt{A_T}$ when $n = 1$, for the case of the single-tuned circuit. The greatest improvement in bandwidth occurs as n is increased from 1 to 2. A given gain of 15 db increases the bandwidth threefold; the improvement is even greater for higher gain.

The technique of broad-banding with a reactive filter circuit assumes the existence of a constant load impedance. In practice, however, this assumption is invalid if presently available circulators are used. S-band circulators, for example, typically have VSWR of 1.02 at the center frequency and 1.3 or greater at frequencies 200 to 300 megacycles on either side. The theoretical bandwidth of a single-tuned amplifier may be far greater than the useful bandwidth of a circulator, i. e., the bandwidth in which the circulator VSWR is within limits specified by amplifier stability requirements. A typical wye ferrite circulator impedance referenced to the center of the circulator is shown by the solid line on the Smith chart in Figure 42. The real part is about 35 ohms at 2.6 gigacycles and 65 ohms at 3.1 gigacycles. The broad-banding technique using lossless filter circuits is therefore impractical if the filter circuit design does not include compensation for the change of circulator characteristics.

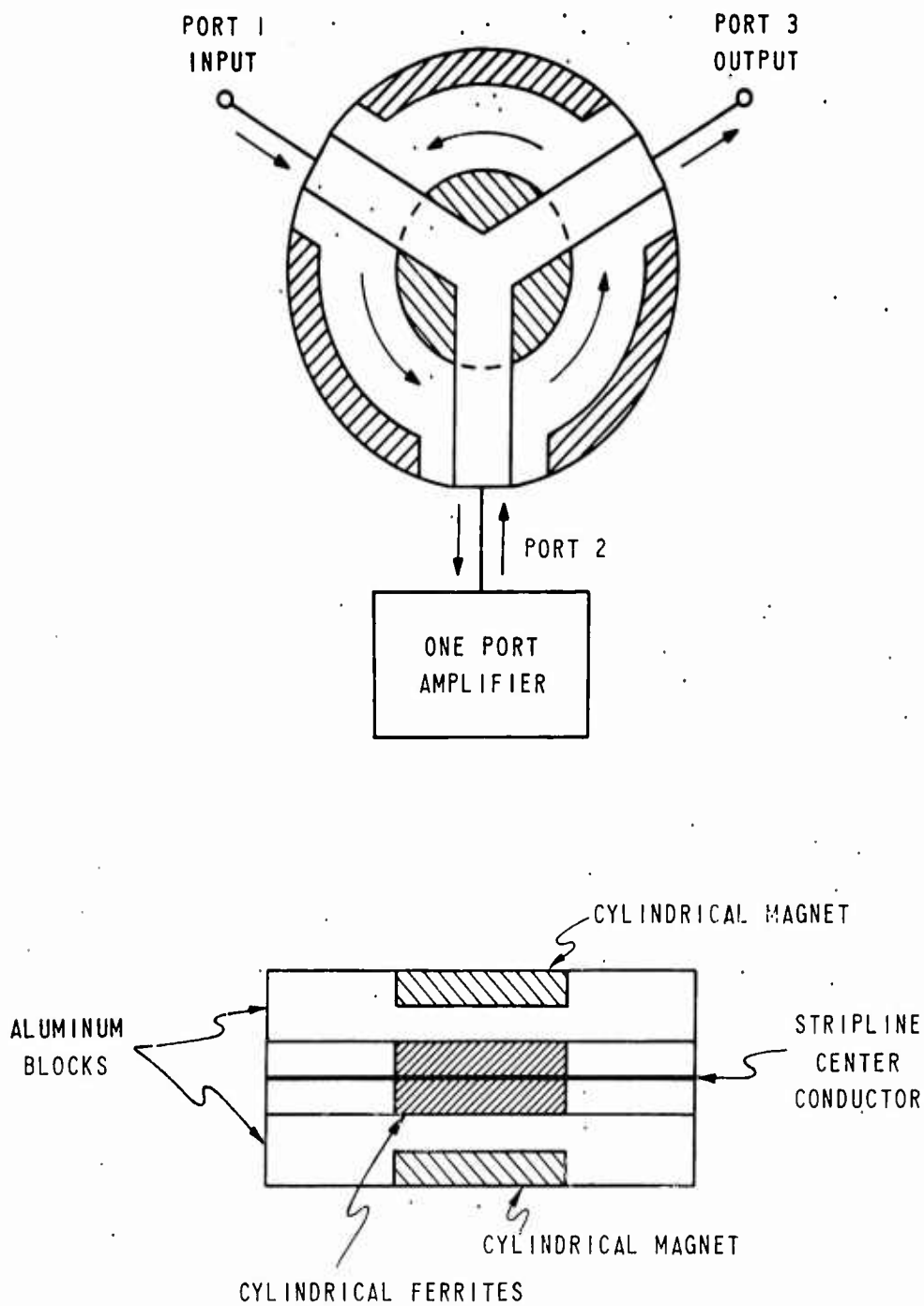


Figure 39
Wye Circulator

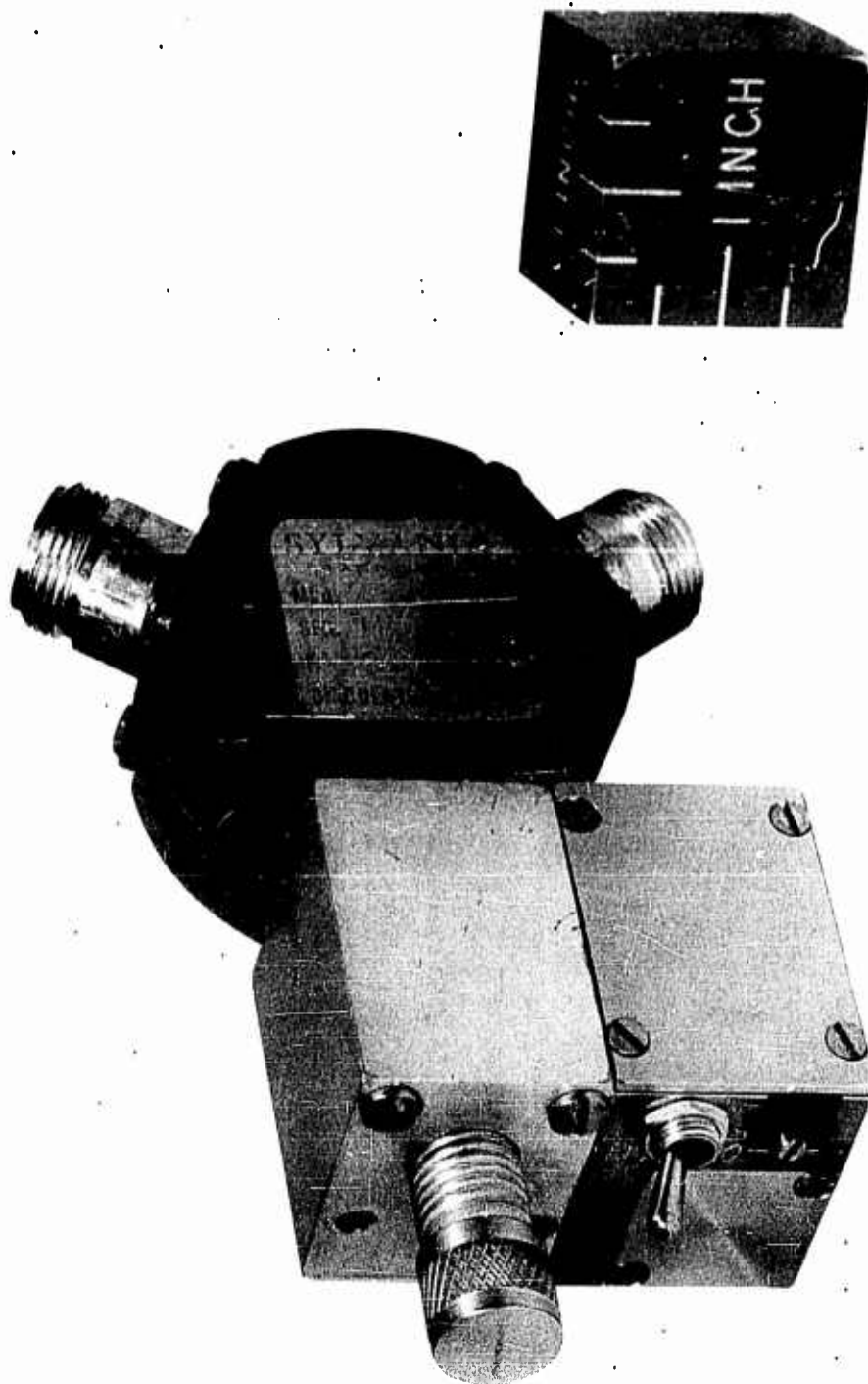


Figure 40
Amplifier with Circulator

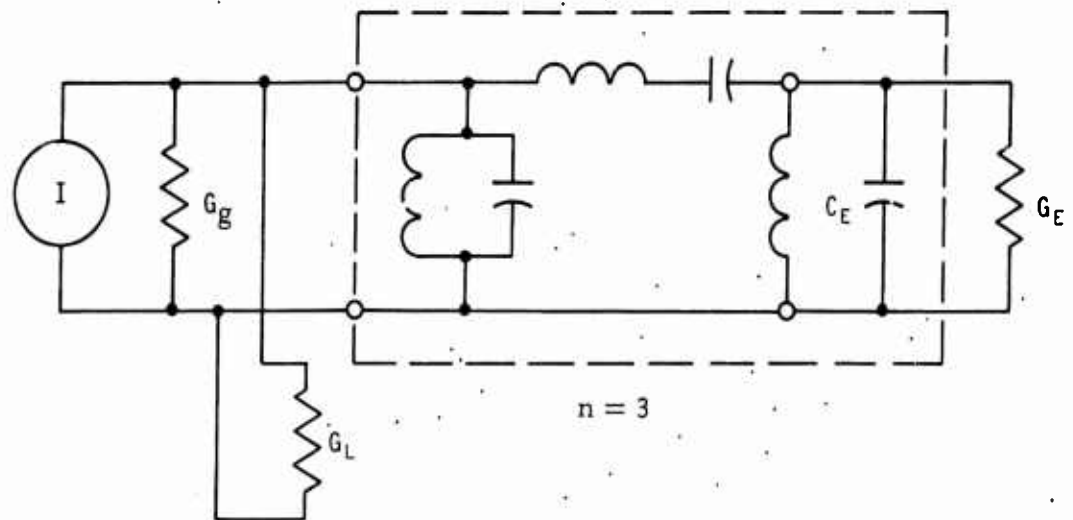
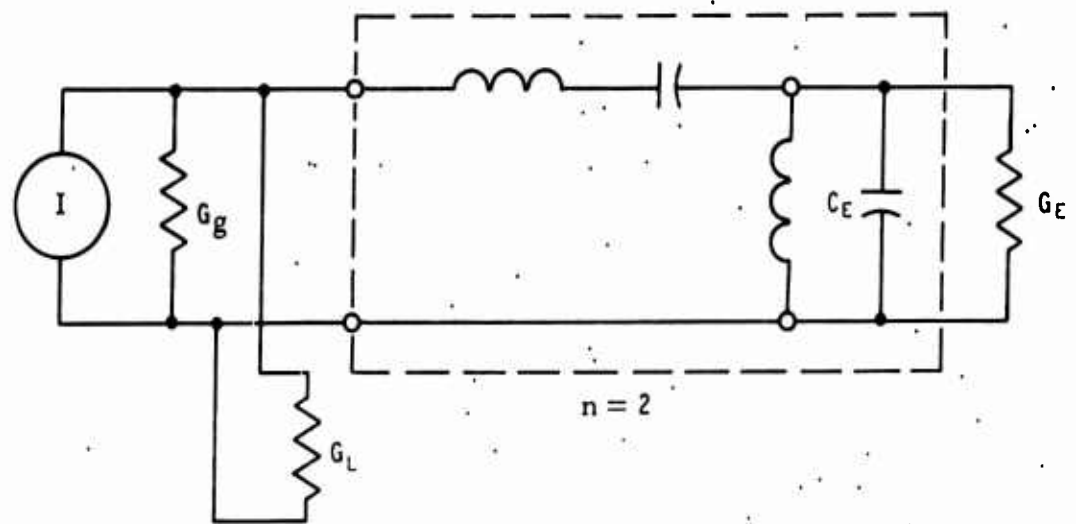


Figure 41
Wide-banding Filter Networks

4.2.3 -- Continued.

A new technique has been developed for the design of broad-banded amplifiers. This technique takes advantage of the existing circulator characteristics and uses, besides the circulator itself, a piece of transmission line connecting to the one-port amplifier. Greater bandwidth is achieved by adjusting the length and the characteristic impedance of the line so that the transferred load conductance at the amplifier port decreases symmetrically at frequencies above and below the resonant amplifier frequency. Figure 42 also shows the transferred load conductance when the transmission line is 3.8 centimeters long and has a characteristic impedance of 50 ohms. Conductance is highest at the resonant frequency and decreases on either side.

Gain bandwidth product of the broad-banded amplifier at high gain is derived from Equation 18 and is given by:

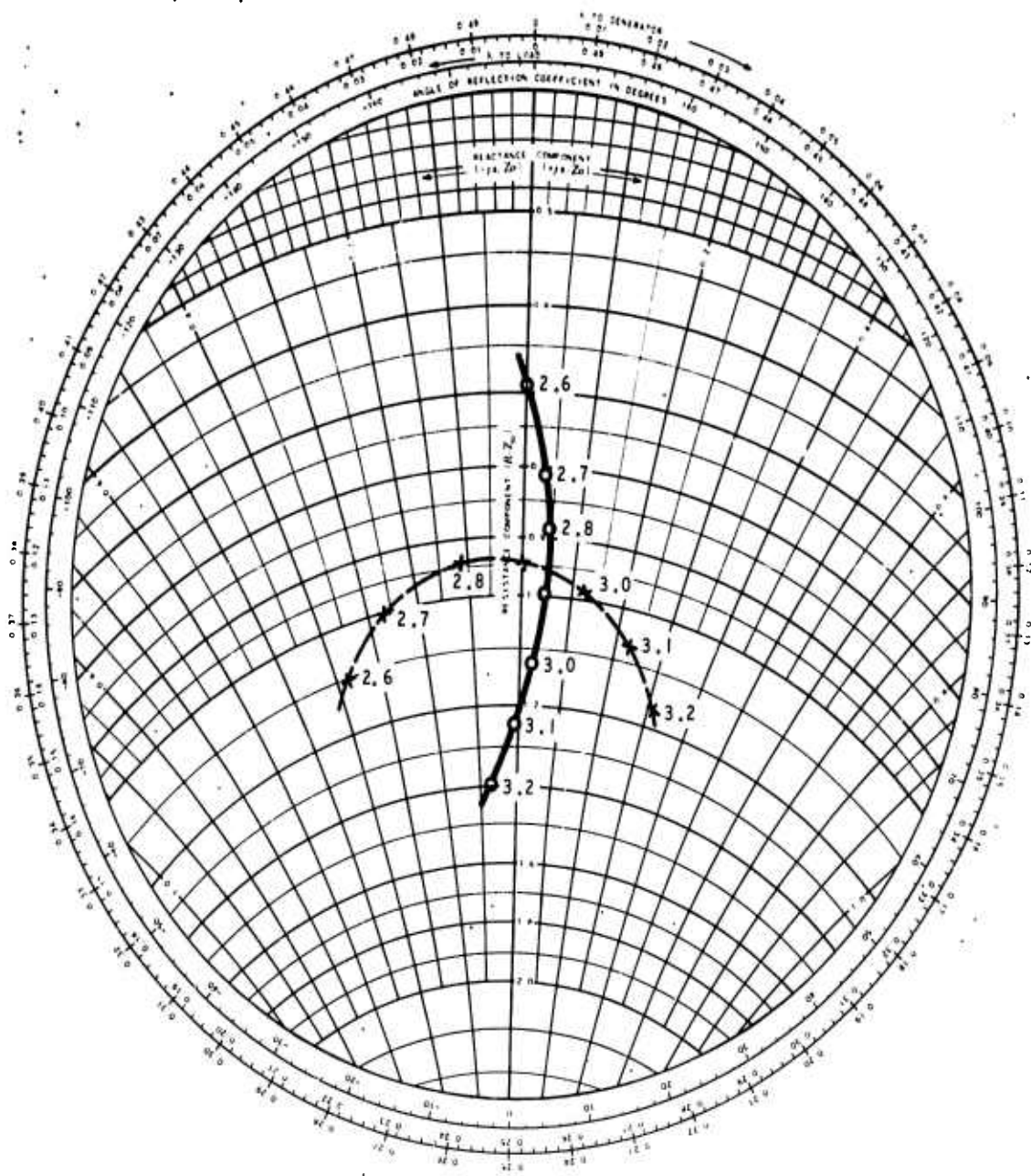
$$B \sqrt{A_{T_0}} = \frac{G_D}{2\pi C_D} \sqrt{1 + \frac{2g}{G_D - G_0}} = \frac{G_D}{2\pi C_D} \sqrt{1 + \frac{2g \sqrt{A_{T_0}}}{G_0}} \quad (29)$$

where G_0 and G_1 are values of G at resonance and at 3-db points, respectively, and $g = G_0 - G_1$. (Mid-band gain A_{T_0} is assumed to be maximum.) The radical factor is the improvement in gain-bandwidth product over the simple one-port amplifier.

Figure 43 shows measured gain of the broad-banded amplifier. Gain-bandwidth product is about 6000 megacycles or three times greater than the theoretical gain-bandwidth of a single-tuned amplifier with the same diode. The factor of improvement agrees reasonably well with the value of the radical in Equation 29 when the value of g/G_0 from Figure 42 is measured as 0.16. Equation 29 also indicates that the gain-bandwidth product is greatly reduced for small negative values of G .

4.2.4 Broad-band Stabilizing Network. The negative resistance of a diode is present at all frequencies from dc to the cutoff frequency, f_r . Stability must, therefore, be considered at these frequencies.

If, for example, an S-band amplifier is connected through a cable to a waveguide horn with a standard coaxial cable-to-waveguide adapter, the diode may become unstable although the horn is well matched in the amplifier pass band. The reason for this is that the coaxial cable-to-waveguide adapter consists of a short probe inside the waveguide and the adapter has a high VSWR below the waveguide cutoff frequency.



NOTE:

SOLID LINE AT CENTER OF CIRCULATOR
 DOTTED LINE AT 3.8 CM FROM CENTER
 FREQUENCY -- GIGACYCLES

Figure 42
 Impedance of Wye Ferrite Circulator

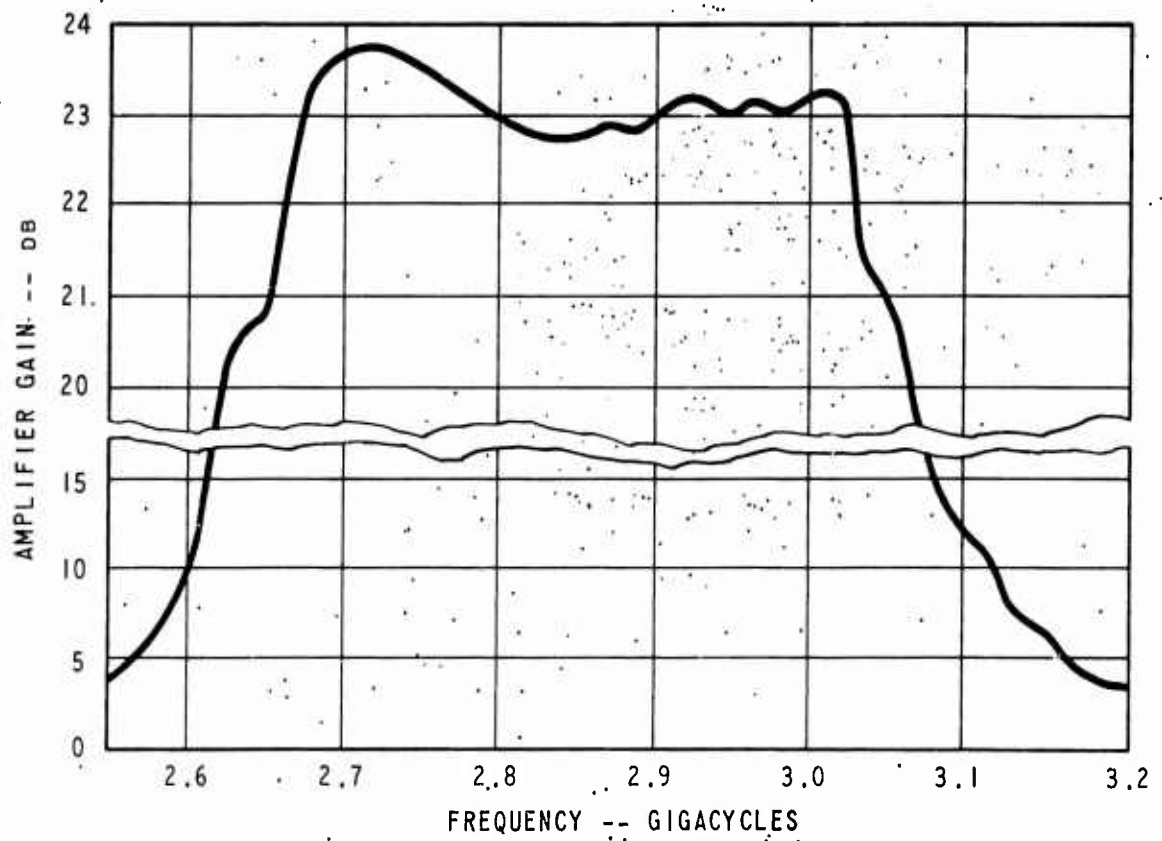
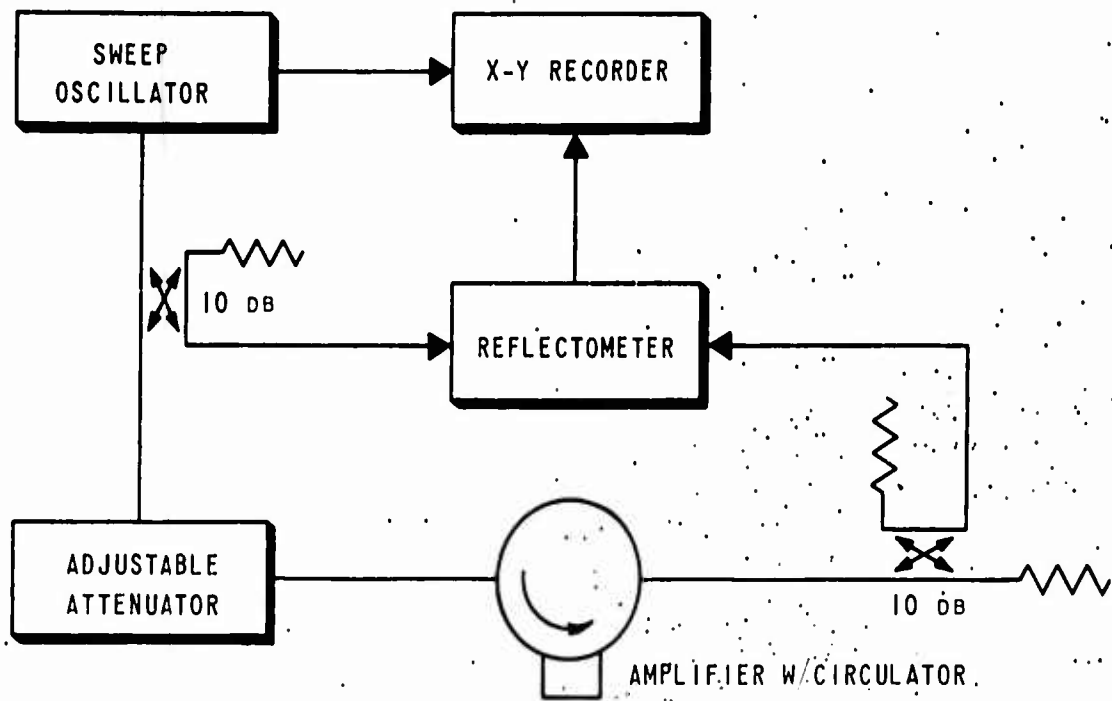


Figure 43 ..
Wide-banded S-band Amplifier

4.2.4 -- Continued.

The diode may see a short or an open circuit at some subharmonic frequency and begin oscillating.

The problem of adapting the amplifier to a waveguide horn was solved by separating the amplifier and horn with a stabilizing network. The network consists of a hybrid coupler and two identical low-pass filters terminated in matched loads. A block diagram of the network, also called a hybrid filter, is shown in Figure 44, and a network built in stripline is shown in Figure 45. The other plate is printed on the other side of the card as is the other filter center conductor. The measured insertion loss of the network is less than 0.5 db from 2.6 to 4.0 gigacycles. When the input terminal is connected to the antenna horn, VSWR of the output terminal is less than 1.5 at frequencies from dc to 3.5 gigacycles.

4.2.5 Amplifier Noise Figure. At resonance, the one-port amplifier has an equivalent circuit consisting of two positive conductances, the signal and the load, and a negative diode conductance. The noise contributed by these conductances can be represented by three current generators in parallel, two Johnson noise sources and one shot-noise source. The noise figure is a function of the ratio of the total current to that contributed by the signal source alone. This value is given approximately by

$$F = 1 + \frac{T_L G_L}{T_s G_s} + \frac{eI_0}{2kT_s G_s} \quad (30)$$

where

T_s and T_L are the absolute temperatures of the source and the load conductances,

I_0 is the net diode junction current,

e is the electron charge, and

k is Boltzmann's constant.^{3, 28}

A more exact expression for the noise figure includes a degradation factor for low gain:²⁹

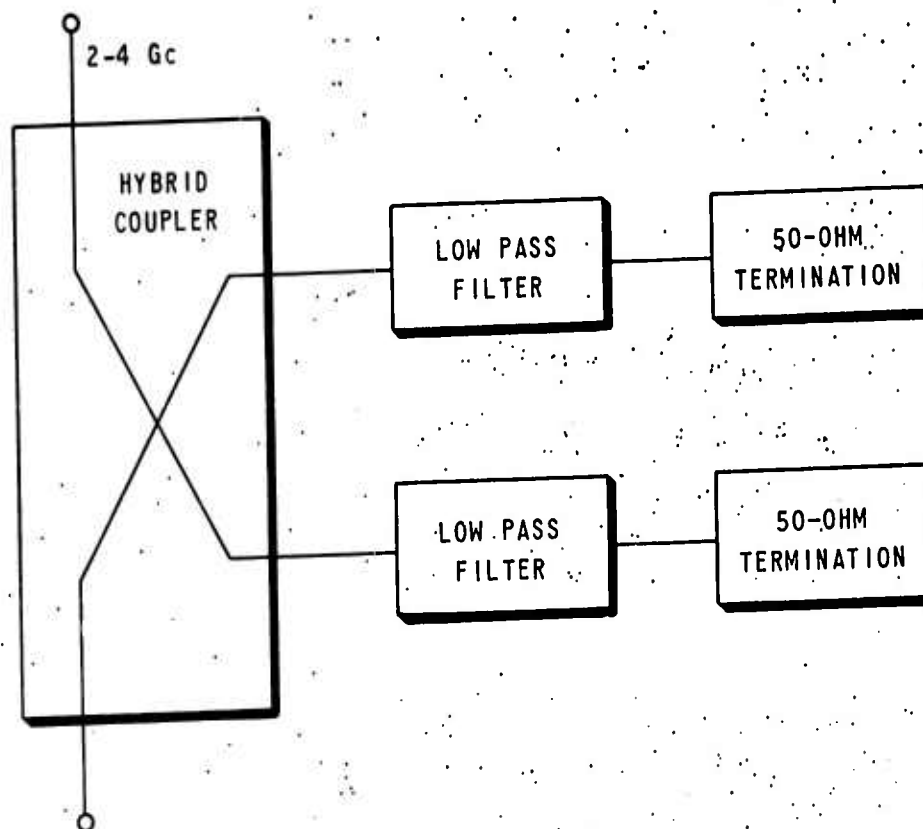


Figure 44
Block Diagram of Stabilizing Network

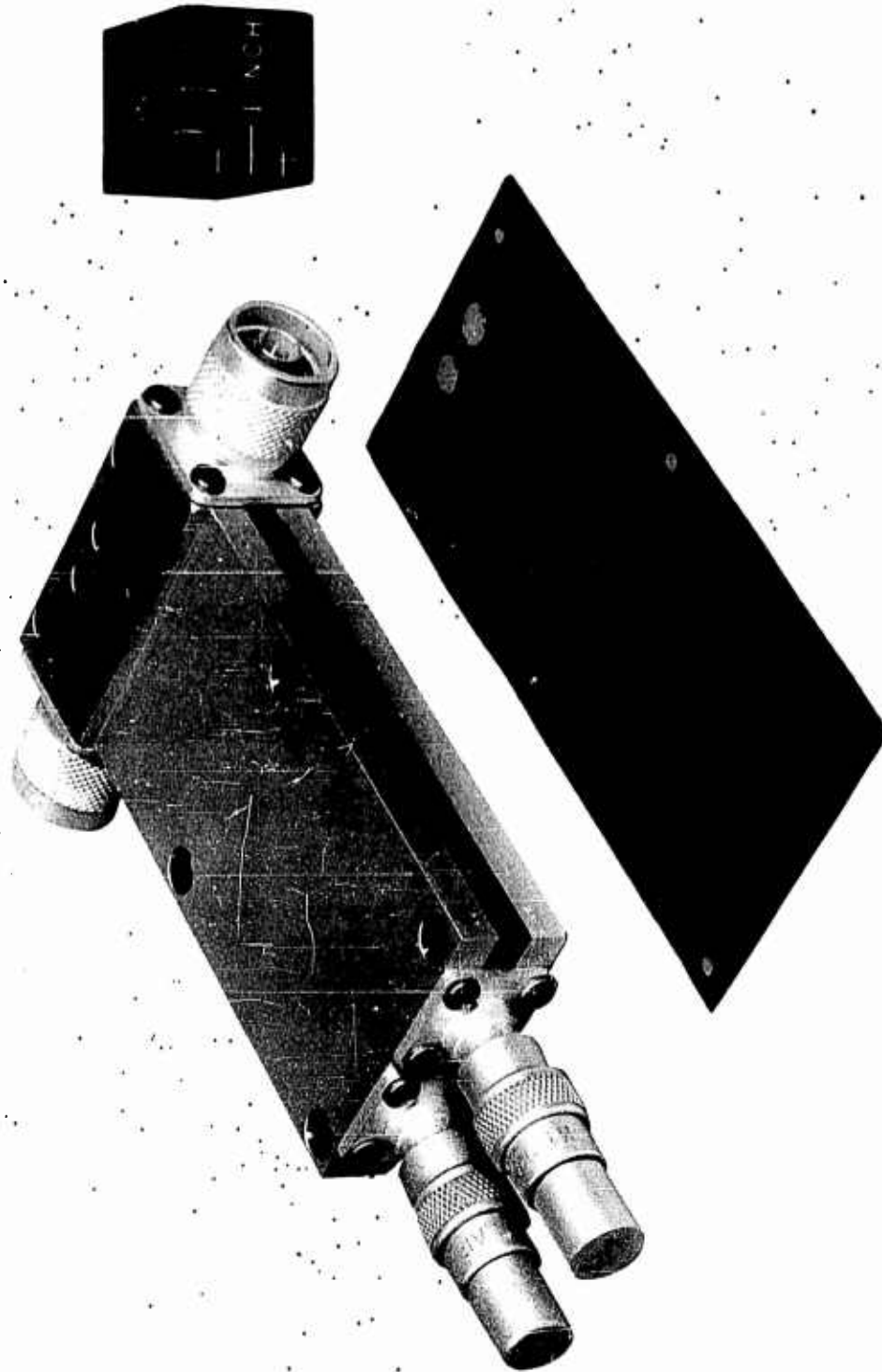


Figure 45
Stripline Configuration of Stabilizing Network

4.2.5 -- Continued.

$$F = 1 + \frac{(\sqrt{A_T} + 1)^2}{A_T} \left[\frac{T_L G_L}{T_s G_s} + \frac{eI_0}{2kT_s G_s} \right] \quad (31)$$

This equation also holds for the hybrid-coupled amplifier with the condition of perfect input match ($\rho_1 = 0$). The degradation is increased when the input reflection coefficient is greater than zero.

Equation 30 shows that the noise figure can be minimized in several ways by:

- (a) operating the amplifier at low temperatures,
- (b) reducing the ratio G_L/G_s , and
- (c) selecting diodes with a low current and high conductance.

Of these methods, only the last is of real importance. A cooling system for the amplifier is not compatible with its prime features, small size and low dc power requirements. Secondly, the required transformer for the reduction of ratio G_L/G_s means added circuit complexity, greater frequency dependence, increased size, and, in addition, a reduction in transducer gain and gain-bandwidth product.

If it is assumed that the amplifier operates at room temperature and that $G_L = G_s = \frac{G}{2}$, Equation 31 reduces to approximately

$$F = 1 + \frac{(\sqrt{A_T} + 1)^2}{A_T} (1 + 20I_0 R_D) \quad (32)$$

A noise figure can now be estimated from the diode characteristics presented in Figure 18. I_0 may be assumed roughly equal to 1/2 of the peak current, I_p . For example, Sylvania D4168 has an operating current of 1.0 millampere and gives, with a gain of 20 db, a noise figure of 5.3 db. The noise figure of the S-band amplifier, including the loss in circulator, was measured as less than 6.2 db at frequencies from 2.6 to 3.1 gigacycles. The measured noise figures of other amplifiers are shown in Figure 46.

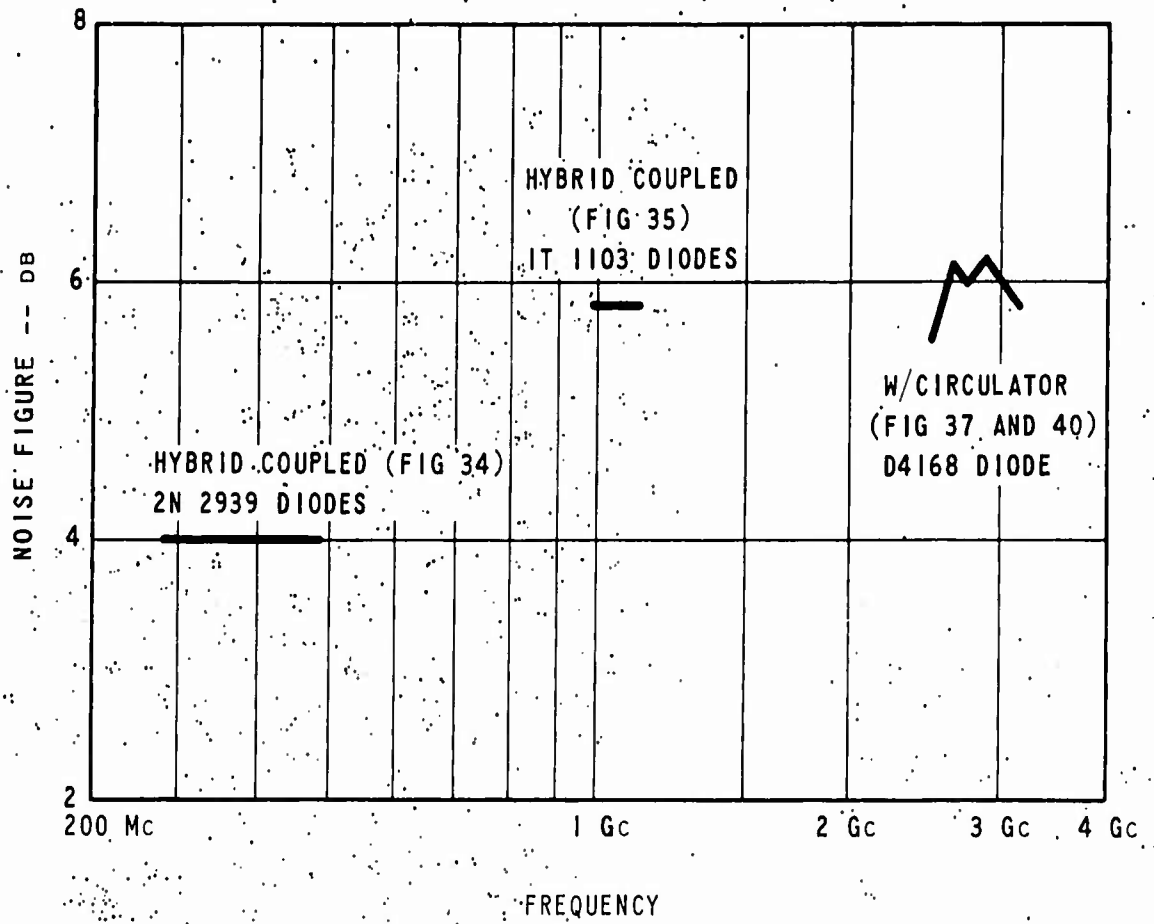


Figure 46
Measured Noise Figures

4.3 Frequency Converters.

The nonlinear characteristic of the negative resistance makes the tunnel diode ideally suited for frequency conversion in superheterodyne receivers. By biasing the diode slightly above the peak of the I-V curve the diode will have an average negative-resistance component useful to sustain oscillation and, in addition, a conversion conductance for the mixing of signal and oscillation frequencies. In this case it is referred to as a self-excited down converter. The diode can also be used as a mixer by keeping the diode stable and providing the oscillating signal from an external source.

The noise characteristics of the mixer or the converter are not inherently degraded by the ratio of the signal and the intermediate frequency as is the case of the parametric down converters. Further, it has been demonstrated that the tunnel-diode mixer can have a noise figure almost as good as that of the amplifier.³⁰

Although the self-excited down converter is inherently more desirable (for its circuit simplicity, small size and low dc power requirements), analysis of tunnel-diode frequency conversion has so far been restricted to the mixer. This is because the self-oscillation of the down converter is not purely sinusoidal, but is greatly distorted over the nonlinear region of the I-V curve. Therefore, it is difficult, if not impossible, to evaluate the conversion conductance and calculate the noise characteristics of the device. Since the down converter is rich in harmonics of the oscillation frequency, its noise figure may be expected to be higher than that of the mixer.

Mixer conversion gain and noise figure are critically dependent on the negative conductance and the conversion conductance. In order to evaluate these, it is assumed that the signal voltage is small and the local-oscillator voltage large. The diode conductance, $g(t)$, can then be considered as varying periodically at the oscillator frequency, as shown in Figure 47. The time-varying conductance may be expressed by a Fourier series of the form:

$$g(t) = g_0 + 2g_1 \cos w_0 t + g_2 \cos 2w_0 t + \dots \quad (33)$$

The average conductance over an oscillator cycle, g_0 , and the conversion conductance, g_1 , vary with bias and oscillation amplitude and can have both positive and negative values. An exact determination

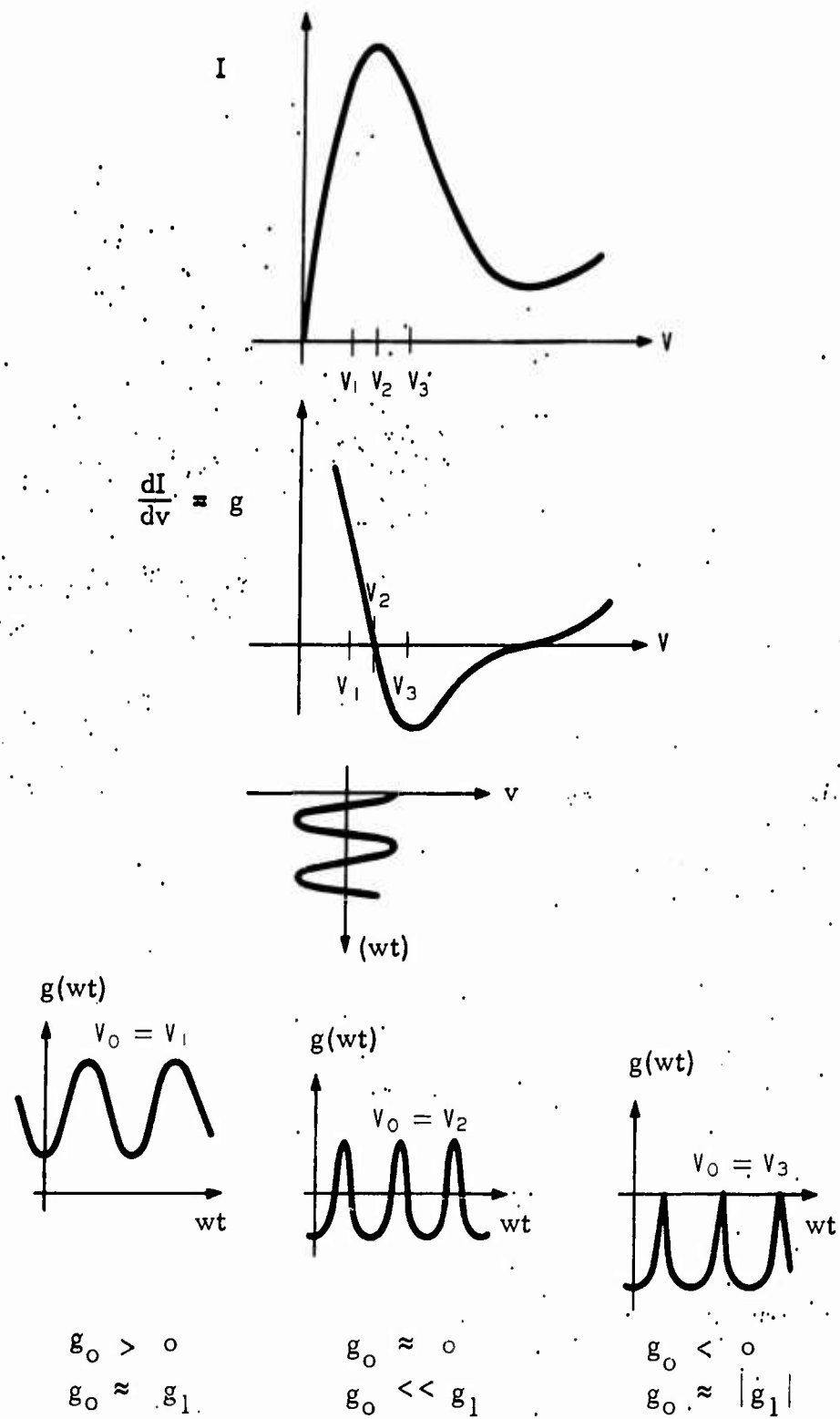


Figure 47

Conversion Conductance and Average Conductance
at Three Bias Points

4.3 -- Continued.

requires either an accurate graphical or numerical evaluation of the Fourier coefficients or both.

The mid-band conversion power gain is given by:

$$G = \frac{4r_1 r_2 g_1^2}{[(1 + g_0 r_1)(1 + g_0 r_2) + g_1^2 r_1 r_2]^2} \quad (34)$$

where r_1 and r_2 are the resistances seen by the diode at signal and intermediate frequencies f_1 and f_2 , respectively. Conversion gain is possible when g_0 is smaller than $|g_1|$. The values of RF input and IF output resistances are given by

$$r_{in} = \frac{1}{g_0(1 - \beta/\alpha)} \quad (35)$$

and

$$r_{out} = \frac{1}{g_0(1 - \gamma/\alpha)} \quad (36)$$

$$\text{where } \alpha = \frac{g_0}{g_1}, \quad \beta = \frac{g_1 r_2}{1 + g_0 r_2}, \quad \text{and } \gamma = \frac{g_1 r_1}{1 + g_0 r_1} \quad (37)$$

The mixer has high gain only if r_{in} and/or r_{out} are negative, i. e., when bias is adjusted so that $g_0 < |g_1|$. A small conversion gain is possible if both r_{in} and r_{out} are positive.

Mixer noise is contributed by r_1 , r_2 and diode shot noise and is given by

$$F = 1 + \frac{g I_0}{2kT_1 g_1} \left[\frac{1 + \gamma^2 \pm 2k\gamma}{\gamma(1 - \alpha\gamma)} \right] + \frac{1}{\gamma(1 - \alpha\gamma)} \frac{1}{g_1 r_2} \frac{T_2}{T_1} \quad (38)$$

where

$$k = -\frac{I_1}{I_0}$$

4.3 -- Continued.

I_1 is the net fundamental component of the diode current and T_1 and T_2 are the temperatures of r_1 and r_2 , respectively.

It is now possible to select a diode, plot its characteristic curve very accurately and calculate g_0 , g_1 , I_0 , and I_1 for various bias points and oscillator amplitudes. A wide choice still exists in the selection of r_1 , r_2 , r_{in} and r_{out} . The noise figure will depend on all these quantities. By making some simplifying assumptions it has been shown that the best values for the noise figure are higher than that of the amplifier noise figure by at least 3 db.³⁰ Under these conditions, both r_{in} and r_{out} were negative, and presented some stability problems. When r_{in} and r_{out} were made positive to ensure unconditional stability,^{32, 33} gain dropped to a very low value and noise figure rose some 4 db, resulting in an overall figure of 12 db. The actual reported measurements are in agreement with theory.^{31, 32}

A circuit diagram of a mixer is shown in Figure 48. The main difference between this circuit and the amplifier circuit, Figure 29, is that the RF bypass capacitor is smaller and is resonated with an inductor at the intermediate frequency. The diode capacitance resonates with the inductance of the tunable short-circuited transmission line. Figure 49 is a photo of a mixer built at EDL.

The mixer has a 200 megacycle bandwidth; its center frequency can be adjusted with the tunable short circuit over a 500 megacycle range in the L-band. As was expected, operation was critically dependent on local oscillator power and bias voltage. The lowest noise figure was measured as 12 db when the local oscillator power was adjusted to -20 dbm; the local oscillator power could therefore easily be supplied from a separate tunnel diode oscillator.

A hybrid coupled mixer, employing two tunnel-diode mixers and a 3-db coupler, has been described in an article by Robertson.³⁴ The main advantage of the hybrid circuit is that like the hybrid-coupled amplifier, it is stable without the use of nonreciprocal devices at the input port.

Several self-excited down converters have been built at EDL; the circuit is the same as that used for the mixer (Figure 48), but the diode is biased far enough into the negative region for the diode to sustain oscillation. A cutaway view of a miniature S-band down converter is presented in Figure 50. The converter uses a Sylvania D4168 diode

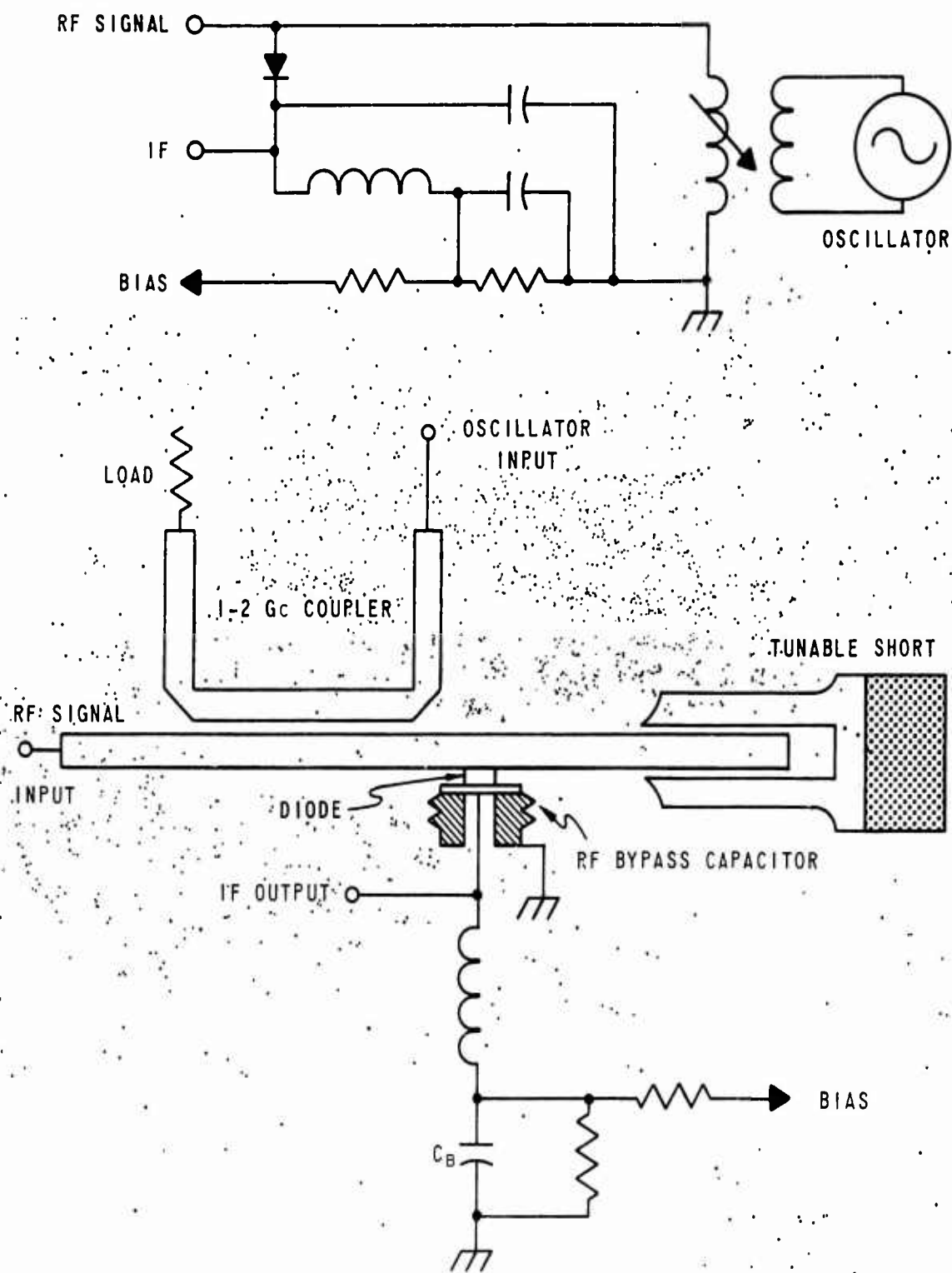


Figure 48

L-band Mixer Circuit Schematic and Component Layout

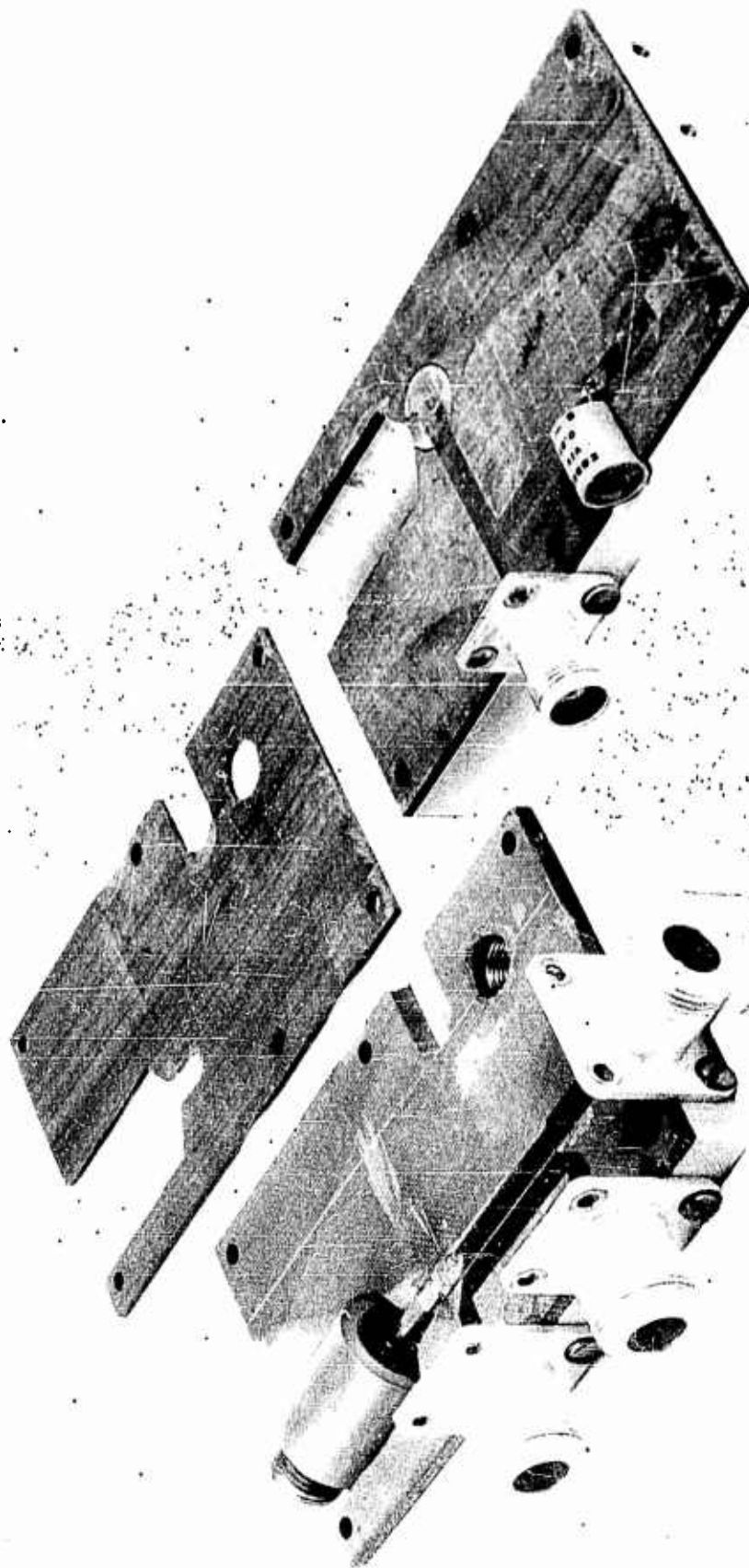


Figure 49
Stripline L-band Mixer

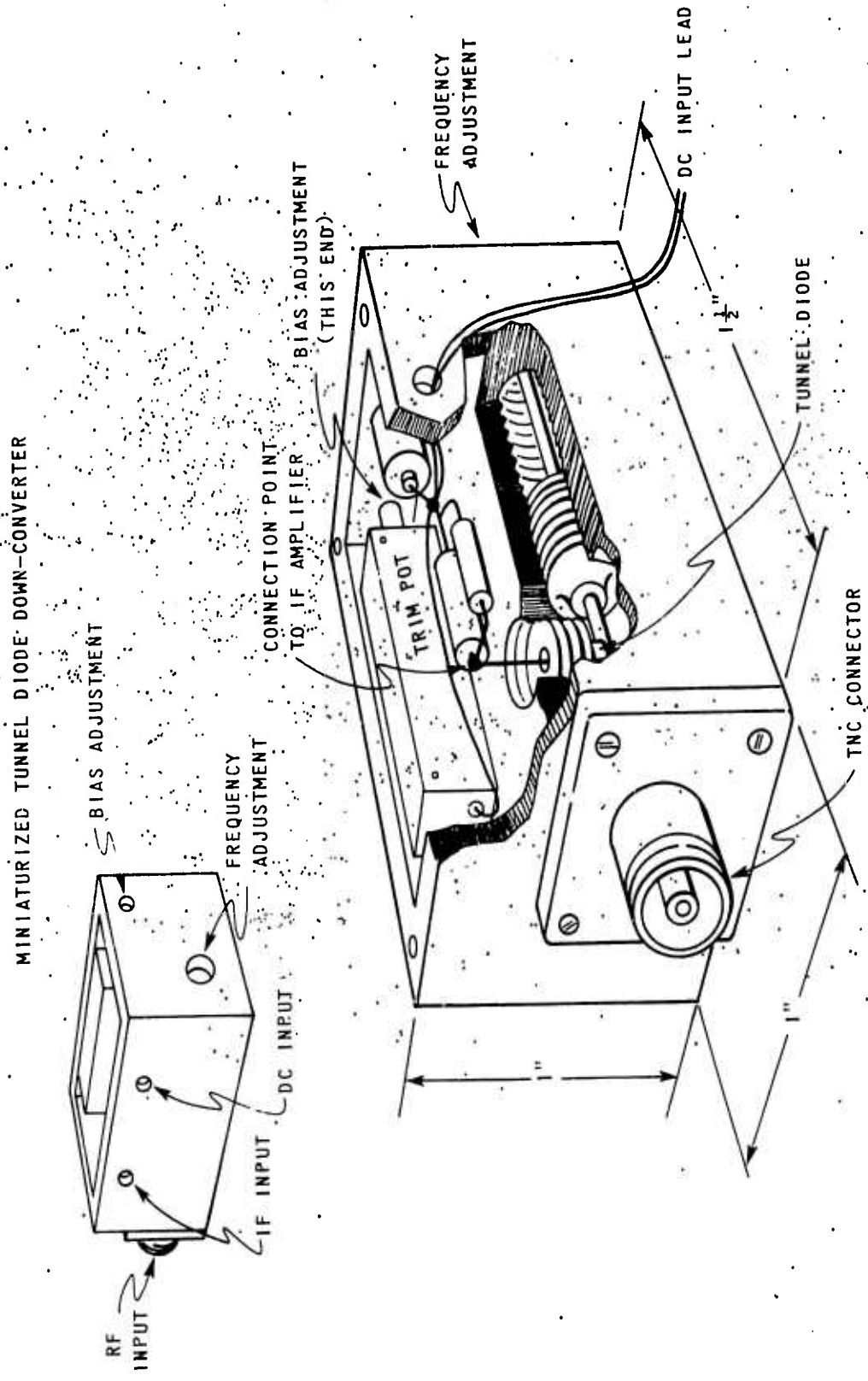


Figure 50
Miniature Tunnel Diode Down Converter

4.3 -- Continued.

and is tunable from 2 to 3 gigacycles. As expected, it is sensitive to changes in input VSWR. Noise figure was measured and found to be between 12 and 15 db. Figure 51 is a photograph of a miniature superheterodyne receiver containing the tunnel diode converter. The receiver also contains a 10-megacycle IF amplifier, detector, video and audio amplifier. Battery, on-off switch and other controls are also shown. A preamplifier, Figure 40, could be connected externally and provide preset amplification over a 400-500 megacycle band. Noise figure of the receiver with preamplifier was between 6 and 7 db.

Another converter was built quite similar to the capacitive-tuned amplifier in Figure 33. A loop coupled the input signal into the oscillating circuit, and IF output was taken across the bias resistor R_0 . Figure 52 is a photo of the capacitive-tuned converter. This converter was tunable from 2.4 to 3.2 gigacycles and noise figure was between 18 and 20 db. The frequency of received signals could be read to within ± 5 megacycles on a digital tuning control.

4.4 Superregenerative Amplifier.

In addition to the circuits discussed in the instant report, a number of other useful and promising circuits have been described in recent papers. It has been shown that the tunnel diode is well suited as a superregenerative amplifier. Quench voltage can be derived from the diode by making it oscillate at a low frequency. Bogusz obtained a voltage gain of 300, and showed a possible theoretical voltage gain of greater than 1000.³⁵

A superregenerative amplifier built at EDL is shown in Figure 53. The circuit configuration is similar to the mixer circuit of Figure 48; however, in the new application, the diode oscillated at a quench frequency, f_q , of 32 megacycles and was stabilized at the signal frequency, f_0 . The output power consisted of amplified signals at the frequencies $f_0 \pm nf_q$, where n is the number of sideband frequencies. The greatest number which n could take depended on f_q and signal amplitude, actually it was measured as greater than 10. Gain-bandwidth product of the center frequency component of the output signals was equivalent to that of a single-tuned one-port amplifier. Gain-bandwidth product as measured with a broad-band crystal detector was 15 to 20 times greater, since the output power at all the frequencies, $f_0 \pm nf_q$, was added by the detector. The measured gain-bandwidth product was from 15 to 17 gigacycles; mid-band gain could be adjusted from 30 db to 58 db.

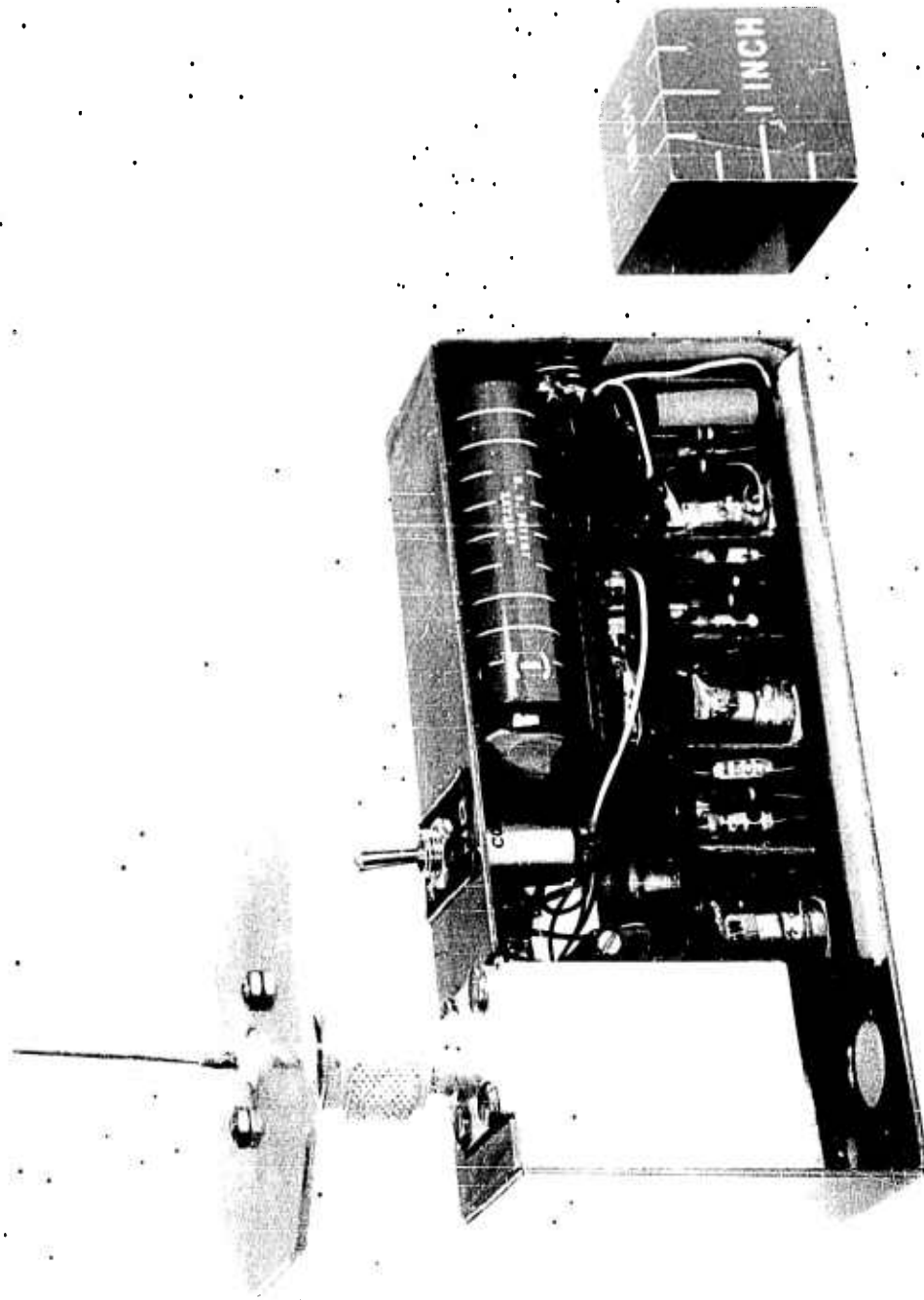


Figure 51
Miniature Solid-State Receiver

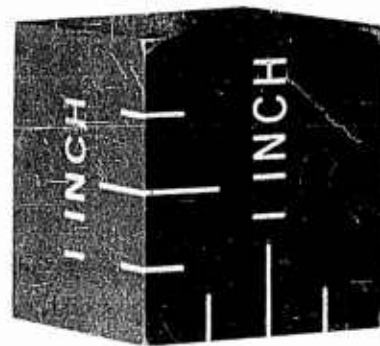
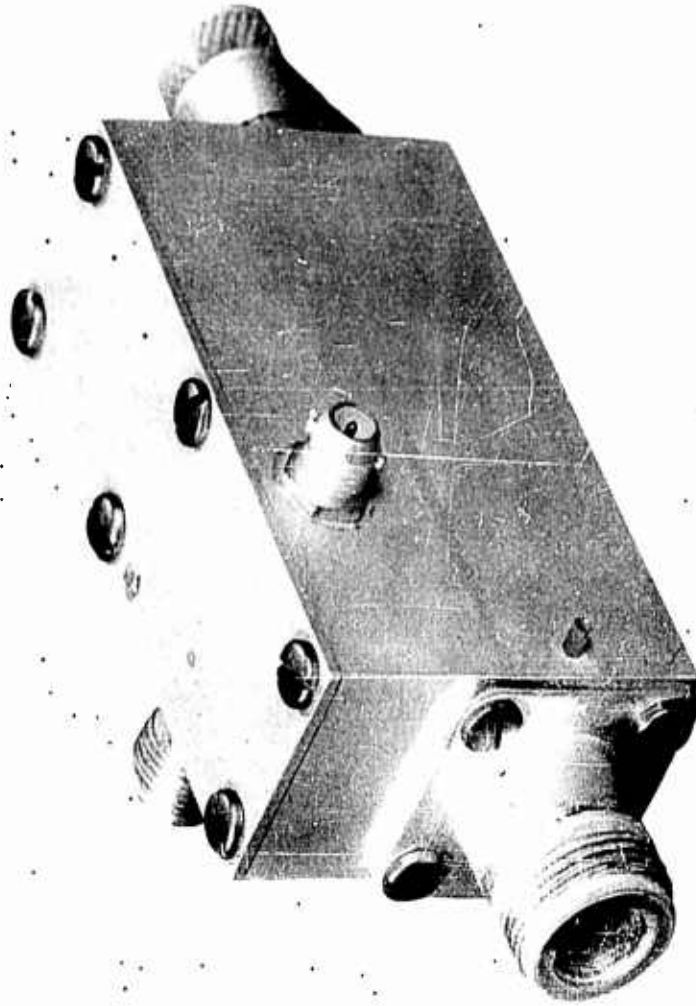


Figure 52
Capacitive-Tuned Down Converter

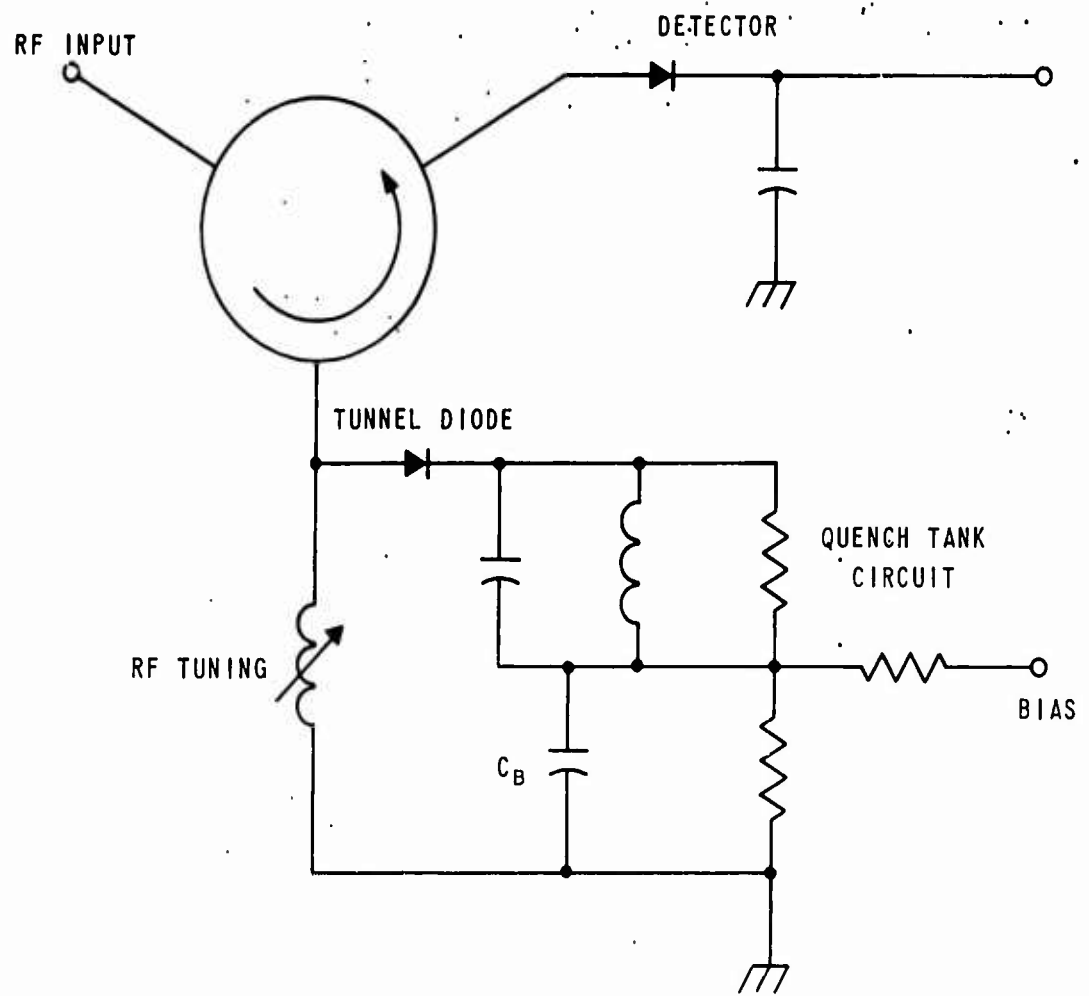


Figure 53
Superregenerative Amplifier

5. TEMPERATURE CHARACTERISTICS.

A preliminary study has been conducted of the stability of tunnel diode circuits in environmental conditions. The temperature characteristic of the negative conductance was checked experimentally by measuring the I-V curve of diode samples as a function of temperature; one such set of curves is shown in Figure 54. The recording shows that the negative conductance changes less than 5 per cent, with a change in temperature from 20° to 85°C. It has been shown theoretically and experimentally² that the negative conductance does not change at low temperatures (down to 4.2°K). Above 100°C, the valley current increases faster than the peak current, and the negative conductance decreases.

Other measurements were made to evaluate the performance of diode circuits in varying environmental temperatures. The mid-band gain of an S-band amplifier was measured as 25 db at 24°C. As the temperature was increased to 65°C, the gain decreased gradually to 22 db. By Equation 21, the gain variation corresponds to a change in negative resistance of 2.5 per cent, and in ohms to 0.03 ohm per degree centigrade.

The frequency stability of an S-band down converter oscillating at 2840 megacycles was measured as 0.05 megacycle per degree centigrade over the temperature change of 25° to 65°C.

6. SUMMARY.

In conclusion, it can be stated that the tunnel diode is a very useful device for many microwave applications. The diode is unequalled for low-noise amplification in lightweight systems where the noise figure requirements are no more demanding than those met by low-noise TWT. The present 500-megacycle bandwidth of the S-band amplifier is still somewhat short of the octave bandwidth capability of present TWT. However, many applications do not require more than the available 500-megacycle bandwidth, and it seems reasonable to expect continued improvements in ferrite devices and tunnel diode circuitry.

In addition, it seems feasible that the self-excited down converter could well replace the microwave mixer and vacuum tube oscillator in many superheterodyne receiving systems, where the 15-18 db noise figure is adequate and size and low power requirements are of importance.

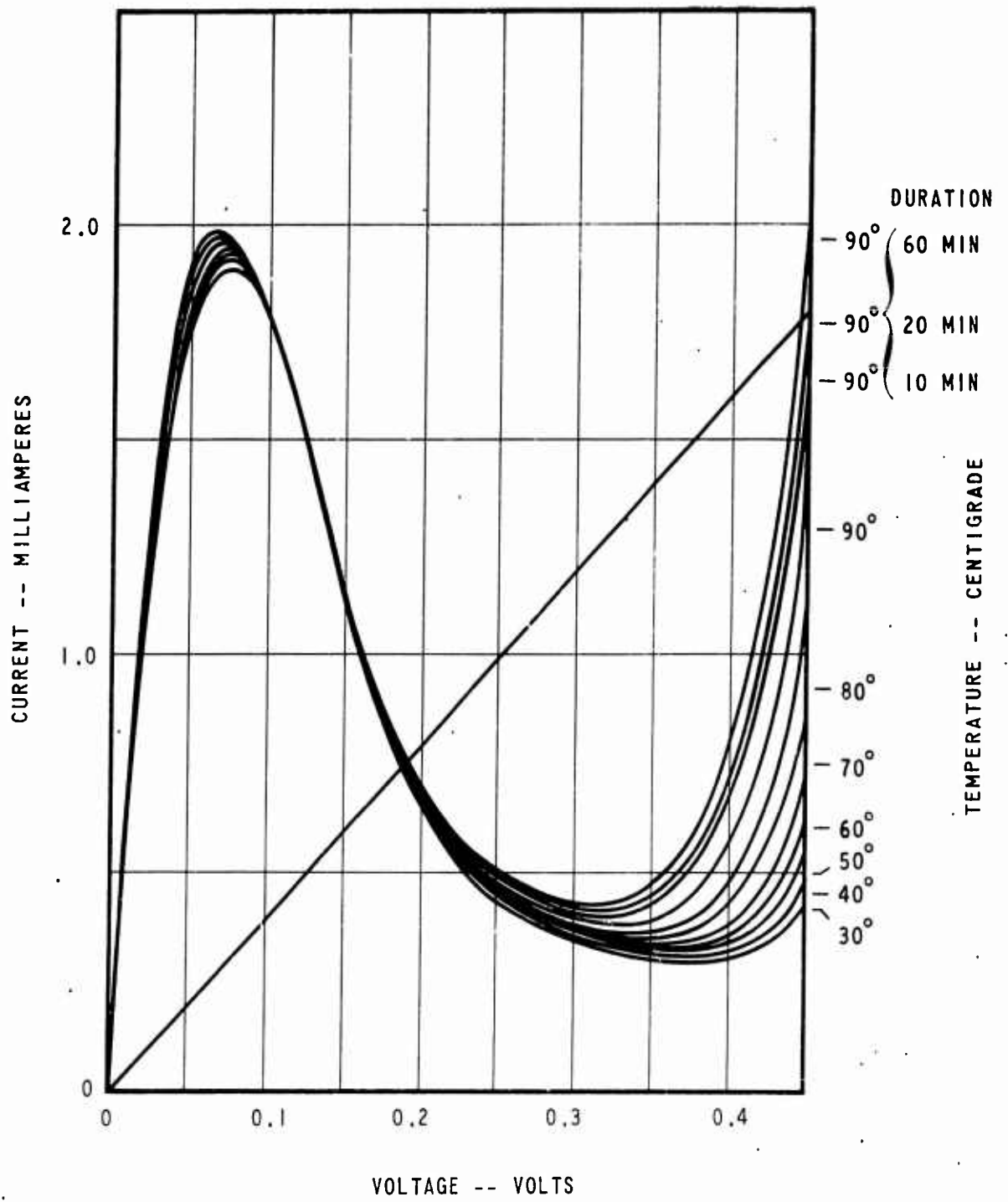


Figure 54
Temperature Characteristics of Sylvania D4115A
Tunnel Diode

7. REFERENCES.

1. L. Esaki, "New Phenomenon in Narrow Ge p-n Junctions," Physical Review, v 109, pp 603-5; January 1958.
2. I. A. Lesk, N. Holonyak, Jr., V. S. Davidsohn, M. W. Aairons, "Germanium and Silicon Tunnel Diodes - Design, Operation and Application," 1959 IRE WESCON Convention Record, v 3, Part 3, Electron Devices, pp 9-32.
3. W. W. Gärtner, "Esaki or Tunnel Diodes," Semiconductor Products, v 3, n 5, pp 31-38; May 1960, and v 3, n 6, pp 36-38; June 1960.
4. Technical Information Sheet on Tunnel Diodes, G. E. Research Lab., Schenectady, N. Y.; 23 July 1959.
5. R. N. Hall, "Tunnel Diodes," IRE Trans., v ED-7, n 1, p 1; January 1960.
6. H. S. Sommers, Jr., "Tunnel Diodes as High-Frequency Devices," Proc. IRE, v 47, n 7, pp 1201-1207; July 1959.
7. H. Fukui, "The Characteristics of Esaki Diodes at Microwave Frequencies," 1960 International Solid-State Circuits Conference, Philadelphia; February 1961.
8. V. S. Davidsohn, Y. C. Hwang, and G. B. Ober, "Designing with Tunnel Diodes," Electronic Design, v 8, n 3 and 4; 3 and 17 February 1960.
9. E. Gottlieb, "General Considerations of Tunnel-Diode Amplifiers," Technical Information Note, Semiconductor Products Dept., G. E. Company, Syracuse, N. Y.; January 1960.
10. K. Von Muller, "Selektive Hf-verstärkung mit Tunnelnioden," Electronik, Nr 2, p 39043; 1961.
11. T. Krueger, "Some Aspects of Tunnel-Diode Applications," U. S. Army Signal Res. & Dev. Lab., For Monmouth, N. J.; ASTIA A. D. 241 784.

7. -- Continued.

12. G. Dermit, "10.8 kmc Germanium Tunnel Diode," Proc. IRE, v 49, n 2, p 519; February 1961.
13. M. E. Hines, "High Frequency Negative-Resistance Circuit Principles for Esaki Diode Applications," G. S. T. J., v 39, n 3, pp 477-513; May 1960.
14. W. B. Hauer, "Definition and Determination of the Series Inductance of Tunnel Diodes," Technical Memorandum 452. 3, GT&E Lab., Inc., Bayside, N. Y.; 12 January 1961.
15. H. G. Dill, and M. R. MacPherson, "Tracing Tunnel Diode Curves," Electronics, v 33, n 32, p 62; 5 August 1960.
16. R. Stratton et al, "Tunnel Diodes, A Special Report," Electrical Design News, v 5, n 5; May 1960.
17. J. Zorzy, "Measurements of the Equivalent-Circuit Parameters of Tunnel Diodes," General Radio Experimenter, v 34, n 7 and 8, pp 3-9; July-August 1960.
18. H. W. Card, "Bridge Measurement of Tunnel-Diode Parameters," IRE, Trans., v ED-8, n 3, p 215; May 1961.
19. D. C. Youla, and L. I. Smilen, "On the Stability of Tunnel Diodes," Networks & Waveguide Group, Memorandum 49; PIBMRI-889-61, Microwave Res. Inst., Polytechnic Institute of Brooklyn.
20. D. C. Youla, and L. I. Smilen, "Exact Theory and Synthesis of a Class of Tunnel-Diode Amplifiers," Proc. of the Natl. Electronic Conference, v 16, 1960.
21. D. E. Nelson, and F. Sterzer, "Tunnel-Diode Microwave Oscillators with Milliwatt Power Output," 1960 IRE WESCON Convention Record, v 4, Part 1, pp 68-73.
22. D. E. Nelson, and F. Sterzer, "Tunnel-Diode Microwave Oscillators," Proc. IRE, v 49, n 4, pp 744-753; April 1961.
23. G. Dermit, "High Frequency Power in Tunnel Diodes," FT&E Internal Letter of Transmittal, 14 December 1960; also, Proc. IRE, v 149, n 6, pp 1033-1043; June 1961.

7. -- Continued.
24. C. A. Burrus, "Gallium Arsenide Esaki Diodes for High-Frequency Applications," *Journal of Applied Physics*, v 32, n 6, pp 1031-1036; June 1961.
25. "Analysis of Negative-Conductance Amplifiers Operated with Ideal 90°-Degree Hybrid," 8th Q. R., June 1960, Airborne Instr. Lab. Contract AF30 (602)-1854, pp 5-18.
26. E. W. Sard, "Tunnel (Esaki) Diode Amplifiers with Unusually Large Bandwidth," *Proc. IRE (corresp.)*, v 48, n 3, pp 357-358; March 1960.
27. R. Aron, "Gain Bandwidth Relations in Negative Resistance Amplifiers," *Proc. IRE*, v 49, n 1, pp 355-356; January 1961.
28. J. J. Tiemann, "Shot Noise in Tunnel-Diode Amplifiers," *Proc. IRE*, v 48, n 8, pp 1418-1423; August 1960.
29. A. Yariv, and J. S. Cook, "A Noise Investigation of Tunnel-Diode Microwave Amplifiers," *Proc. IRE*, v 49, n 4, pp 739-743; April 1961.
30. D. I. Breitzer, "Noise Figure of Tunnel-Diode Mixer," *Proc. IRE*, v 48, n 5, pp 935-936; May 1960.
31. J. C. Greene, and E. W. Sard, "Experimental Tunnel-Diode Mixer," *Proc. IRE*, v 49, n 1, pp 350-351; January 1961.
32. J. C. Greene, and E. W. Sard, "Experimental Verification of Theoretical Gain and Noise Factor of Tunnel-Diode Mixer," 8th Q. R., June 1960, Contr. AF30-602-1854, pp 19-26, Airborne Inst. Lab.
33. J. C. Greene, and E. W. Sard, "Additional Design Considerations for Tunnel-Diode Mixer," 9th Q. R., Airborne Inst. Lab., Contr. AF30 (602)-1854, pp 19-27; September 1960.
34. W. J. Robertson, "A Broadband Hybrid Coupled Tunnel-Diode Down Converter," *Proc. IRE*, v 48, n 12, pp 2023-2024; December 1960.

7. -- Continued.

35. J. F. Bogusz, and H. H. Schaffer, "Superregenerative Circuits Using Tunnel Diodes," 1961 International Solid State Circuits Conference, Philadelphia; February 1961.

<p>AD Accession No.</p> <p>Electronic Defense Labs., Mountain View, Calif. TUNNEL DIODE CIRCUITS AT MICROWAVE FREQUENCIES - John Reindel. Technical Memo- randum EDL-M397, 15 August 1961 (Contract DA 36-039 SC-87475) UNCLASSIFIED Report.</p> <p>This report presents results of recent studies in tunnel diode microwave circuits at the Electronic Defense Laboratories. Descriptions are also offered of an S-band low-noise amplifier with a voltage gain bandwidth product of 6000 mega- cycles and of designs of mechanically tunable down converters. The prime features of the tunnel diode, its small size and low dc power requirements, are taken advantage of in the circuit designs.</p>	<p>AD Accession No.</p> <p>Electronic Defense Labs., Mountain View, Calif. TUNNEL DIODE CIRCUITS AT MICROWAVE FREQUENCIES - John Reindel. Technical Memo- randum EDL-M397, 15 August 1961 (Contract DA 36-039 SC-87475) UNCLASSIFIED Report.</p> <p>This report presents results of recent studies in tunnel diode microwave circuits at the Electronic Defense Laboratories. Descriptions are also offered of an S-band low-noise amplifier with a voltage gain bandwidth product of 6000 mega- cycles and of designs of mechanically tunable down converters. The prime features of the tunnel diode, its small size and low dc power requirements, are taken advantage of in the circuit designs.</p>	<p>UNCLASSIFIED Copy No.</p> <ol style="list-style-type: none"> 1. Amplifier 2. Bandwidth 3. Broadbanding 4. Circuits 5. Conductance 6. Converter 7. Diodes 8. Function 9. Gain 10. Frequencies 11. Microwave 12. Noise 13. Oscillator 14. S-band 15. Stability 16. Tunable 17. Tunnel 18. Voltage <p>I. Reindel, John II. Contract DA 36-039 SC-87475 8.2</p>	<p>UNCLASSIFIED Copy No.</p> <ol style="list-style-type: none"> 1. Amplifier 2. Bandwidth 3. Broadbanding 4. Circuits 5. Conductance 6. Converter 7. Diodes 8. Function 9. Gain 10. Frequencies 11. Microwave 12. Noise 13. Oscillator 14. S-band 15. Stability 16. Tunable 17. Tunnel 18. Voltage <p>I. Reindel, John II. Contract DA 36-039 SC-87475 8.2</p>
<p>AD Accession No.</p> <p>Electronic Defense Labs., Mountain View, Calif. TUNNEL DIODE CIRCUITS AT MICROWAVE FREQUENCIES - John Reindel. Technical Memo- randum EDL-M397, 15 August 1961 (Contract DA 36-039 SC-87475) UNCLASSIFIED Report.</p> <p>This report presents results of recent studies in tunnel diode microwave circuits at the Electronic Defense Laboratories. Descriptions are also offered of an S-band low-noise amplifier with a voltage gain bandwidth product of 6000 mega- cycles and of designs of mechanically tunable down converters. The prime features of the tunnel diode, its small size and low dc power requirements, are taken advantage of in the circuit designs.</p>	<p>AD Accession No.</p> <p>Electronic Defense Labs., Mountain View, Calif. TUNNEL DIODE CIRCUITS AT MICROWAVE FREQUENCIES - John Reindel. Technical Memo- randum EDL-M397, 15 August 1961 (Contract DA 36-039 SC-87475) UNCLASSIFIED Report.</p> <p>This report presents results of recent studies in tunnel diode microwave circuits at the Electronic Defense Laboratories. Descriptions are also offered of an S-band low-noise amplifier with a voltage gain bandwidth product of 6000 mega- cycles and of designs of mechanically tunable down converters. The prime features of the tunnel diode, its small size and low dc power requirements, are taken advantage of in the circuit designs.</p>	<p>UNCLASSIFIED Copy No.</p> <ol style="list-style-type: none"> 1. Amplifier 2. Bandwidth 3. Broadbanding 4. Circuits 5. Conductance 6. Converter 7. Diodes 8. Function 9. Gain 10. Frequencies 11. Microwave 12. Noise 13. Oscillator 14. S-band 15. Stability 16. Tunable 17. Tunnel 18. Voltage <p>I. Reindel, John II. Contract DA 36-039 SC-87475 8.2</p>	<p>UNCLASSIFIED Copy No.</p> <ol style="list-style-type: none"> 1. Amplifier 2. Bandwidth 3. Broadbanding 4. Circuits 5. Conductance 6. Converter 7. Diodes 8. Function 9. Gain 10. Frequencies 11. Microwave 12. Noise 13. Oscillator 14. S-band 15. Stability 16. Tunable 17. Tunnel 18. Voltage <p>I. Reindel, John II. Contract DA 36-039 SC-87475 8.2</p>

<p>AD Accession No. Electronic Defense Labs., Mountain View, Calif. TUNNEL DIODE CIRCUITS AT MICROWAVE FREQUENCIES - John Reindel. Technical Memo- randum EDL-M397, 15 August 1961 (Contract DA 36-039 SC-87475) UNCLASSIFIED Report.</p> <p>This report presents results of recent studies in tunnel diode microwave circuits at the Electronic Defense Laboratories. Descriptions are also offered of an S-band low-noise amplifier with a voltage gain bandwidth product of 6000 mega- cycles and of designs of mechanically tunable down converters. The prime features of the tunnel diode, its small size and low dc power requirements, are taken advantage of in the circuit designs.</p>	<p>UNCLASSIFIED Copy No. 1. Amplifier 2. Bandwidth 3. Broadbanding 4. Circuits 5. Conductance 6. Converter 7. Diodes 8. Function 9. Gain 10. Frequencies 11. Microwave 12. Noise 13. Oscillator 14. S-band 15. Stability 16. Tunable 17. Tunnel 18. Voltage</p> <p>I. Reindel, John II. Contract DA 36-039 SC-87475 8.2</p>	<p>UNCLASSIFIED Copy No. 1. Amplifier 2. Bandwidth 3. Broadbanding 4. Circuits 5. Conductance 6. Converter 7. Diodes 8. Function 9. Gain 10. Frequencies 11. Microwave 12. Noise 13. Oscillator 14. S-band 15. Stability 16. Tunable 17. Tunnel 18. Voltage</p> <p>I. Reindel, John II. Contract DA 36-039 SC-87475 8.2</p>
<p>AD Accession No. Electronic Defense Labs., Mountain View, Calif. TUNNEL DIODE CIRCUITS AT MICROWAVE FREQUENCIES - John Reindel. Technical Memo- randum EDL-M397, 15 August 1961 (Contract DA 36-039 SC-87475) UNCLASSIFIED Report.</p> <p>This report presents results of recent studies in tunnel diode microwave circuits at the Electronic Defense Laboratories. Descriptions are also offered of an S-band low-noise amplifier with a voltage gain bandwidth product of 6000 mega- cycles and of designs of mechanically tunable down converters. The prime features of the tunnel diode, its small size and low dc power requirements, are taken advantage of in the circuit designs.</p>	<p>UNCLASSIFIED Copy No. 1. Amplifier 2. Bandwidth 3. Broadbanding 4. Circuits 5. Conductance 6. Converter 7. Diodes 8. Function 9. Gain 10. Frequencies 11. Microwave 12. Noise 13. Oscillator 14. S-band 15. Stability 16. Tunable 17. Tunnel 18. Voltage</p> <p>I. Reindel, John II. Contract DA 36-039 SC-87475 8.2</p>	<p>UNCLASSIFIED Copy No. 1. Amplifier 2. Bandwidth 3. Broadbanding 4. Circuits 5. Conductance 6. Converter 7. Diodes 8. Function 9. Gain 10. Frequencies 11. Microwave 12. Noise 13. Oscillator 14. S-band 15. Stability 16. Tunable 17. Tunnel 18. Voltage</p> <p>I. Reindel, John II. Contract DA 36-039 SC-87475 8.2</p>

<p>AD Accession No. Electronic Defense Labs., Mountain View, Calif. TUNNEL DIODE CIRCUITS AT MICROWAVE FREQUENCIES - John Reindel. Technical Memo- randum EDL-M397, 15 August 1961 (Contract DA 36-039 SC-87475) UNCLASSIFIED Report.</p> <p>This report presents results of recent studies in tunnel diode microwave circuits at the Electronic Defense Laboratories. Descriptions are also offered of an S-band low-noise amplifier with a voltage gain bandwidth product of 6000 mega- cycles and of designs of mechanically tunable down converters. The prime features of the tunnel diode, its small size and low dc power requirements, are taken advantage of in the circuit designs.</p>	<p>UNCLASSIFIED Copy No. 1. Amplifier 2. Bandwidth 3. Broadbanding 4. Circuits 5. Conductance 6. Converter 7. Diodes 8. Function 9. Gain 10. Frequencies 11. Microwave 12. Noise 13. Oscillator 14. S-band 15. Stability 16. Tunable 17. Tunnel 18. Voltage</p> <p>I. Reindel, John II. Contract DA 36-039 SC-87475 8.2</p>	<p>UNCLASSIFIED Copy No. 1. Amplifier 2. Bandwidth 3. Broadbanding 4. Circuits 5. Conductance 6. Converter 7. Diodes 8. Function 9. Gain 10. Frequencies 11. Microwave 12. Noise 13. Oscillator 14. S-band 15. Stability 16. Tunable 17. Tunnel 18. Voltage</p> <p>I. Reindel, John II. Contract DA 36-039 SC-87475 8.2</p>
<p>AD Accession No. Electronic Defense Labs., Mountain View, Calif. TUNNEL DIODE CIRCUITS AT MICROWAVE FREQUENCIES - John Reindel. Technical Memo- randum EDL-M397, 15 August 1961 (Contract DA 36-039 SC-87475) UNCLASSIFIED Report.</p> <p>This report presents results of recent studies in tunnel diode microwave circuits at the Electronic Defense Laboratories. Descriptions are also offered of an S-band low-noise amplifier with a voltage gain bandwidth product of 6000 mega- cycles and of designs of mechanically tunable down converters. The prime features of the tunnel diode, its small size and low dc power requirements, are taken advantage of in the circuit designs.</p>	<p>UNCLASSIFIED Copy No. 1. Amplifier 2. Bandwidth 3. Broadbanding 4. Circuits 5. Conductance 6. Converter 7. Diodes 8. Function 9. Gain 10. Frequencies 11. Microwave 12. Noise 13. Oscillator 14. S-band 15. Stability 16. Tunable 17. Tunnel 18. Voltage</p> <p>I. Reindel, John II. Contract DA 36-039 SC-87475 8.2</p>	<p>UNCLASSIFIED Copy No. 1. Amplifier 2. Bandwidth 3. Broadbanding 4. Circuits 5. Conductance 6. Converter 7. Diodes 8. Function 9. Gain 10. Frequencies 11. Microwave 12. Noise 13. Oscillator 14. S-band 15. Stability 16. Tunable 17. Tunnel 18. Voltage</p> <p>I. Reindel, John II. Contract DA 36-039 SC-87475 8.2</p>